Groundwater Resources Program

The Mississippi Embayment Regional Aquifer Study (MERAS): Documentation of a Groundwater-Flow Model Constructed to Assess Water Availability in the Mississippi Embayment

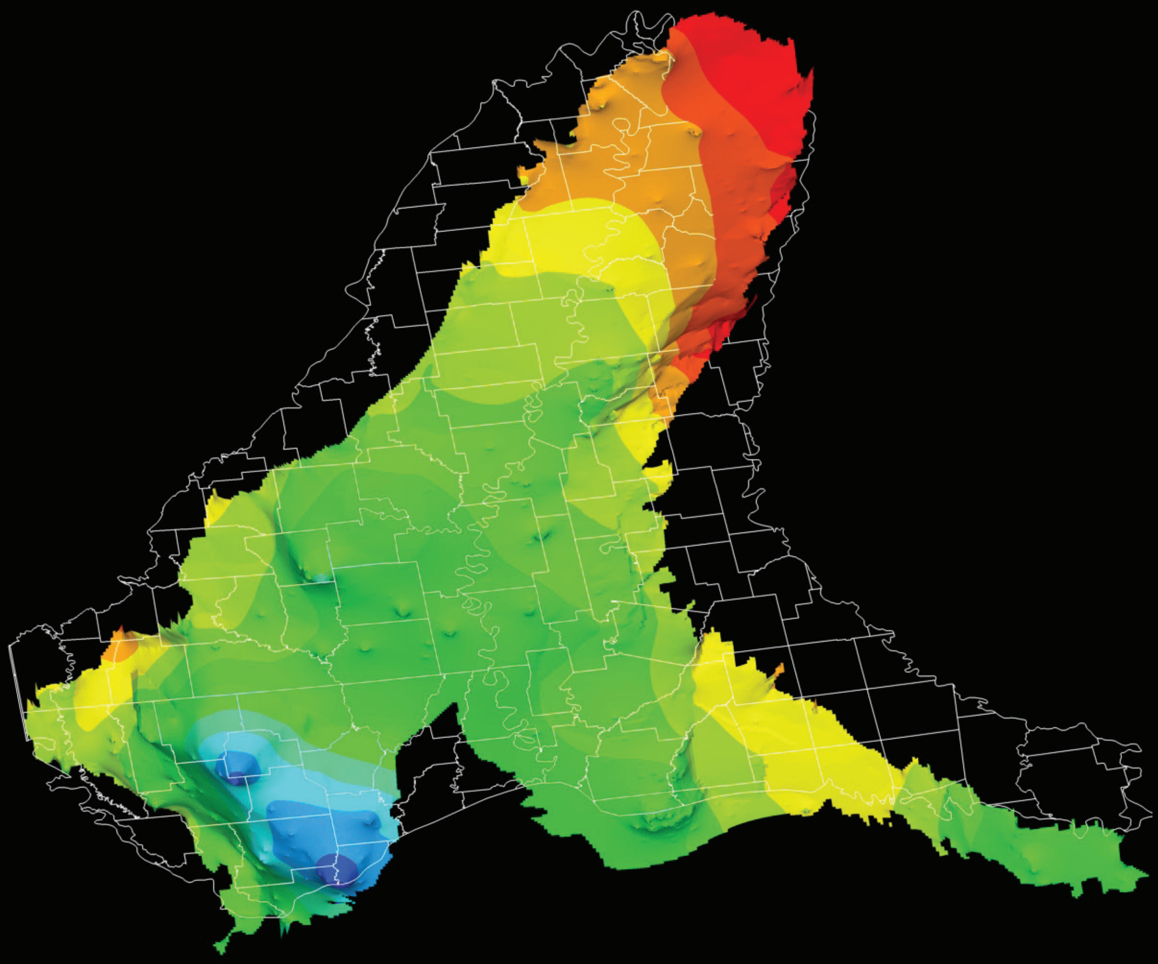

Scientific Investigations Report 2009–5172

U.S. Department of the Interior
U.S. Geological Survey

Cover description. Oblique view of 2007 simulated hydraulic heads of the middle Claiborne aquifer.

The Mississippi Embayment Regional Aquifer Study (MERAS): Documentation of a Groundwater-Flow Model Constructed to Assess Water Availability in the Mississippi Embayment

By Brian R. Clark and Rheannon M. Hart

Groundwater Resources Program

Scientific Investigations Report 2009-5172

U.S. Department of the Interior
U.S. Geological Survey

U.S. Department of the Interior
KEN SALAZAR, Secretary

U.S. Geological Survey
Suzette M. Kimball, Acting Director

U.S. Geological Survey, Reston, Virginia: 2009

For product and ordering information:
World Wide Web: http://www.usgs.gov/pubprod
Telephone: 1-888-ASK-USGS

For more information on the USGS--the Federal source for science about the Earth, its natural and living resources, natural hazards, and the environment:
World Wide Web: http://www.usgs.gov
Telephone: 1-888-ASK-USGS

Suggested citation:
Clark, B.R., and Hart, R.M., 2009, The Mississippi Embayment Regional Aquifer Study (MERAS): Documentation of a groundwater-flow model constructed to assess water availability in the Mississippi Embayment: U.S. Geological Survey Scientific Investigations Report 2009-5172, 61 p.

Contents

Figures

Tables

Conversion Factors

Multiply	By	To obtain
	Length	
inch (in.)	2.54	centimeter (cm)
inch (in.)	25.4	millimeter (mm)
foot (ft)	0.3048	meter (m)
mile (mi)	1.609	kilometer (km)
	Area	
square mile (mi^2)	259.0	hectare (ha)
square mile (mi^2)	2.590	square kilometer (km^2)
	Flow rate	
acre-foot per year (acre-ft/yr)	1,233	cubic meter per year (^{3}/yr)
foot per day (ft/d)	0.3048	meter per day (m/d)
cubic foot per second (ft^3/s)	0.02832	cubic meter per second (m^3/s)
cubic foot per day (ft^3/d)	0.02832	cubic meter per day (m^3/d)
gallon per minute (gal/min)	0.06309	liter pr second (L/s)
million gallons per day (Mgal/d)	0.04381	cubic meters per second (m^3/s)
inch per year (in/yr)	25.4	millimeter per year (mm/yr)
	Hydraulic conductivity	
foot per day (ft/d)	0.3048	meter per day (m/d)

Temperature in degrees Celsius (°C) may be converted to degrees Fahrenheit (°F) as follows:

°F=(1.8×°C)+32

Temperature in degrees Fahrenheit (°F) may be converted to degrees Celsius (°C) as follows:

°C=(°F-32)/1.8

Vertical coordinate information is referenced to the National Geodetic Vertical Datum of 1929 (NGVD 29).

Horizontal coordinate information is referenced to the North American Datum of 1983 (NAD 83).

Altitude as used in this report, refers to distance above the vertical datum.

*Transmissivity: The standard unit for transmissivity is cubic foot per day per square foot times foot of aquifer thickness [(ft^3/d)/ft^2]ft. In this report the mathematically reduced form, foot squared per day (ft^2/d), is used for convenience.

Specific conductance is given in microsiemens per centimeter at 25 degrees Celsius (µS/cm at 25°C).

Concentrations of chemical constituents in water are given in milligrams per liter (mg/L) or micrograms per liter (µg/L).

The Mississippi Embayment Regional Aquifer Study (MERAS): Documentation of a Groundwater-Flow Model Constructed to Assess Water Availability in the Mississippi Embayment

By Brian R. Clark and Rheannon M. Hart

Abstract

The Mississippi Embayment Regional Aquifer Study (MERAS) was conducted with support from the Groundwater Resources Program of the U.S. Geological Survey Office of Groundwater. This report documents the construction and calibration of a finite-difference groundwater model for use as a tool to quantify groundwater availability within the Mississippi embayment. To approximate the differential equation, the MERAS model was constructed with the U.S. Geological Survey's modular three-dimensional finite-difference code, MODFLOW-2005; the preconditioned conjugate gradient solver within MODFLOW-2005 was used for the numerical solution technique. The model area boundary is approximately 78,000 square miles and includes eight States with approximately 6,900 miles of simulated streams, 70,000 well locations, and 10 primary hydrogeologic units. The finite-difference grid consists of 414 rows, 397 columns, and 13 layers. Each model cell is 1 square mile with varying thickness by cell and by layer. The simulation period extends from January 1, 1870, to April 1, 2007, for a total of 137 years and 69 stress periods. The first stress period is simulated as steady state to represent predevelopment conditions.

Areal recharge is applied throughout the MERAS model area using the MODFLOW-2005 Recharge Package. Irrigation, municipal, and industrial wells are simulated using the Multi-Node Well Package. There are 43 streams simulated by the MERAS model. Each stream or river in the model area was simulated using the Streamflow-Routing Package. The perimeter of the model area and the base of the flow system are represented as no-flow boundaries. The downgradient limit of each model layer is a no-flow boundary, which approximates the extent of water with less than 10,000 milligrams per liter of dissolved solids.

The MERAS model was calibrated by making manual changes to parameter values and examining residuals for hydraulic heads and streamflow. Additional calibration was achieved through alternate use of UCODE-2005 and PEST. Simulated heads were compared to 55,786 hydraulic-head measurements from 3,245 wells in the MERAS model area. Values of root mean square error between simulated and observed hydraulic heads of all observations ranged from 8.33 feet in 1919 to 47.65 feet in 1951, though only six root mean square error values are greater than 40 feet for the entire simulation period. Simulated streamflow generally is lower than measured streamflow for streams with streamflow less than 1,000 cubic feet per second, and greater than measured streamflow for streams with streamflow more than 1,000 cubic feet per second. Simulated streamflow is underpredicted for 18 observations and overpredicted for 10 observations in the model. These differences in streamflow illustrate the large uncertainty in model inputs such as predevelopment recharge, overland flow, pumpage (from stream and aquifer), precipitation, and observation weights.

The groundwater-flow budget indicates changes in flow into (inflows) and out of (outflows) the model area during the pregroundwater-irrigation period (pre-1870) to 2007. Total flow (sum of inflows or outflows) through the model ranged from about 600 million gallons per day prior to development to 18,197 million gallons per day near the end of the simulation. The pumpage from wells represent the largest outflow components with a net rate of 18,197 million gallons per day near the end of the model simulation in 2006. Groundwater outflows are offset primarily by inflow from aquifer storage and recharge.

Introduction

Fresh groundwater in the Mississippi embayment can be found in alternating formations of sand, silt, and clay. The uppermost of these formations is the Mississippi River Valley alluvial aquifer (alluvial aquifer), which can provide well yields of 300 to 2,000 gal/min. The alluvial aquifer exists at land surface and covers much of the embayment area within the Mississippi Alluvial Plain. One of the next most widely used aquifers is the middle Claiborne aquifer, which can provide well yields of 100 to 500 gal/min (up to 1,500 gal/min in the Memphis area). The middle Claiborne aquifer, in some areas, lies several hundred feet beneath land surface. Decades of pumping from the alluvial aquifer for irrigation and from the middle Claiborne aquifer for industry and public-water supply have affected groundwater levels throughout the northern Mississippi Embayment in Arkansas, Louisiana, Mississippi, and Tennessee. Since the Gulf Coast Regional Aquifer System Analysis (GCRASA) study was completed in 1985, groundwater withdrawals have increased ranging from 37 percent at Memphis, Tennessee (17th largest city in the United States), to 132 percent in the agricultural areas of Arkansas from 1985 to 2000. Groundwater withdrawals for agriculture have caused water-level declines in the alluvial aquifer in Arkansas of at least 40 feet in 40 years (Schrader, 2001) while withdrawals from the middle Claiborne aquifer in Arkansas have resulted in declines of more than 360 feet since the 1920's (Scheiderer and Freiwald, 2006). These declines have prompted concerns over water availability and quality for agriculture and industry.

The Mississippi Embayment Regional Aquifer Study (MERAS) was conducted with support from the Groundwater Resources Program of the U.S. Geological Survey (USGS) Office of Groundwater to assess groundwater availability within the Mississippi embayment (fig. 1). The primary tool used in the assessment of groundwater availability is the MERAS groundwater-flow model.

Purpose and Scope

The purpose of this report is to document the construction and calibration of the MERAS groundwater-flow model of the Mississippi embayment. The current purpose of the model is to assist in the estimation of available groundwater in the Mississippi embayment aquifer system. The model was constructed to benefit concurrent and future investigations involving groundwater-withdrawal scenarios, optimization, particle transport, and monitoring network analysis.

Previous Investigations

Previous investigations of groundwater flow in the Mississippi embayment are numerous. Some early examples were the 1906 investigation of the underground waters of northern Louisiana (Veach, 1906) and 1928 investigation of groundwater resources of Mississippi (Stephenson and others, 1928). In the 1980's, the USGS began the GCRASA. The GCRASA compiled data and simulated groundwater flow in three main parts: the Mississippi River Valley alluvial aquifer, the Mississippi embayment aquifer system, and the gulf coastal lowland aquifer system (U.S. Geological Survey, 2008a). Other reports documenting groundwater-flow simulations within the MERAS flow system include Reed (1972), Brahana and Mesko (1988), Fitzpatrick and others (1990), Mahon and Ludwig (1990), Sumner and Wasson (1990), Mahon and Poynter (1993), Ackerman (1996), Arthur and Taylor (1998), Hays and others (1998), Arthur (2001), Brahana and Broshears (2001), McKee and Clark (2003), Stanton and Clark (2003), and Reed (2003).

Methods of Analyses

The primary method used to analyze the groundwater-flow systems is through the use of a numerical model to simulate groundwater flow. The viability of the numerical model is tested by comparing transient, simulated hydraulic-head values and streamflows from the groundwater-flow model with measurements from wells and stream gages. Details of the numerical model are listed in the next section, followed by a description of the limitations and assumptions of the model.

Numerical Model

For the MERAS model, the modular finite-difference code, USGS MODFLOW-2005 (Harbaugh, 2005), was used to approximate the solution of the equations governing three-dimensional (3D) groundwater flow. Because MODFLOW-2005 was used as the model simulation code, an additional advantage is the ability to investigate local areas within MERAS using the Local Grid Refinement package of MODFLOW-2005 (Mehl and Hill, 2007). The preconditioned conjugate gradient solver (Hill, 1990) was used for the numerical solution technique. The groundwater-flow system is represented by a set of grid cells, within which the hydraulic properties are the same. Each cell has three finite-difference equations describing the flow through it, which can be solved for either steady-state or transient conditions to simulate water-level changes within the flow system resulting from pumping stress over discrete periods of time. The model simulates 137 years (1870–2007) of system response to stress by using 69 stress periods.

Study Area Description

The model area encompasses approximately 78,000 mi^2 in an area known as the Mississippi embayment, referred to hereafter as the embayment (fig. 1). The model area boundary crosses eight States and includes approximately 6,900 mi of simulated streams, 70,000 well locations, and 10 primary hydrogeologic units. These hydrogeologic units include two primary aquifers—the Mississippi River Valley alluvial aquifer and the Middle Claiborne aquifer (Hart and others, 2008). The model area lies within parts of three physiographic sections, West Gulf Coastal Plain, East Gulf Coastal Plain, and Mississippi Alluvial Plain sections of the Coastal Plain physiographic province (fig. 1).

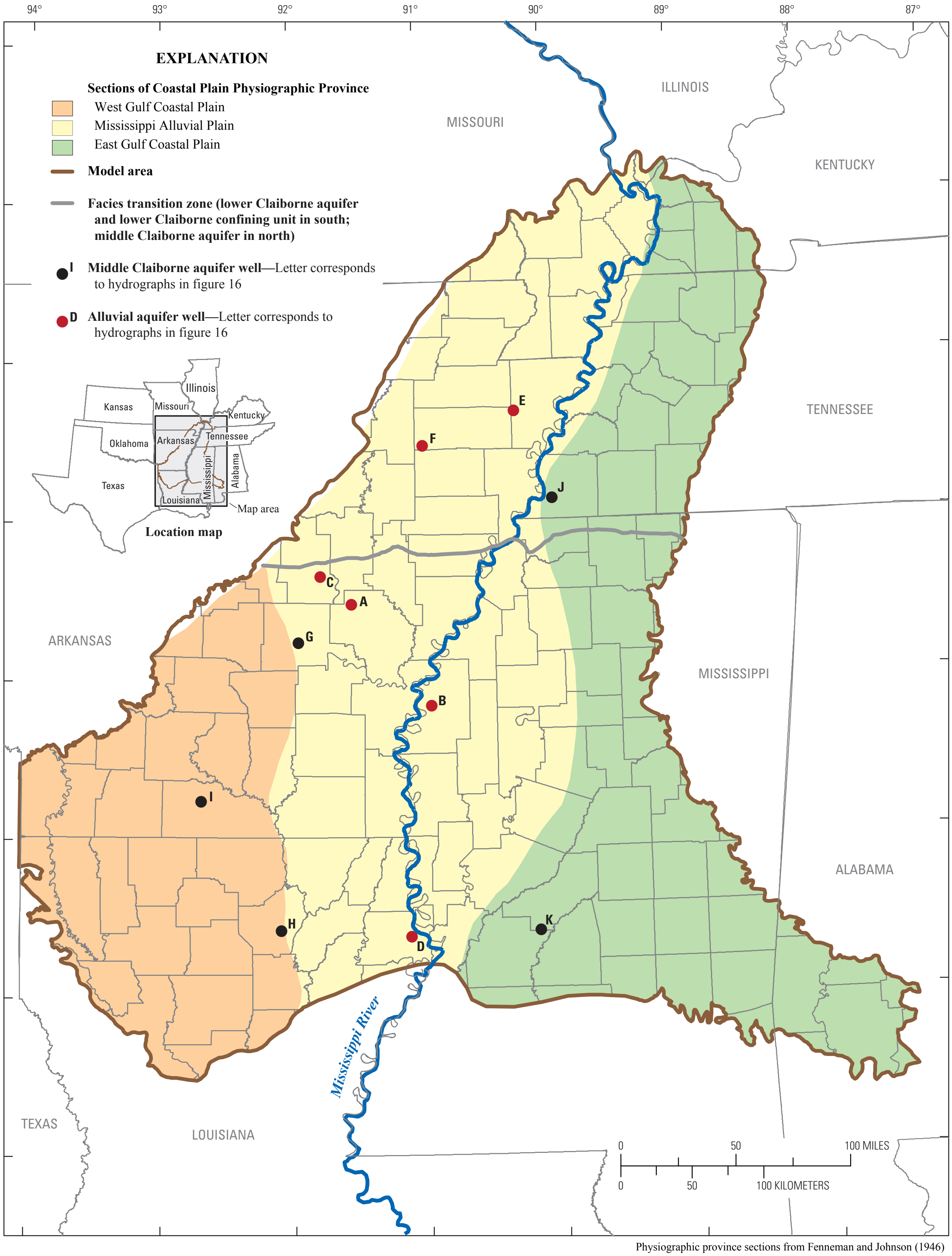

Figure 1. Location of the model area and Coastal Plain physiographic province sections.

Geologic History and Setting

The geologic history of the area began as downwarping and rifting as a result of the Ouachita orogeny occurring at the end of the Paleozoic era. Downwarping and downfaulting proceeded as a result of sediment loading during the Mesozoic era (Hosman, 1996). Many of the structural features and fault zones continued to develop into the Tertiary Period. Because of the continental extension, the embayment lies within a plunging syncline with the axis roughly paralleling the present-day Mississippi River and plunges south toward the Gulf of Mexico. Cyclic invasions by transgressing and regressing seas through the Cretaceous and Tertiary Periods created the synclinal shape resulting in older rock units cropping out on the periphery of the embayment (Arthur and Taylor, 1998). The units exposed within the model area are Cenozoic in age and consist primarily of Tertiary and Quaternary sands and gravels, silts, and clays.

Geologic Structural Features

The primary geologic structures in the model area consist of fault zones, basins, and uplifts, which were created in the late Paleozoic era and continued into the Tertiary Period. The New Madrid fault zone is located in the northern part of the model area and roughly parallels the axis of the embayment and is responsible for the downfaulting of the upper end of the syncline (Hosman, 1996). The Arkansas fault zone generally trends west-east across southern Arkansas and consists of multiple parallel normal faults and grabens (fig. 2). The Pickens-Gilbertown fault zone appears to be in alignment with the Arkansas fault zone and trends from west-central Mississippi southeastward across Mississippi and southwestern Alabama (Hosman and Weiss, 1991). There are three major structural highs within the model area. The Sabine uplift is located in eastern Texas and western Louisiana, the Monroe uplift located in southeastern Arkansas-northwestern Louisiana, and the Jackson dome in southern Mississippi. These uplifts control the alignment and position of axis of the embayment in the southern part of the model area.

Climate

The climate of the embayment is moderate with a mean annual precipitation of 48 inches in the north to 56 inches in the south. Precipitation is distributed fairly evenly throughout the year with the greatest amounts generally occurring in April and the least in October (Kleiss and others, 2000). The average temperature ranges from 58ºF in the north to 66ºF in the south (Cushing and others, 1970; National Oceanic and Atmospheric Administration, 2009). Much of the precipitation is lost through evapotranspiration and runoff to the streams in the model area (fig. 3).

Land Use

Land use in the embayment is primarily agricultural (fig. 4). Approximately 8 billion gallons per day of groundwater is pumped each year to meet irrigation requirements in Arkansas, Louisiana, and Mississippi (Hutson and others, 2004). Irrigated land accounts for approximately 45 percent of the model area, forested land is 38 percent, water and wetlands is 14 percent, and urban land is 3 percent of the total area (U.S. Geological Survey, 2008b). About 7 percent of the irrigated land is used for rice production, 22 percent for cotton, 35 percent for soybean, 5 percent for corn and wheat, 10 percent for pasture, and 2 percent for other crops or nonagricultural land (Stuart and others, 1996). The largest urban area includes the city of Memphis, Tennessee, which historically has relied heavily on groundwater pumpage to meet its municipal requirements (Parks and Lounsbury, 1976). Ninety-four percent of groundwater withdrawals in Arkansas were for irrigation, and surface irrigation is the predominant application method in Arkansas, Louisiana, Mississippi, and Missouri (Hutson and others, 2004).

Recharge

Recharge within the embayment is from infiltration of precipitation, stream losses, and infiltration of irrigation return flow. Though few (if any) studies have been conducted in the embayment to determine actual recharge rates, many model simulations have used recharge rates of 0.8 to 2.6 in/yr (Ackerman, 1996; Arthur, 2001; Mahon and Poynter, 1993; Stanton and Clark, 2003). Additional recharge may be introduced through adjacent or underlying aquifers, such as the McNairy-Nacatoch system or the Ozark aquifer system. Groundwater flow from the adjacent and underlying systems is considered negligible compared to the overall flow within the Mississippi embayment aquifer system and is ignored in this study.

Hydrogeologic Units

The major hydrogeologic units in the MERAS model include 10 units described by Hart and others (2008) (table 1). These include the Mississippi River Valley alluvial aquifer (hereafter referred to as the alluvial aquifer), the Vicksburg-Jackson confining unit, the upper Claiborne aquifer, the middle Claiborne confining unit, the middle Claiborne aquifer, the lower Claiborne confining unit, the lower Claiborne aquifer, the middle Wilcox aquifer, the lower Wilcox aquifer, and the Midway confining unit (table 1). As noted in Hart and others (2008), the lower Claiborne confining unit and the lower Claiborne aquifer undergo a facies transition and merge into the middle Claiborne aquifer in the northern part of the model area (fig. 1).

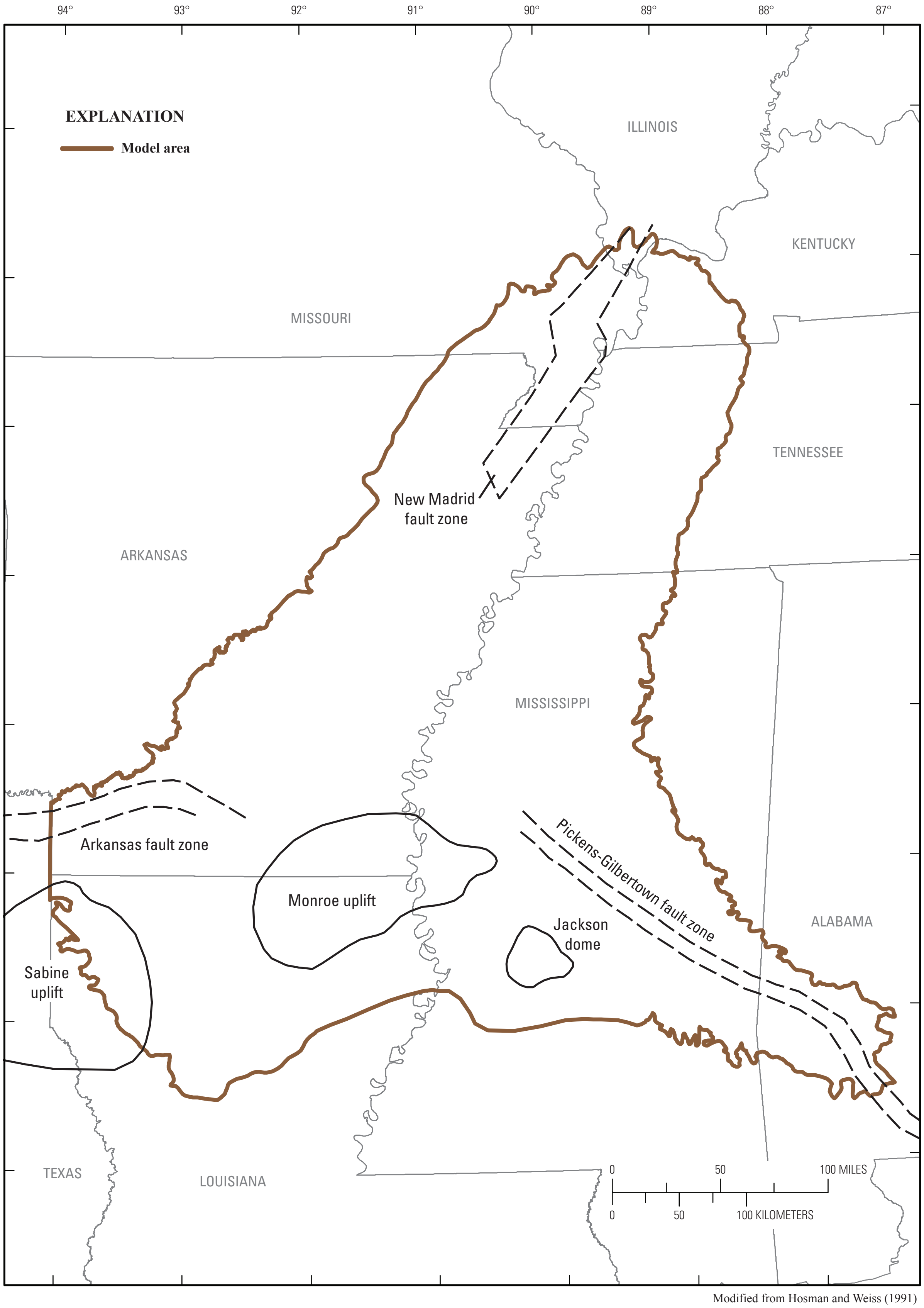

Figure 2. Primary geologic structural features.

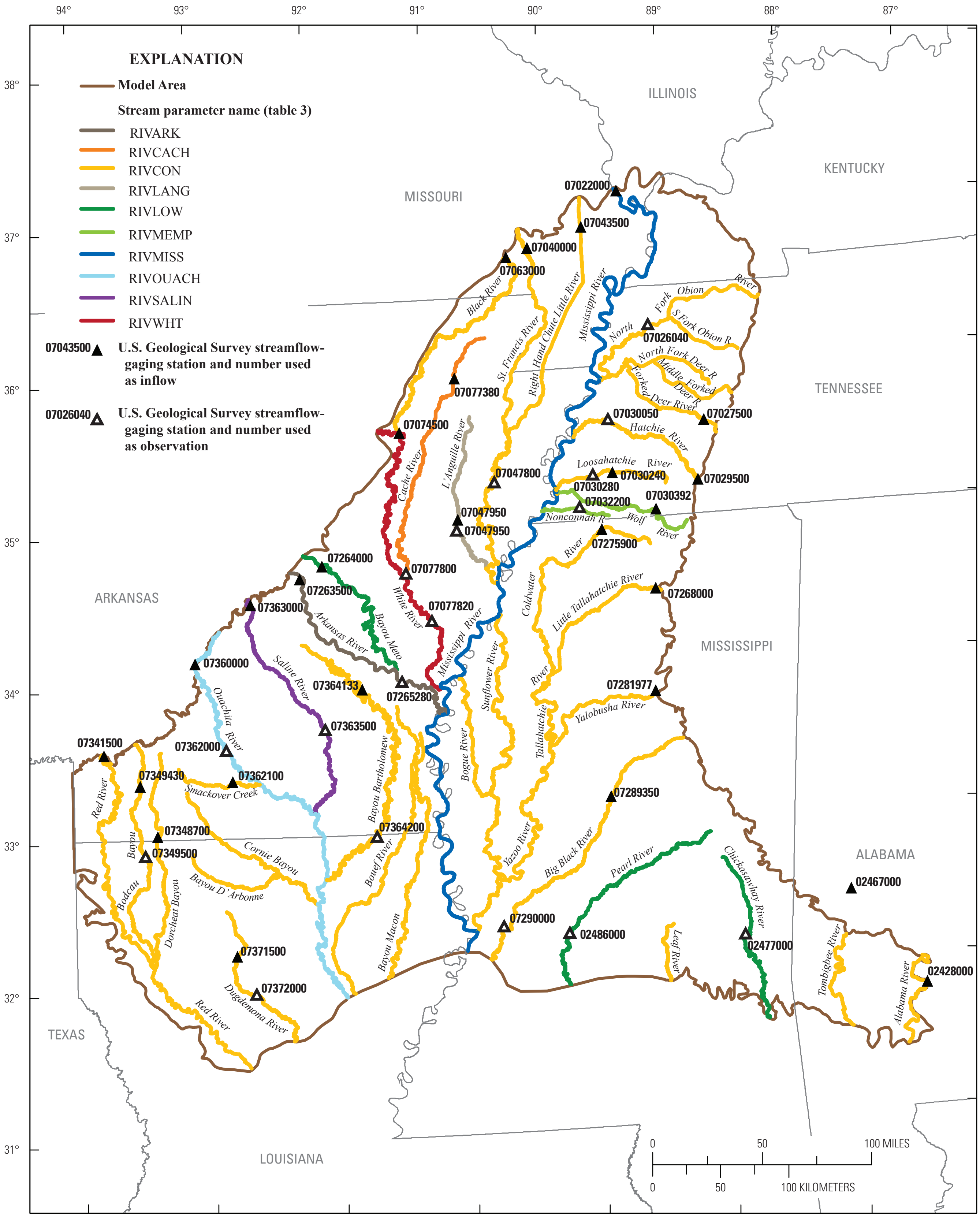

Figure 3. Streams simulated in the model area.

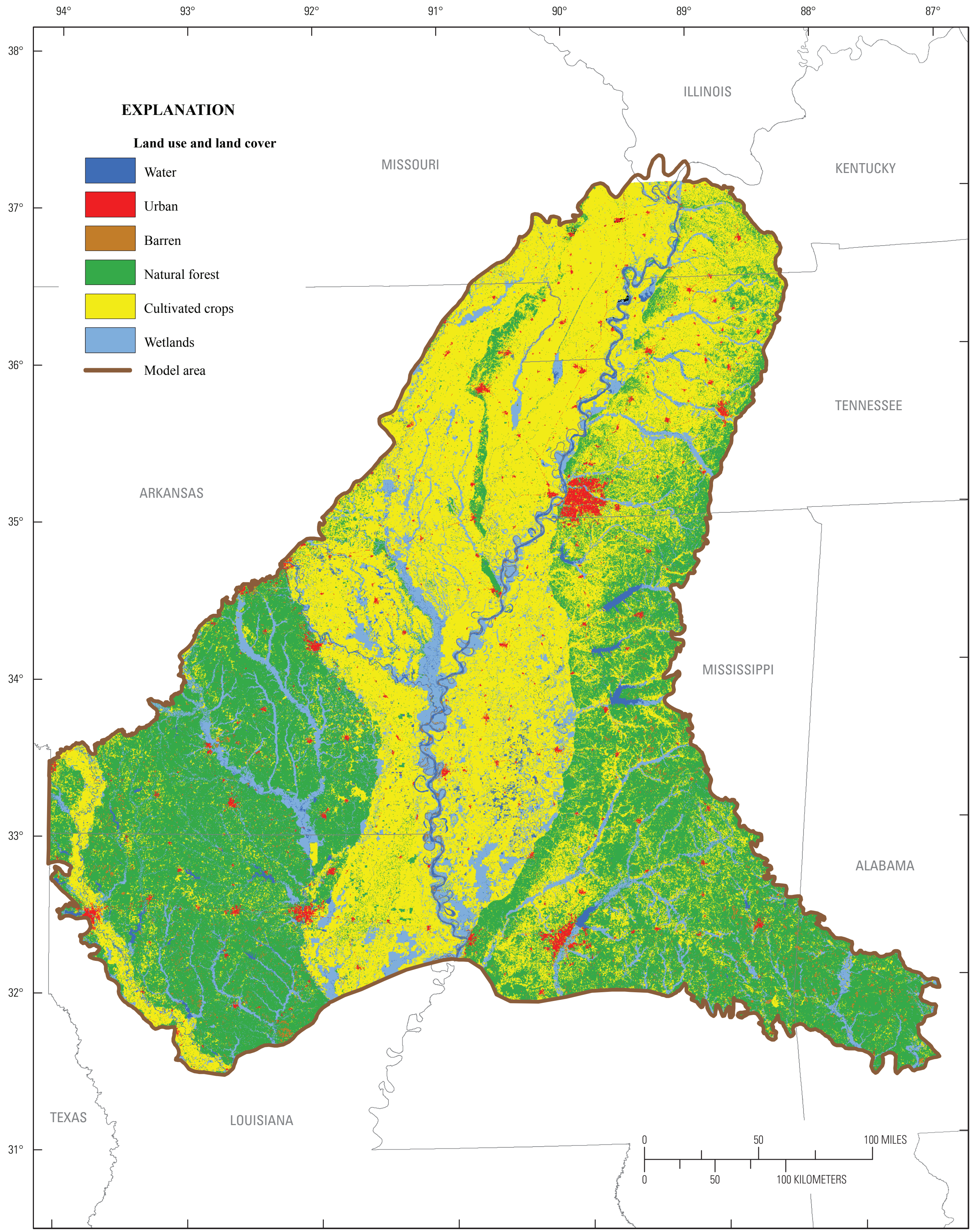

Figure 4. Typical land-use types within the Mississippi embayment.

Table 1. Hydrogeologic and geologic units and their correlation across the States within the Mississippi Embayment Regional Aquifer Study.

ERATHEM	SYSTEM	EPOCH	GROUP	LOUISIANA	ARKANSAS Southern	ARKANSAS Northeastern	MISSOURI	KENTUCKY	TENNESSEE	MISSISSIPPI	ALABAMA	Hydrogeologic units	Model layer number
CENOZOIC	QUATERNARY	HOLOCENE / PLEISTOCENE		Alluvium and terrace deposits				Alluvium and loess deposits		Alluvium, terrace, and loess deposits	Alluvium and terrace deposits	Mississippi River Valley alluvial aquifer	1
	TERTIARY	OLIGOCENE	Vicksburg	Vicksburg Formation	Not present in study area					Vicksburg Formation		Vicksburg-Jackson confining unit	2
		EOCENE	Jackson	Jackson Formation									
			Claiborne	Cockfield Formation							Gosport Sand	Upper Claiborne aquifer	3
				Cook Mountain Formation								Middle Claiborne confining unit	4
				Sparta Sand		Memphis Sand		Sparta Sand	Memphis Sand	Sparta Sand	Lisbon Formation	Middle Claiborne aquifer[4]	5–7
				Cane River Formation				Tallahatta Formation		Zilpha Clay Winona Sand Tallahatta Formation	Tallahatta Formation	Lower Claiborne confining unit[2]	8–9
				Carrizo Sand						Meridian Sand Member		Lower Claiborne aquifer[1]	10
		UPPER PALEOCENE	Wilcox	Dolet Hills Formation	Undifferentiated	Flour Island Formation		Wilcox Formation	Flour Island Formation	Undifferentiated	Hatchetigbee Formation	Middle Wilcox aquifer	11
						Fort Pillow Sand		No Wilcox deposits identified as being of Paleocene age	Fort Pillow Sand		Bashi Formation Tuscahoma Sand Nanafalia Formation	Lower Wilcox aquifer[3]	12–13
				Undifferentiated Naborton Formation		Old Breast-works Formation			Old Breast-works Formation				
			Mid-way	Midway Group								Midway confining unit	Base of model

[1] Lower Claiborne aquifer includes the upper Wilcox aquifer in some parts of Mississippi.
[2] Winona-Tallahatta Formation is included with lower Claiborne confining unit in Hart and others (2008).
[3] Old Breastworks confining unit is included with middle Wilcox aquifer in Hart and others (2008).
[4] El Dorado confining unit and El Dorado Sand are included with middle Claiborne aquifer.

Modified from Hosman and Weiss, 1991

Four additional minor hydrogeologic units not described by Hart and others (2008) consist of the El Dorado confining unit, the El Dorado Sand, the Winona-Tallahatta aquifer, and the Old Breastworks confining unit, which will be more fully discussed here and shown in figures 5–7. These minor hydrogeologic units are included because of extensive use in local areas in southern Arkansas, northern Louisiana, and Mississippi. The El Dorado Sand is the lower part of the middle Claiborne aquifer in south-central Arkansas and north-central Louisiana. The El Dorado Sand is separated from the upper part of the middle Claiborne aquifer by a locally extensive confining unit termed the El Dorado confining unit in this report, which is as much as 155 ft thick (fig. 5). The Winona-Tallahatta aquifer is the lower part of the lower Claiborne confining unit throughout much of Mississippi and includes the Tallahatta Formation and the Winona Sand (fig. 6). The Tallahatta Formation consists of a greenish-gray, siliceous, sandy claystone, and the Winona Sand consists of glauconitic, fossiliferous, medium- to coarse-grained sandstone with a combined thickness up to 800 ft (Mancini and Tew, 1994; Spiers, 1977). Additionally, throughout most of Arkansas and Louisiana, the middle and lower Wilcox aquifers are undifferentiated; however, in areas of Tennessee and Mississippi, the lower Wilcox aquifer (Hart and others 2008, figs. 20 and 21) may be separated into two units, the lower Wilcox aquifer and the Old Breastworks confining unit (fig. 7). The lower Wilcox aquifer consists of the lower part of the Wilcox Formation and is the lowermost aquifer in Tertiary rocks within the Embayment (Lloyd and Lyke, 1995). This aquifer includes the Old Breastworks Formation in Missouri and Tennessee that consists of clay, silt, and lignite (Warwick and others, 1997).

Groundwater-Flow Model Construction

The following sections describe the spatial and temporal discretization, hydrologic boundaries, initial conditions, and hydraulic properties formulated for the MERAS model. In some instances, such as the temporal discretization, information from previous investigations was used as a basis (McKee and Clark, 2003; Stanton and Clark, 2003; Brahana and Broshears, 2001).

Spatial Discretization and Layering

The finite-difference grid is oriented north-south and consists of 414 rows, 397 columns, and 13 layers. Though a single model layer of the rectangular finite-difference grid contains over 164,000 cells, many cells are inactive because they fall outside of the active model area. Cells are a uniform 1 mi^2 (1 mile on a side) with varying thickness by cell and by layer. The northwestern corner of the grid is located at 37º 27’ 28” north latitude and 93º 57’ 19” west longitude. Vertically, the hydrogeologic units are discretized into 13 model layers (table 1). Layer 1 (fig. 8) represents primarily the alluvial aquifer where present, but also represents loess in Tennessee and Mississippi or other surficial units such as Pleistocene deposits on Crowleys Ridge or other sediments overlying the Vicksburg-Jackson confining unit in Louisiana, southern Mississippi, and Alabama. Layer 2 represents the Vicksburg-Jackson confining unit where present. Where the Vicksburg-Jackson confining unit is not present, the properties of layer 2 are modified to match that of the overlying surficial unit, such as the alluvial aquifer. The thickness of layer 2 also is modified to represent a partial thickness of the surficial unit, which in turn modifies the thickness of layer 1 to represent the remaining thickness of the surficial unit. The same technique of applying hydrologic properties and partial thickness of the surficial unit to layers that represent areas where formations pinch out or subcrop was applied to each layer below layer 1; therefore, the top layer of the model could be represented by characteristics of a single layer or combination of layers (1–13), depending on location. This was done to accommodate the requirement of continuous model layers throughout the finite-difference model grid. Layer 3 represents the upper Claiborne aquifer, where present, and the surficial unit beyond the upper Claiborne aquifer extent. Layer 4 represents the middle Claiborne confining unit where present, and the surficial unit beyond the middle Claiborne confining unit extent. The middle Claiborne aquifer begins in layer 5 and varies from 3 to 6 layers depending on spatial location. South of the facies transition zone (fig. 1), the middle Claiborne aquifer occupies layers 5 through 7, with a portion of layer 6 representing the El Dorado confining unit and layer 7 representing the El Dorado Sand. Layer 8 represents the lower Claiborne confining unit, layer 9 represents the Winona-Tallahata, and layer 10 represents the lower Claiborne aquifer. North of the transition zone, the middle Claiborne aquifer occupies layers 5 through 10. Layer 11 represents the middle Wilcox aquifer, and layer 12 represents the lower Wilcox aquifer. Layer 13 also represents the lower Wilcox aquifer or the Old Breastworks confining unit where present (fig. 8)

Temporal Discretization

The simulation period extends from January 1, 1870, to April 1, 2007, for a total of 137 years and 69 stress periods (table 2). The first stress period is simulated as steady state to represent predevelopment conditions. Stress periods 2 through 27 are variable length to reflect embayment-wide changes in groundwater withdrawals. These stress periods also mimic the temporal discretization used by McKee and Clark (2003), Stanton and Clark (2003), Reed (2003), Mahon and Poynter (1993), and Brahana and Broshears (2001). Stress periods 28 (beginning in 1986) through 69 are each 6 months in length to reflect spring–summer (April–September) and fall–winter (October–March) conditions related to irrigation.

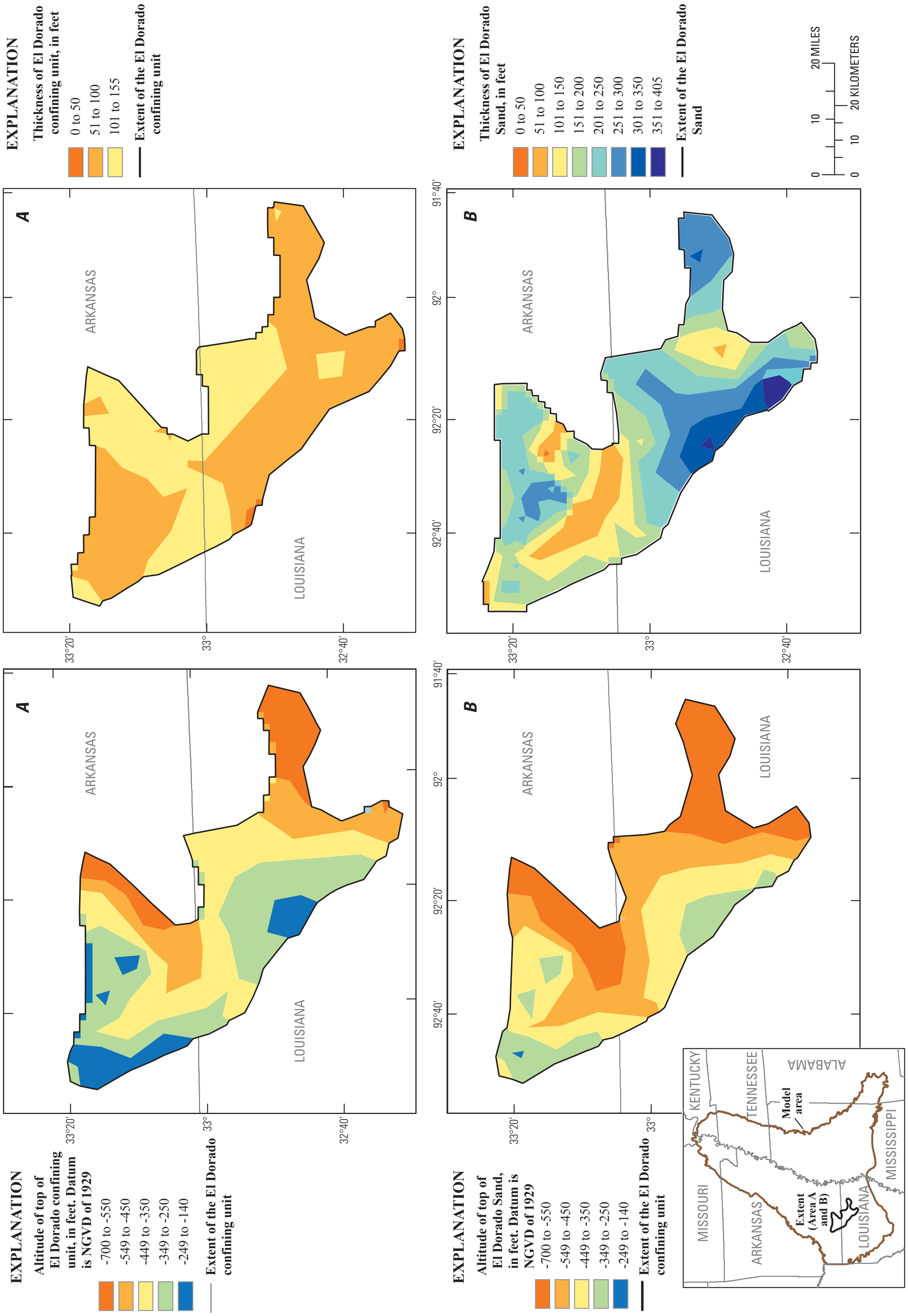

Figure 5. Top and thickness of (A) the El Dorado confining unit and (B) El Dorado Sand.

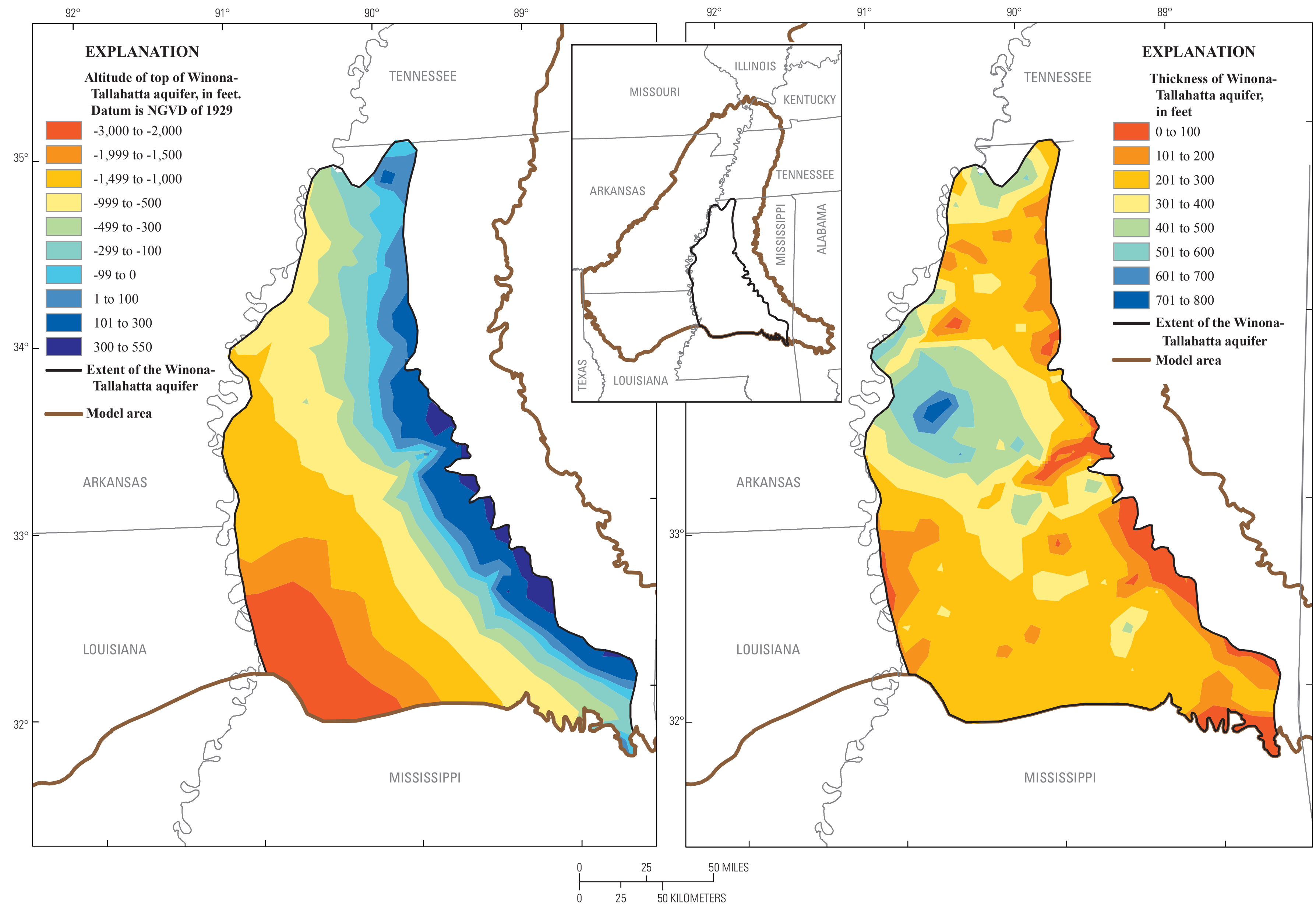

Figure 6. Top and thickness of the Winona-Tallahatta aquifer.

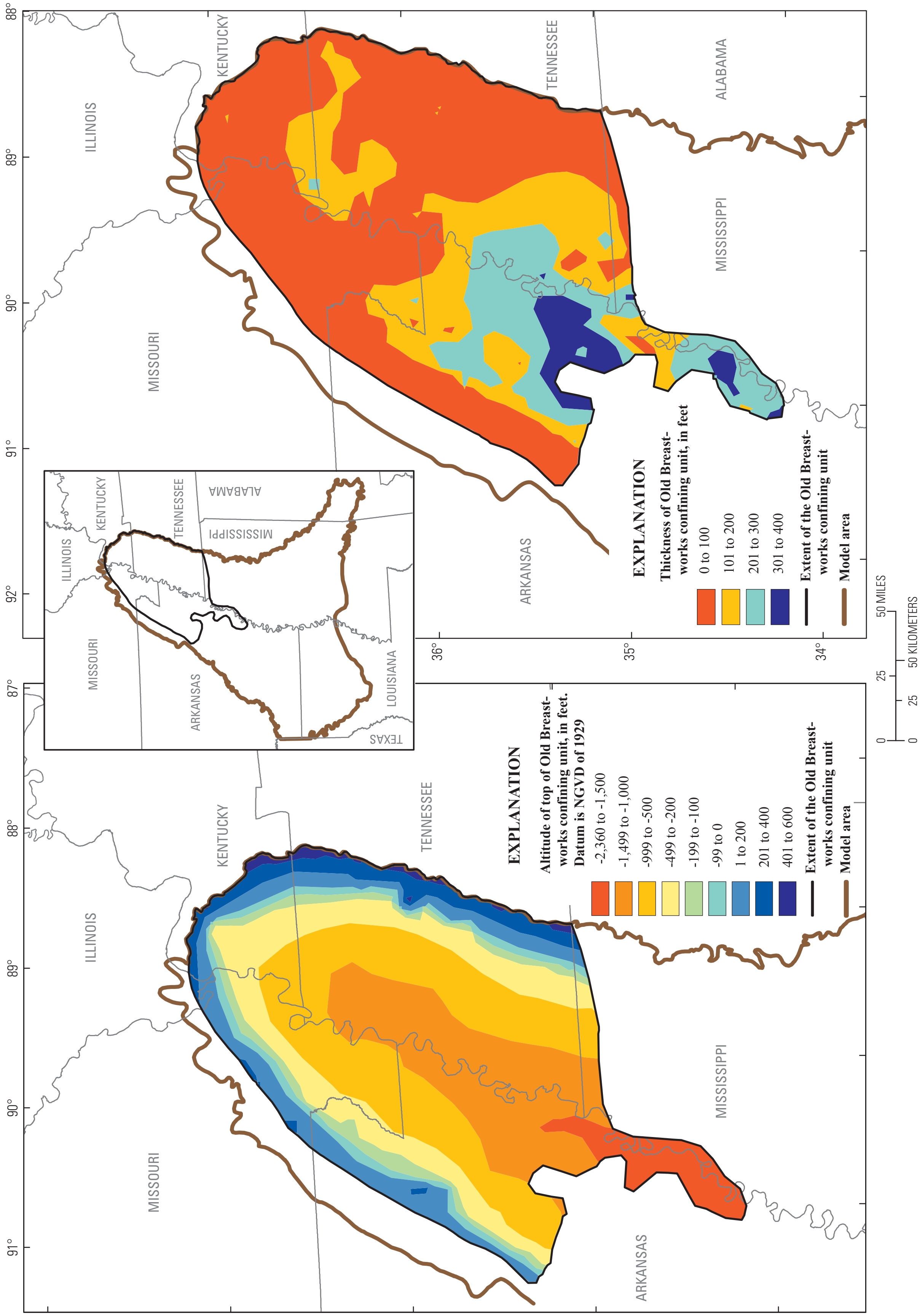

Figure 7. Top and thickness of the Old Breastworks confining unit.

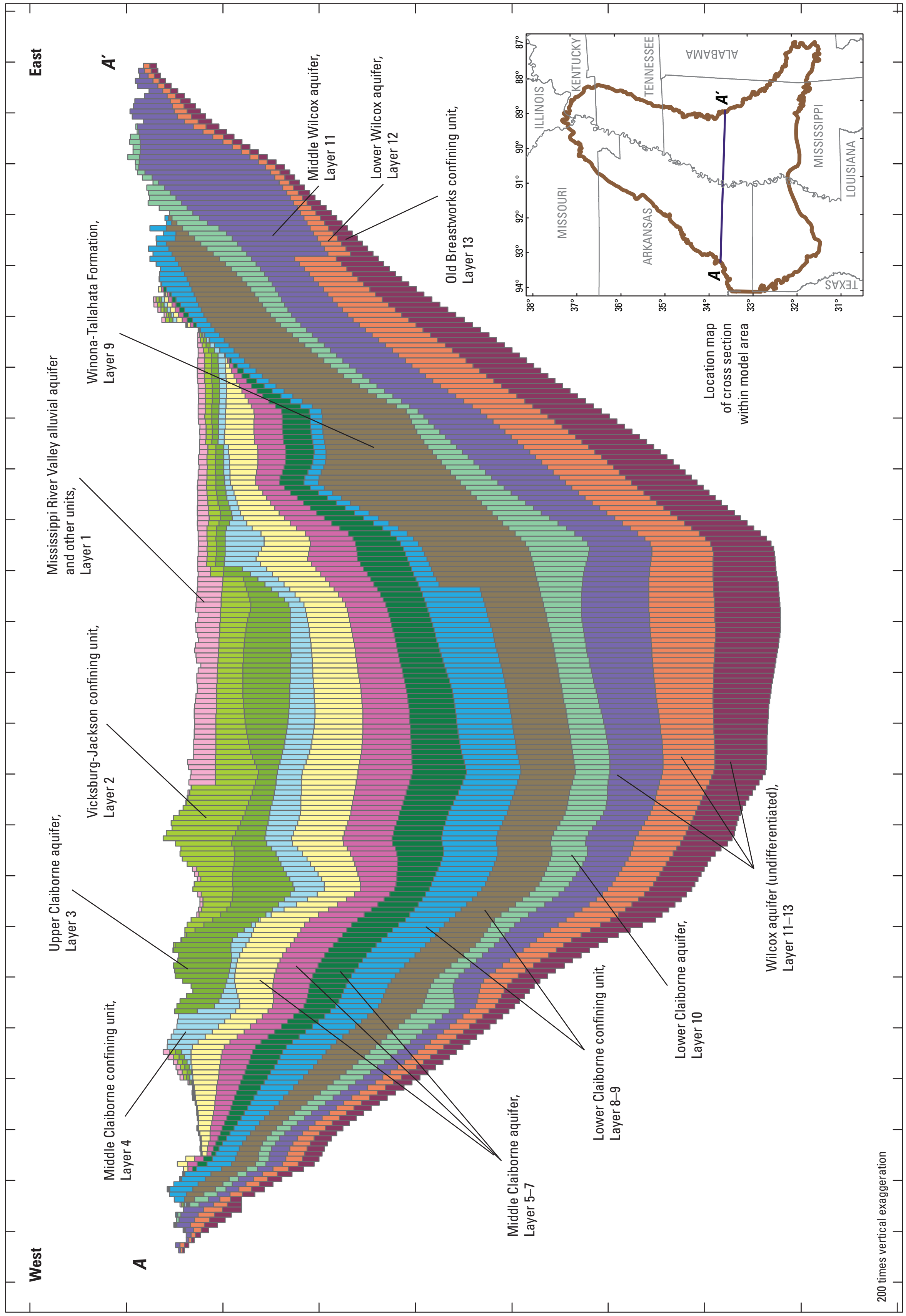

Figure 8. Cross section of model grid from west to east through row 258. Cross-section location is shown on inset map.

Table 2. Model simulation stress periods.

Beginning of stress period	Season	Stress period number	Days in stress period	Years in stress period	Cumulative year
01/01/1870	steady state	1	0	0	0
01/01/1870	multiyear	2	10,227	28.0	28.0
01/01/1898	multiyear	3	730	2.0	30.0
01/01/1900	multiyear	4	7,305	20.0	50.0
01/01/1920	multiyear	5	1,827	5.0	55.0
01/01/1925	multiyear	6	1,826	5.0	60.0
01/01/1930	full year	7	365	1.0	61.0
01/01/1931	multiyear	8	1,461	4.0	65.0
01/01/1935	multiyear	9	1,096	3.0	68.0
01/01/1938	multiyear	10	1,826	5.0	73.0
01/01/1943	full year	11	365	1.0	74.0
01/01/1944	multiyear	12	1,461	4.0	78.0
01/01/1948	multiyear	13	731	2.0	80.0
01/01/1950	multiyear	14	730	2.0	82.0
01/01/1952	multiyear	15	1,096	3.0	85.0
01/01/1955	multiyear	16	731	2.0	87.0
01/01/1957	full year	17	365	1.0	88.0
01/01/1958	multiyear	18	1,826	5.0	93.0
01/01/1963	multiyear	19	731	2.0	95.0
01/01/1965	multiyear	20	1,095	3.0	98.0
01/01/1968	multiyear	21	731	2.0	100.0
01/01/1970	full year	22	365	1.0	101.0
01/01/1971	multiyear	23	731	2.0	103.0
01/01/1973	multiyear	24	1,826	5.0	108.0
01/01/1978	multiyear	25	1,096	3.0	111.0
01/01/1981	multiyear	26	730	2.0	113.0
01/01/1983	multiyear	27	1,186	3.2	116.2
04/01/1986	spring-summer	28	183	0.5	116.7
10/01/1986	fall-winter	29	182	0.5	117.2
04/01/1987	spring-summer	30	183	0.5	117.7
10/01/1987	fall-winter	31	183	0.5	118.2
04/01/1988	spring-summer	32	183	0.5	118.7
10/01/1988	fall-winter	33	182	0.5	119.2
04/01/1989	spring-summer	34	183	0.5	119.7
10/01/1989	fall-winter	35	182	0.5	120.2
04/01/1990	spring-summer	36	183	0.5	120.7
10/01/1990	fall-winter	37	182	0.5	121.2
04/01/1991	spring-summer	38	183	0.5	121.7
10/01/1991	fall-winter	39	183	0.5	122.2
04/01/1992	spring-summer	40	183	0.5	122.7

Table 2. Model simulation stress periods.—Continued

Beginning of stress period	Season	Stress period number	Days in stress period	Years in stress period	Cumulative year
10/01/1992	fall-winter	41	182	0.5	123.2
04/01/1993	spring-summer	42	183	0.5	123.7
10/01/1993	fall-winter	43	182	0.5	124.2
04/01/1994	spring-summer	44	183	0.5	124.7
10/01/1994	fall-winter	45	182	0.5	125.2
04/01/1995	spring-summer	46	183	0.5	125.7
10/01/1995	fall-winter	47	183	0.5	126.2
04/01/1996	spring-summer	48	183	0.5	126.7
10/01/1996	fall-winter	49	182	0.5	127.2
04/01/1997	spring-summer	50	183	0.5	127.7
10/01/1997	fall-winter	51	182	0.5	128.2
04/01/1998	spring-summer	52	183	0.5	128.7
10/01/1998	fall-winter	53	182	0.5	129.2
04/01/1999	spring-summer	54	183	0.5	129.7
10/01/1999	fall-winter	55	183	0.5	130.2
04/01/2000	spring-summer	56	183	0.5	130.7
10/01/2000	fall-winter	57	182	0.5	131.2
04/01/2001	spring-summer	58	183	0.5	131.7
10/01/2001	fall-winter	59	182	0.5	132.2
04/01/2002	spring-summer	60	183	0.5	132.7
10/01/2002	fall-winter	61	182	0.5	133.2
04/01/2003	spring-summer	62	183	0.5	133.7
10/01/2003	fall-winter	63	183	0.5	134.2
04/01/2004	spring-summer	64	183	0.5	134.7
10/01/2004	fall-winter	65	182	0.5	135.2
04/01/2005	spring-summer	66	183	0.5	135.7
10/01/2005	fall-winter	67	182	0.5	136.2
04/01/2006	spring-summer	68	183	0.5	136.7
10/01/2006	fall-winter	69	182	0.5	137.2
04/01/2007	spring-summer		END DATE		

Hydrologic Boundaries

Hydrologic boundaries determine the locations and quantities of simulated flow into and out of the model; therefore, the selection of appropriate boundaries for the model is a major concern in a modeling effort. The selection of model boundaries for the aquifers in the current model is based on a conceptual interpretation of the flow system developed using information reported by Payne (1968), Hosman (1988), and Petersen and others (1985). Boundaries require the definition of model input variables, also called parameters.

Areal Recharge

Areal recharge is applied throughout the MERAS model area using the MODFLOW-2005 Recharge Package (Harbaugh, 2005). While many factors such as type and intensity of precipitation, land use, vegetation type, soil moisture, and slope determine recharge, the concept of parsimony (start simple, build complexity as needed) was used to develop a method of applying recharge in the MERAS model. This method consists of estimating recharge rates as a fraction (ranging from 1.25×10^{-4} to 7.06×10^{-2}) of precipitation based on typical literature values and soil type or geology and modified locally or regionally during calibration of the model into zones. Early attempts to use a land-use classification for recharge zones did not yield acceptable results. Therefore, 19 zones, based on soil type, geomorphology, or surficial geology, were assigned in the MERAS model (fig. 9). Alluvial recharge zones were classified based on soil type and geomorphology, and all other units' recharge zones were classified based on geology. The zone numbers on figure 9 are used for recharge distribution and hydraulic property parameters for surficial units defined later in the “Hydraulic Properties” section. Zone numbers for the alluvial aquifer are numbered 101 through 108. Recharge zone numbers of other units are generally sequential from the youngest to the oldest. Exceptions are zone number 61 for the eastern outcrop of the middle Claiborne aquifer and zone 10 representing surficial deposits other than the loess in Tennessee and Mississippi. Annual precipitation grids were downloaded from the Parameter-elevation Regressions on Independent Slopes Model (PRISM) group for the period of 1895 to 2005 (Daly and others, 2000; PRISM Group, 2006). Annual precipitation grids were averaged together for stress periods that encompass multiple years. Precipitation amounts were divided evenly for stress periods representing 6-month periods of spring–summer and fall–winter. Each averaged or split precipitation grid then was multiplied by the recharge fraction assigned to each recharge zone. Recharge amounts to each respective recharge zone were a percentage of precipitation from the PRISM grids and, therefore, varied for each stress period. The precipitation percentage was determined from previous model simulations and adjustments were made during model calibration. While this method of recharge estimation neglects temporal increases in pumpage, the model fit described later in the “Model Fit and Model Error” section is considered reasonable given the scale and discretization of the model area, and reflects the concept of parsimony used during model construction.

Groundwater Pumpage

Pumpage from irrigation, municipal, and industrial wells is simulated using the Multi-Node Well (MNW) Package (Halford and Hanson, 2002). The MNW Package allows simulation of flow in wells that are completed in multiple aquifers or model layers. Flow through the well bore of a MNW is distributed dynamically based on transmissivity and hydraulic head differences between the respective layers. The MNW Package also allows the user to specify drawdown constraints for each well simulated. Flow into or out of the well bore can be affected by the contrast in transmissivity between the formation and the disrupted radius around the well bore, noted by a Skin coefficient. For all withdrawal wells, a final, calibrated Skin value of 4 was used, which results in a contrast of the transmissivity of the formation (T) to transmissivity of the disrupted radius (Tskin) value of 6.77 (T/Tskin). The contrast of T/Tskin allows variation in flow into and out of hydrogeologic units based on the different hydraulic properties of each unit. The final, calibrated Skin values are comparable to the values used by Clark and others (2008) and Hanson and others (2004), in which the Skin value was increased from 5 to 15 during calibration.

Pumpage from each MNW was input from site-specific data, 5-year water-use reports (Hall, 1989; Johnson, 1994; Sholar and Wood, 1995; Mooty and Richardson, 1998; Holland, 1999; Sargent, 2007), and trend analysis. Site-specific data were used to estimate the amount of pumpage per well for each aquifer to calculate a ratio of the number of wells to total pumpage. The ratio then could be used to estimate the number of wells required to pump a given amount of water. Site-specific pumpage information was averaged by stress period for each well and used as input to the model. Average annual pumpage from each aquifer and within each county contained by the model area was compiled from 5-year water-use reports generally from the period 1960–2005 or 1985–2005. For each county and aquifer, the number of wells used in a given stress period was estimated using the ratio of the number of wells to total pumpage amount. For most aquifers, the placement of wells within each county was selected from a list of known well locations in the USGS National Water Information System (NWIS) (http://waterdata.usgs.gov/nwis). The 5-year pumpage amount for each county and aquifer was distributed to the well locations for the given stress period. Thus, the number of wells increased through the simulation time as pumpage increased (fig. 10).

For wells in the middle Claiborne aquifer and the alluvial aquifer within Arkansas, the fraction of total pumpage from 2005 by county was calculated and assigned to the well. The 5-year pumpage amount then was partitioned to each well based on the pumpage fraction rather than evenly distributed to each well. This produced the desired effect of higher concentrations of pumpage in intensely agricultural or populated areas based on 2005 information, and also accounted for the jump in number of wells from stress period 17 to 18 (fig. 10). The trend analysis was based on a best fit exponential trend of water-use applications for the site-specific period of record, if available, and 5-year published data for each aquifer simulated by the model. The best fit exponential trend allows an estimation of pumpage for a given aquifer and stress period prior to 5-year water-use reporting. After the estimation of pumpage, well selection and pumpage distribution were assigned using a similar method described above for the 5-year pumpage amounts.

Streams

There are 43 streams included within the MERAS model (fig. 3). Each stream in the model area was represented using the Streamflow-Routing (SFR) package of MODFLOW (Prudic and others, 2004). The use of the SFR Package is considered an improvement over past simulations of the embayment because it “…uses the continuity equation to route surface-water flow through one or more simulated rivers, streams, canals, or ditches” (Prudic and others, 2004), rather than using a specified head boundary or river stage. The initial criterion

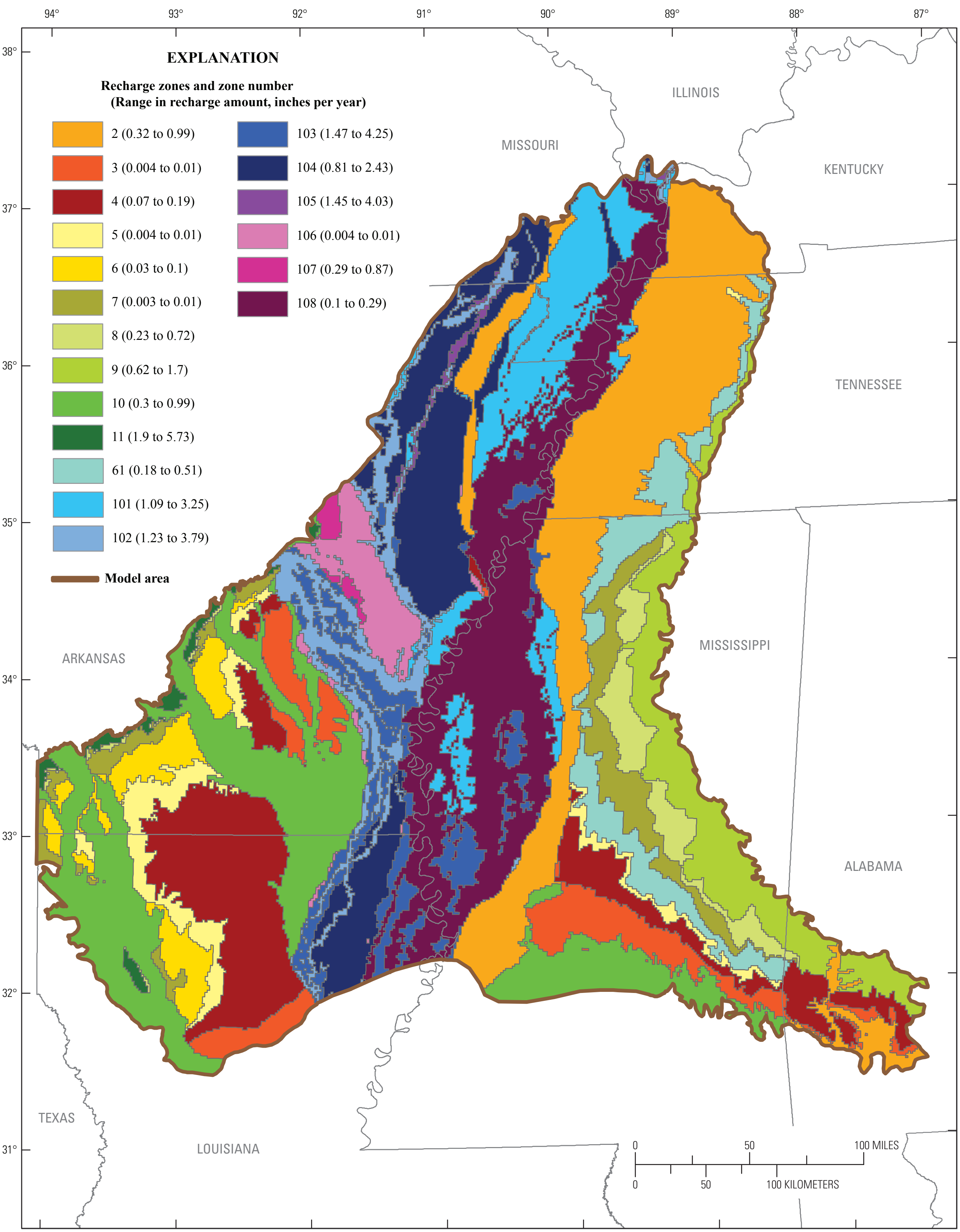

Figure 9. Zones used for both recharge and hydraulic property parameters in the model area.

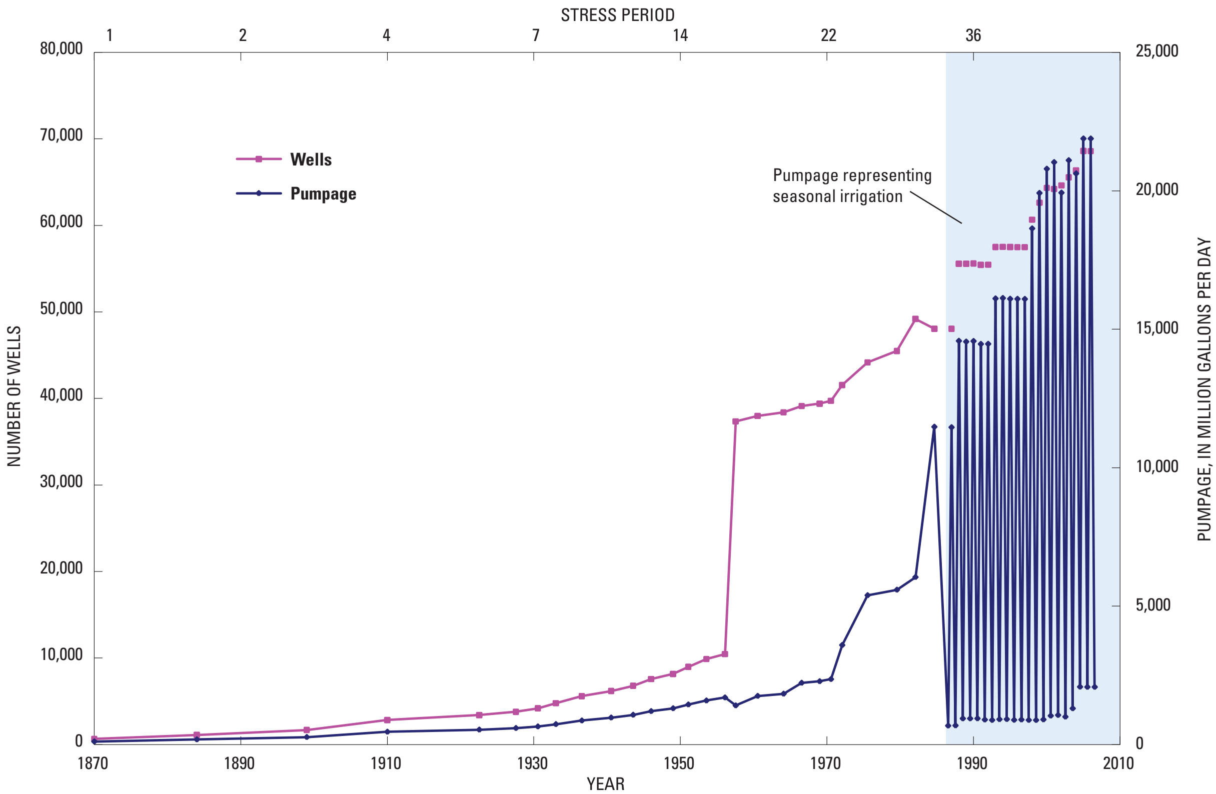

Figure 10. Number of wells and amount of pumpage in model simulation.

for the inclusion of streams in the model was a mean annual flow of 1,000 ft^3/s or more. Other streams were added based on inclusion by previous model studies that demonstrated the interaction of the streams with surficial aquifers (Reed, 2003; McKee and Clark, 2003; Stanton and Clark, 2003). Streams also were added in the Memphis, Tennessee, area where known interactions occur between the streams and the Memphis aquifer (Nyman, 1965). Streambed hydraulic conductivities were chosen as the stream parameters to be adjusted during simulations of the MERAS model. A streambed thickness of 10 ft was used, and an approximate stream width was measured from 1:24,000 topographic maps at the midpoint of the stream length for each simulated stream in the model area. The SFR package requires stream inflow at the model boundary or at the headwaters of the stream for each stress period of the simulation. Of the 43 streams simulated, 20 streams were assigned zero inflow because the headwaters started within the model area or near the model boundary; 12 streams with gages within 10 mi of the model boundary used the mean annual streamflow at the gage for model inflow (U.S. Geological Survey, 2008c); and inflows for 4 streams with gages that were further than 10 mi from the model boundary were corrected for the drainage area not gaged. For example, given a gage 15 mi upstream from the model boundary, the streamflow for the additional 15 mi of stream was calculated based on the drainage area from the model boundary to the upstream gage and the ratio of drainage area to streamflow at the gage. This streamflow then was added to the mean annual streamflow at the gage to approximate the streamflow at the model boundary.

The SFR package also allows input for overland runoff to streams. Runoff to simulated streams for each stress period was estimated from the 30-year average runoff (Williamson and others, 1990). The average runoff was divided by average precipitation for the same time period (1951-1980) to obtain a fraction for the average amount of precipitation that becomes runoff. The fraction of precipitation then could be multiplied by the precipitation for a given stress period to produce an estimate of runoff for each model cell and each stress period. The runoff estimates then were distributed to simulated streams by drainage basin.

No-Flow Boundaries

The perimeter of the model area and the base of the flow system are represented as no-flow boundaries. The perimeter of the model area represents an area where the hydrogeologic units do not exist or where flow into or out of the model area is assumed to be neglibible. The base of the flow system coincides with the top of the Midway confining unit. This unit is composed of thick marine clays; the effect of the thick marine clays allows for a small amount of flow leaking up through the Midway confining unit, which is considered to be minor compared to the volume of flow in the aquifers above it, and, therefore, chosen as the base of the model (Williamson and others, 1990). Brahana and Mesko (1988) delineated the Midway confining unit as a very low leakance unit except in the extreme northwestern part of the embayment where the Midway confining unit is absent and the alluvial aquifer directly overlies the Upper Cretaceous McNairy-Nacotoch aquifer.

Saltwater Interface

An increase in dissolved solids concentrations in milligrams per liter has been documented by Pettijohn and others (1988) in an area that extends from western Mississippi into Louisiana and Arkansas. Dissolved solids concentrations increase approximately 1,000 mg/L or more in a downdip direction over a distance of several miles (Pettijohn and others, 1988). Within the model area there are two large salt basins containing salt domes located in northern Louisiana and eastern Louisiana-central Mississippi. Salt domes have been noted to penetrate up through the base of the upper Claiborne aquifer (Beckman and Williamson, 1990). For the model simulation presented in this report, it is assumed that density of water remains constant with time. The downgradient limit of each model layer is a no-flow boundary, which approximates the extent of water with less than 10,000 mg/L dissolved solids. The downgradient limit of portions of layers 5 through 13 terminate north of the 10,000 mg/L dissolved solids line in an area that approximates the freshwater boundary delineated by Payne (1968). The assumption of a no-flow boundary at the freshwater-saltwater interface and constant density of water may not be entirely valid, but may be justified because most pumpage in each layer tends to be upgradient from the interface.

Initial Conditions

There are no known predevelopment potentiometric surfaces for the portion of the alluvial aquifer simulated by the MERAS model. Williams and Williamson (1989) calculated an average depth to water of 25.7 ft using the first nonpumping, pre-1960 hydraulic-head value in 6,825 wells less than 150 ft deep. Before the development of the groundwater resource in the early 1900s, hydraulic head in the alluvial aquifer is presumed to generally follow land surface and slope toward major rivers (Ackerman, 1989). Predevelopment potentiometric surfaces for the middle Claiborne aquifer also are scarce. Reed (1972) presents a potentiometric surface of the middle Claiborne for 1886 “based on measurements made prior to extensive development.”

Initial conditions are simulated using a steady-state stress period (representing conditions prior to January 1, 1870) at the beginning of the simulation. Stream inflows for this steady-state stress period were the mean annual flow average of the first 10 years of available flow data for each stream. While the potential exists that the first 10 years of available flow data could be affected by human actions, in many cases, data for streamflow began prior to the 1950’s. The average of the first 10 years of streamflow is thought to approximate early streamflow conditions in a way that is acceptable to create initial conditions from which to base the transient simulation. Recharge for the first stress period is the same as that used in the second stress period. There is no groundwater pumpage specified in the first stress period because it is designed to represent predevelopment conditions before pumping began.

Hydraulic Properties

In many groundwater-flow models, grid cells assumed to have similar hydraulic properties are grouped together as a zone and assigned a parameter value that can be adjusted during the calibration process (Hill and others, 2000). The MERAS model uses a total of 104 hydraulic parameters (table 3). These parameters include hydraulic properties of horizontal hydraulic conductivity, specific yield, specific storage, and vertical anisotropy. Parameter values of the aquifers and confining units also are affected by the amount (percent) of coarse (sand) or fine (clay) material within the unit. A discussion of the method used to assign the percent of sand within each unit is presented in the “Sand Percentage” section. In addition, selected faults present in some areas (Arkansas fault zone, Pickens-Gilbertown fault zone, fig. 2) are represented in the model, and the properties associated with faults were specified.

Hydraulic Conductivity

Horizontal hydraulic-conductivity parameters generally consist of a single zone for each aquifer and confining unit. The exceptions are the alluvial aquifer (or equivalent surficial unit), middle Claiborne confining unit, middle Claiborne aquifer, and Wilcox Group. Zone numbers generally coincide with model layers in multiples of 10. For example, layer 2 is 20, layer 3 is 30, layer 4 is 40, and so on. Using this design, 10 zone numbers per layer are available for use to define different areas within each layer. For example, there are four zones within layer 5; 50, 51, 52, and 53. Zone numbers may extend through multiple layers once they are defined for a hydrogeologic unit. Zone numbers for the alluvial aquifer are the same values used for recharge zones of the alluvial aquifer (fig. 9). Parameter zones for the alluvial aquifer are based on grouped classifications of geomorphology (Saucier, 1994) to create eight zones (zone 101 to 108, fig. 9). Equivalent surficial units are represented by two additional zones: one zone for the surficial unit covering Crowleys Ridge and loess in Tennessee and Mississippi or other equivalent units in the eastern half of the model area (zone 2, fig. 9), and one zone for other Quaternary age deposits in southeastern Arkansas (zone 10, fig. 9). There are three parameter zones to represent the middle Claiborne confining unit: one zone represents the majority of the confining unit (zone 40, fig. 11), a second zone represents areas where the middle Claiborne confining unit is absent in western Tennessee (Parks, 1990) (zone 30, fig. 11), and a third

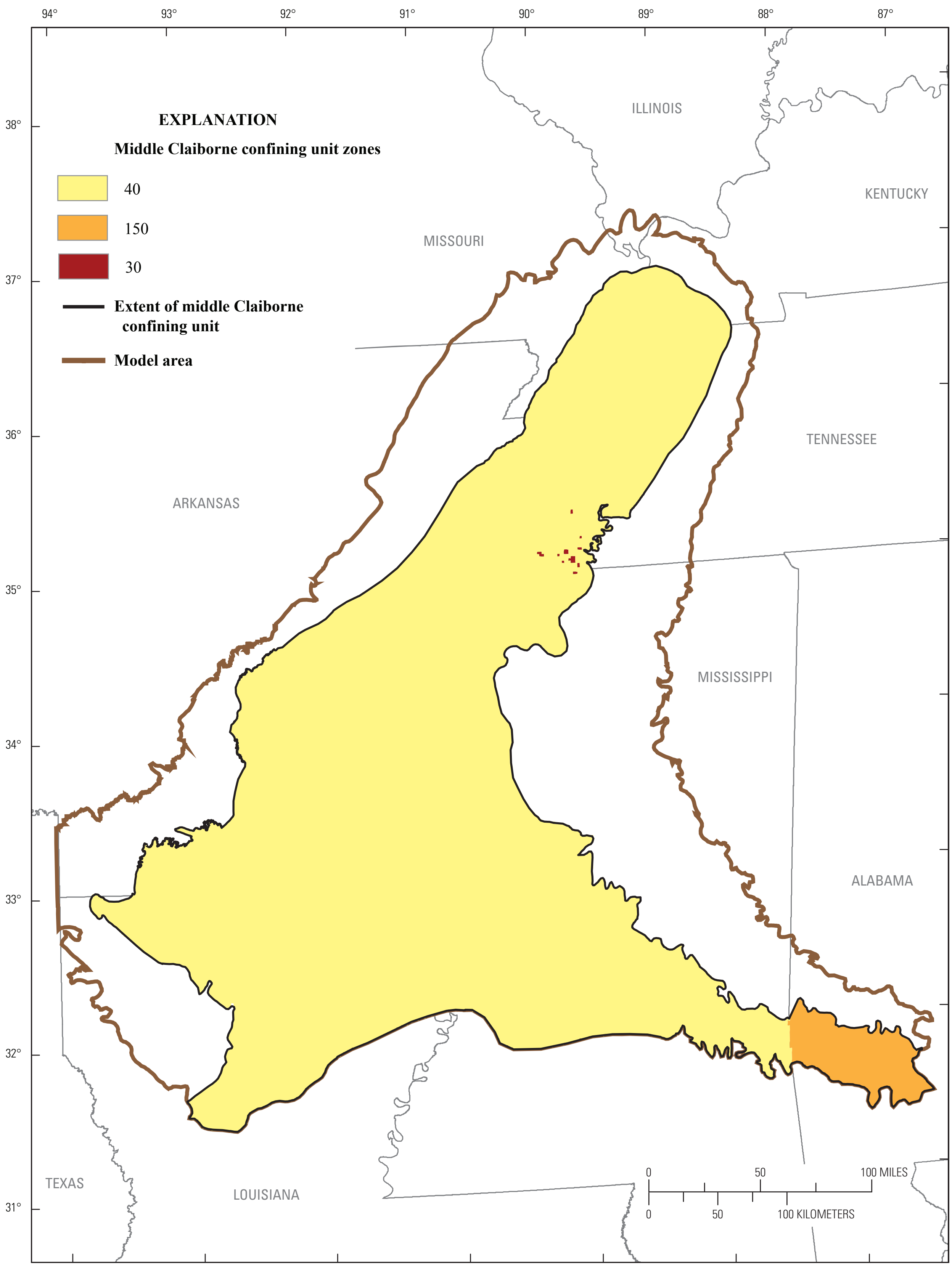

Figure 11. Parameter zones of the middle Claiborne confining unit.

zone represents the undifferentiated Claiborne Group in Alabama (zone 150, fig. 11). Zone 150 defines an area in Alabama that represents the undifferentiated Claiborne Group, which includes the upper Claiborne aquifer, middle Claiborne confining unit, middle Claiborne aquifer, lower Claiborne confining unit, and the lower Claiborne aquifer. Seven parameter zones define the properties of the middle Claiborne aquifer (fig. 12). Four zones, 50 through 53, were delineated based on hydraulic conductivity values estimated by Prudic (1991) and modified during the calibration procedure. Two zones, 60 and 70 (same area, different layers), were delineated based on a locally extensive clay layer within the middle Claiborne aquifer. Zone 60, which occurs only in layer 6, represents the finer material that confines the lower portion of the middle Claiborne aquifer (El Dorado confining unit). Zone 70, which occurs only in layer 7, represents the coarser material in the lower portion of the Middle Claiborne aquifer (El Dorado Sand), from which most wells are screened for municipal and industrial use. Four parameter zones define the properties of the Wilcox Group (fig. 13, 7). Zone 110 occurs in layer 11, 12, and 13 in areas where the Wilcox Group is undifferientated. Zone 111 represents the middle Wilcox aquifer in layer 11, and zone 120 represents the lower Wilcox aquifer in layer 12. Zone 130 represents the Old Breastworks Formation in the northern part of the embayment as shown in figure 7 as the extent of the Old Breastworks confining unit.

Vertical Anisotropy and Storage

Zones used for vertical anisotropy, specific yield, and specific storage were identical to those used for horizontal hydraulic conductivity. Initial estimates of vertical anisotropy, specific yield, and specific storage were based on literature values (Fetter, 1994; Freeze and Cherry, 1979) and were adjusted during model calibration.

Sand Percentage

An analysis of sand percentage for each formation was conducted through the use of geophysical logs (Hart and others, 2008; Hart and Clark, 2008b). Sand percentage grids, created using automated interpolation methods, then were used as a multiplier array on model parameters, such as hydraulic conductivity, for select aquifers or confining units in the MERAS model.

Normal-resistivity and natural gamma logs for the sand percentage analysis were selected to maximize spatial distribution. A 25-percent subset of approximately 2,700 geophysical logs was digitized and exported to Log ASCII Standard (LAS) format. The short normal resistivity curve was digitized and the LAS data for each geophysical log were queried to determine percent coarse material and thickness of the coarse material for each hydrogeologic unit. Distinction between coarse and fine material for each individual geophysical log was determined by using 20 percent of the maximum resistivity as the division between coarse and fine material. Materials with resistivities greater than 20 percent of the maximum resistivities were considered coarse materials (sand) and materials with resistivities less than 20 percent of the maximum resistivities were considered fine materials (clay).

Sand thickness was calculated by summing the intervals of material with resistivity greater than 20 percent of the maximum resistivity. Sand percentage was determined by dividing sand thickness by total hydrogeologic unit thickness and multiplying by 100 for grid cells equal in size and shape of each model cell (fig. 14). Total thickness for each hydrogeologic unit was determined from Hart and Clark (2008a) to obtain the tops and bottoms of each unit from each geophysical log. The units selected for use with sand percentage grids were the alluvial aquifer (fig. 14 A), Vicksburg-Jackson confining unit (fig. 14 B), upper Claiborne aquifer (fig. 14 C), middle Claiborne confining unit (fig. 14 D), middle Claiborne aquifer (fig. 14 E-J), lower Claiborne confining unit (fig. 14 K), portions of the middle Wilcox aquifer (fig. 14 L), and portions of the lower Wilcox aquifer (fig. 14 M). The middle Claiborne aquifer is represented by three model layers south of the facies transition zone (fig. 1) and six model layers north of the transition zone. To accommodate multilayering of the middle Claiborne aquifer, sand percentage grids also were divided vertically into three to six layers depending on location. In general, sand percentages of each unit are higher in the north and east, and lower in the south and west, which correspond to the conceptual depositional environment of shallow, high energy environment in the north, and deep, low energy environment in the south.

Faults

The existence of faults in the model area is supported by multiple studies (Hosman, 1982; Petersen and others, 1985; Albin 1964, Kingsbury and Parks, 1993). McKee and Clark (2003) included inferred faults to improve hydraulic-head value matching in simulations of flow within the middle Claiborne aquifer.

Seven faults were represented in the model using the Horizontal Flow Barrier (HFB) package that allows a reduction in horizontal hydraulic conductivity between adjacent cells (fig. 12). All simulated faults extend from layer 5 (Tertiary age middle Claiborne aquifer) to the base of the model domain. For simplification, the width of the horizontal flow barrier is assumed to be 1.0 ft.

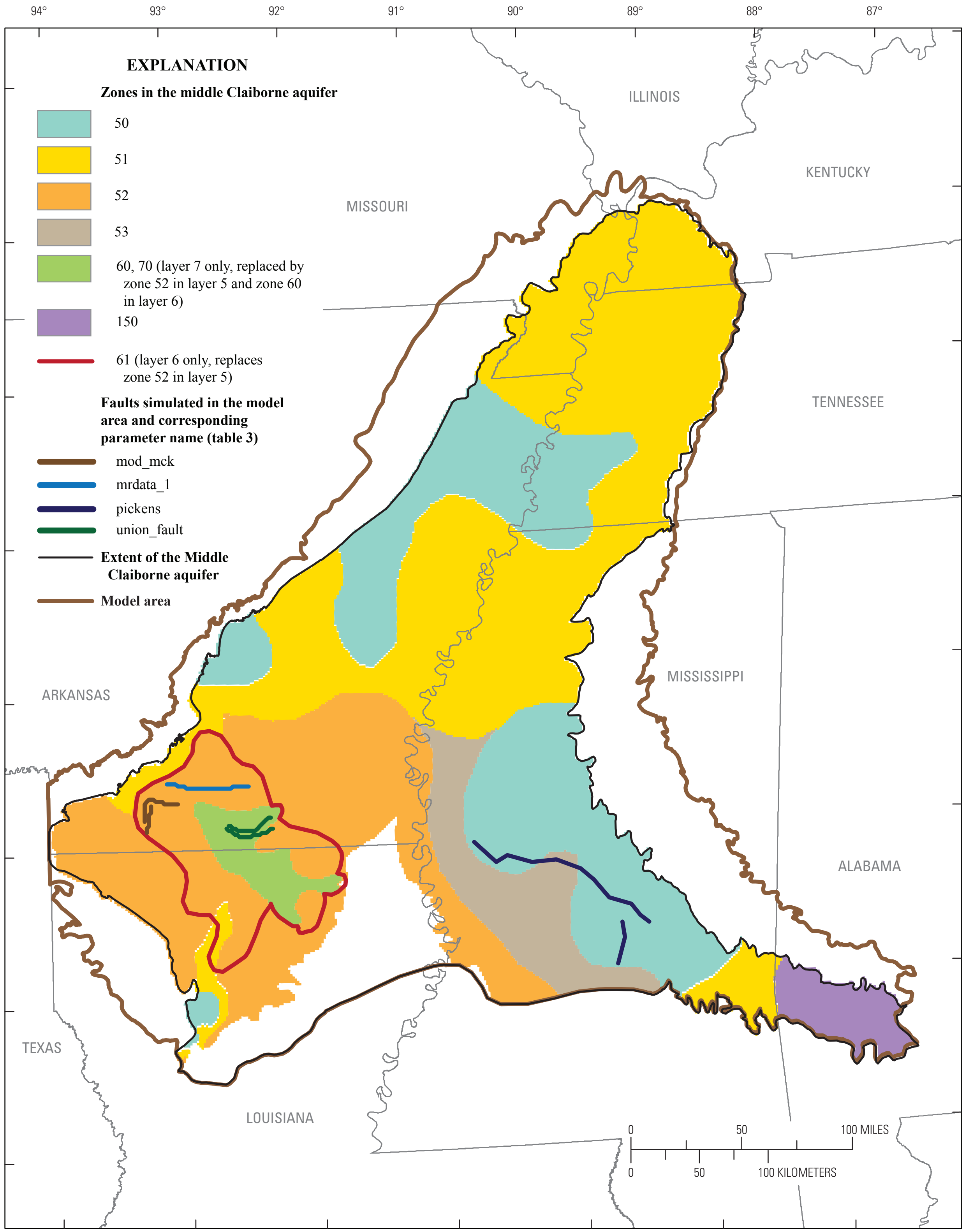

Figure 12. Parameter zones of the middle Claiborne aquifer and the location of faults simulated.

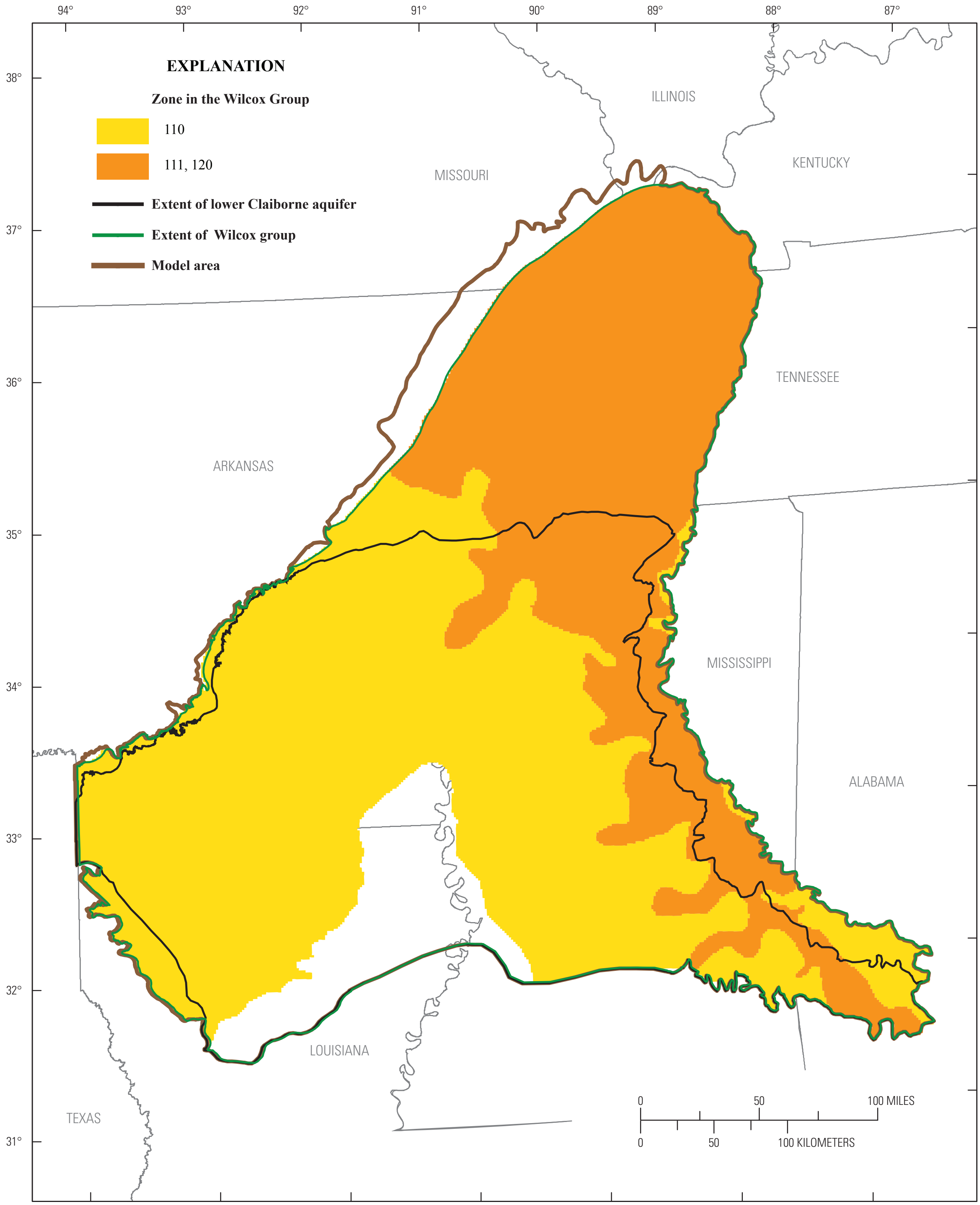

Figure 13. Parameter zones of the Wilcox Group and extent of the lower Claiborne aquifer.

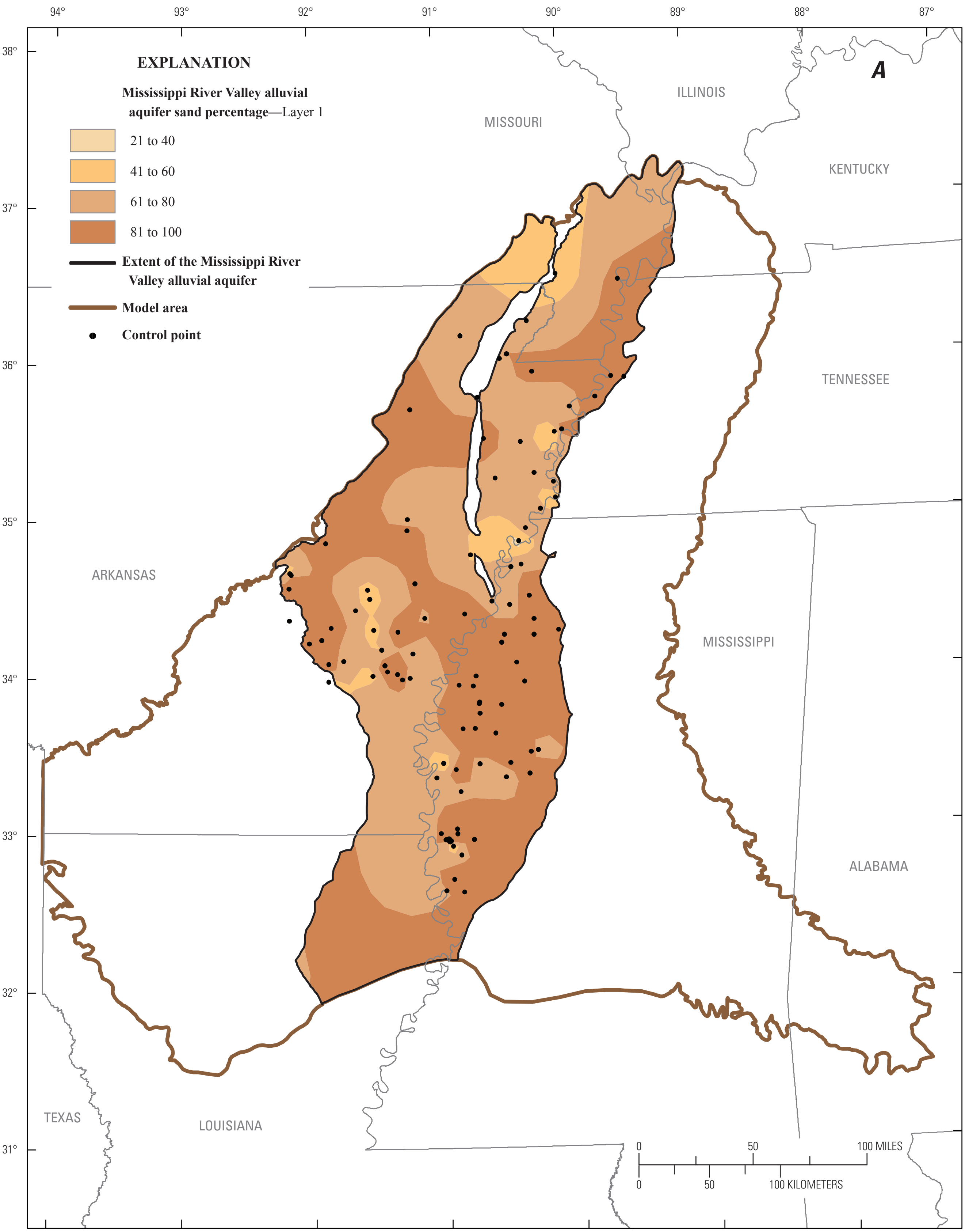

Figure 14. Sand percentage for select hydrogeologic units in the Mississippi Embayment Regional Aquifer Study area.

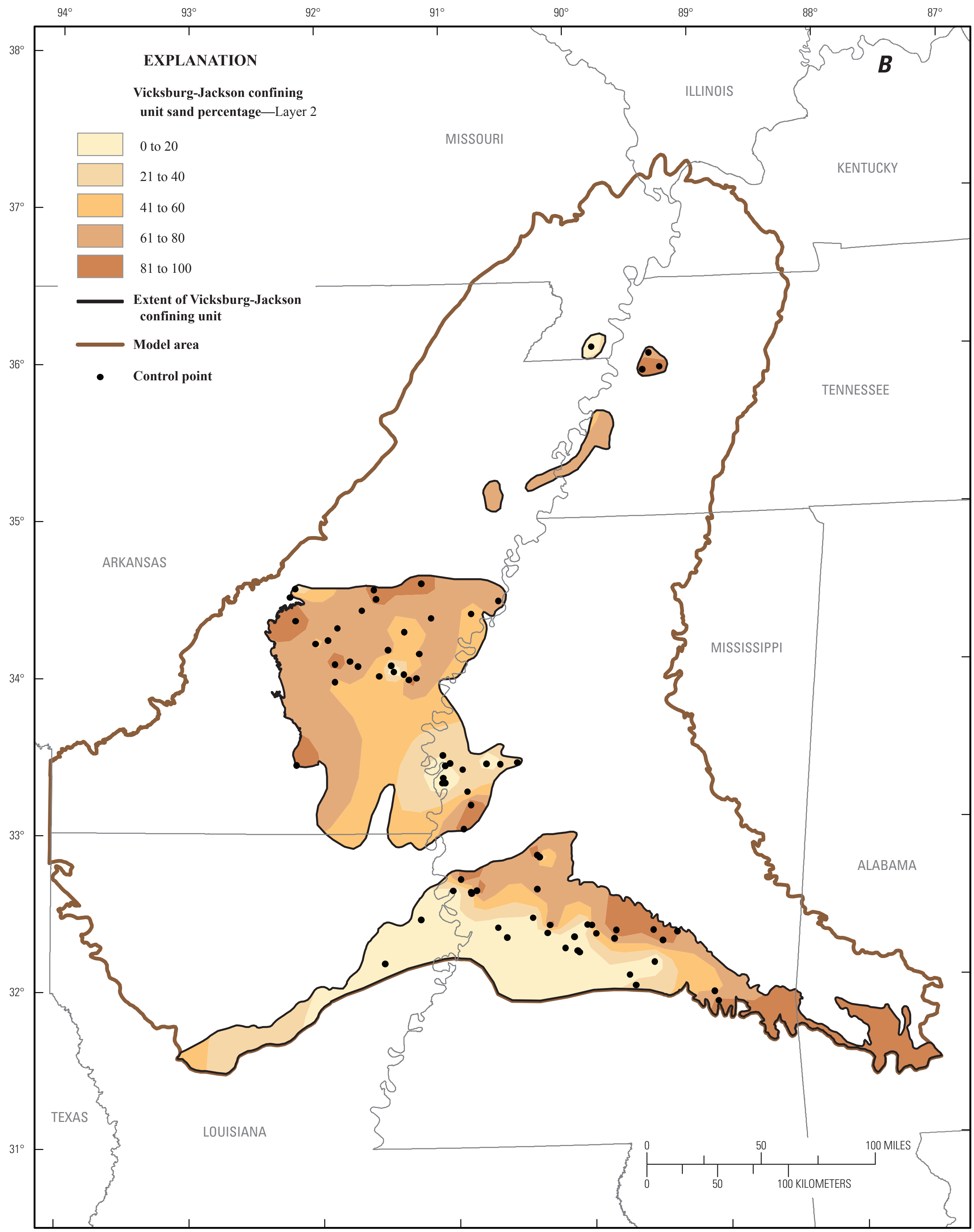

Figure 14. Sand percentage for select hydrogeologic units in the Mississippi Embayment Regional Aquifer Study area.—Continued

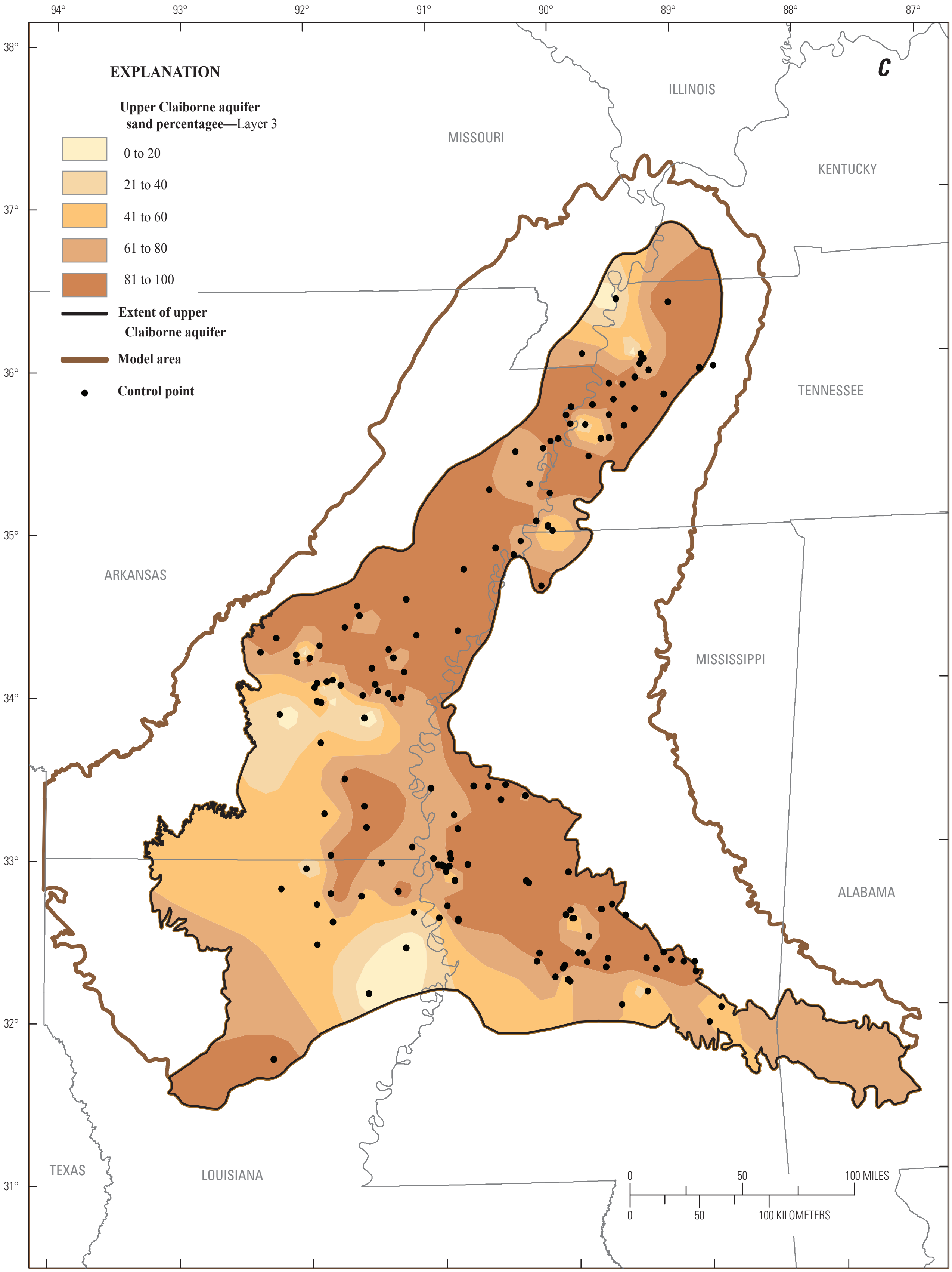

Figure 14. Sand percentage for select hydrogeologic units in the Mississippi Embayment Regional Aquifer Study area.—Continued

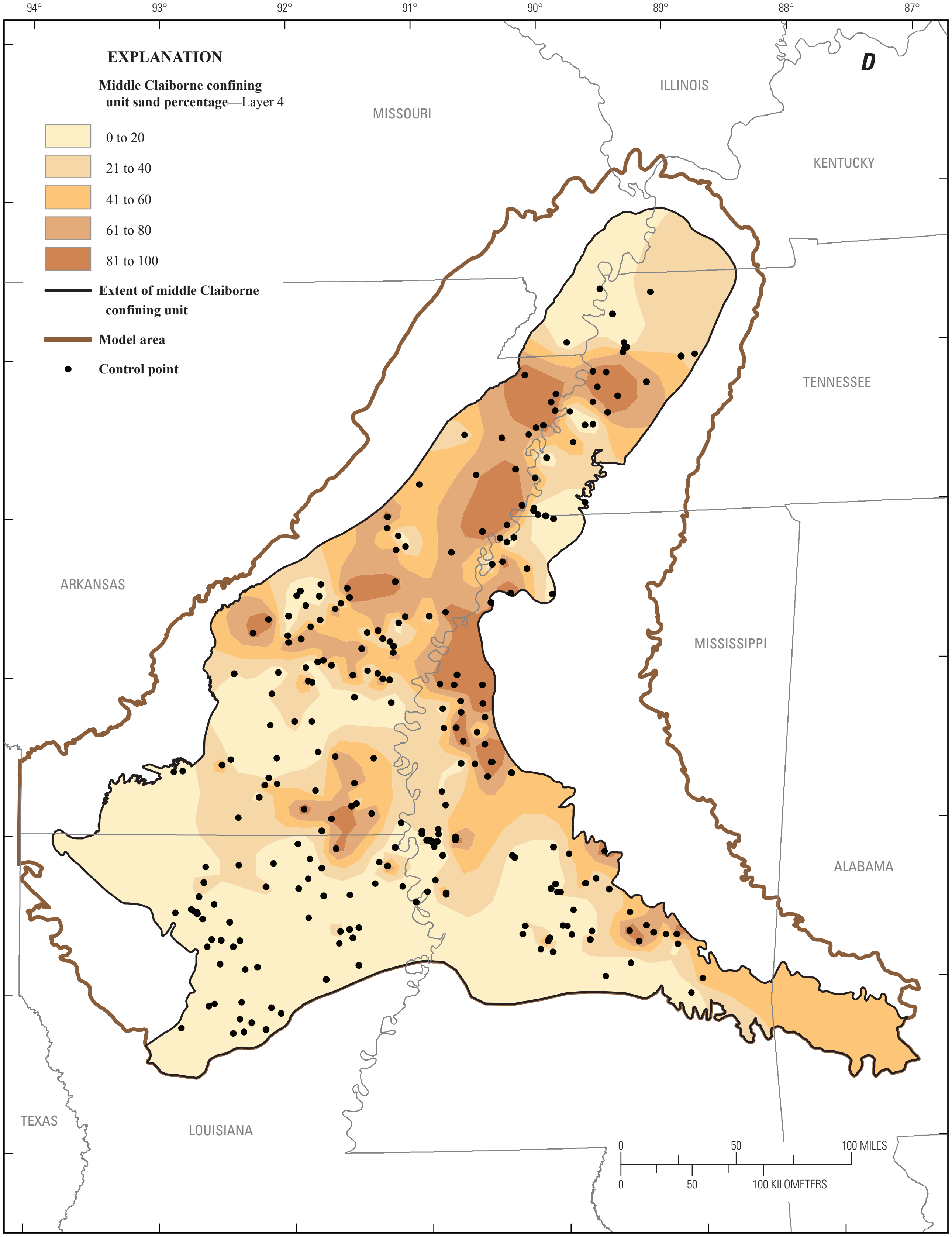

Figure 14. Sand percentage for select hydrogeologic units in the Mississippi Embayment Regional Aquifer Study area.—Continued

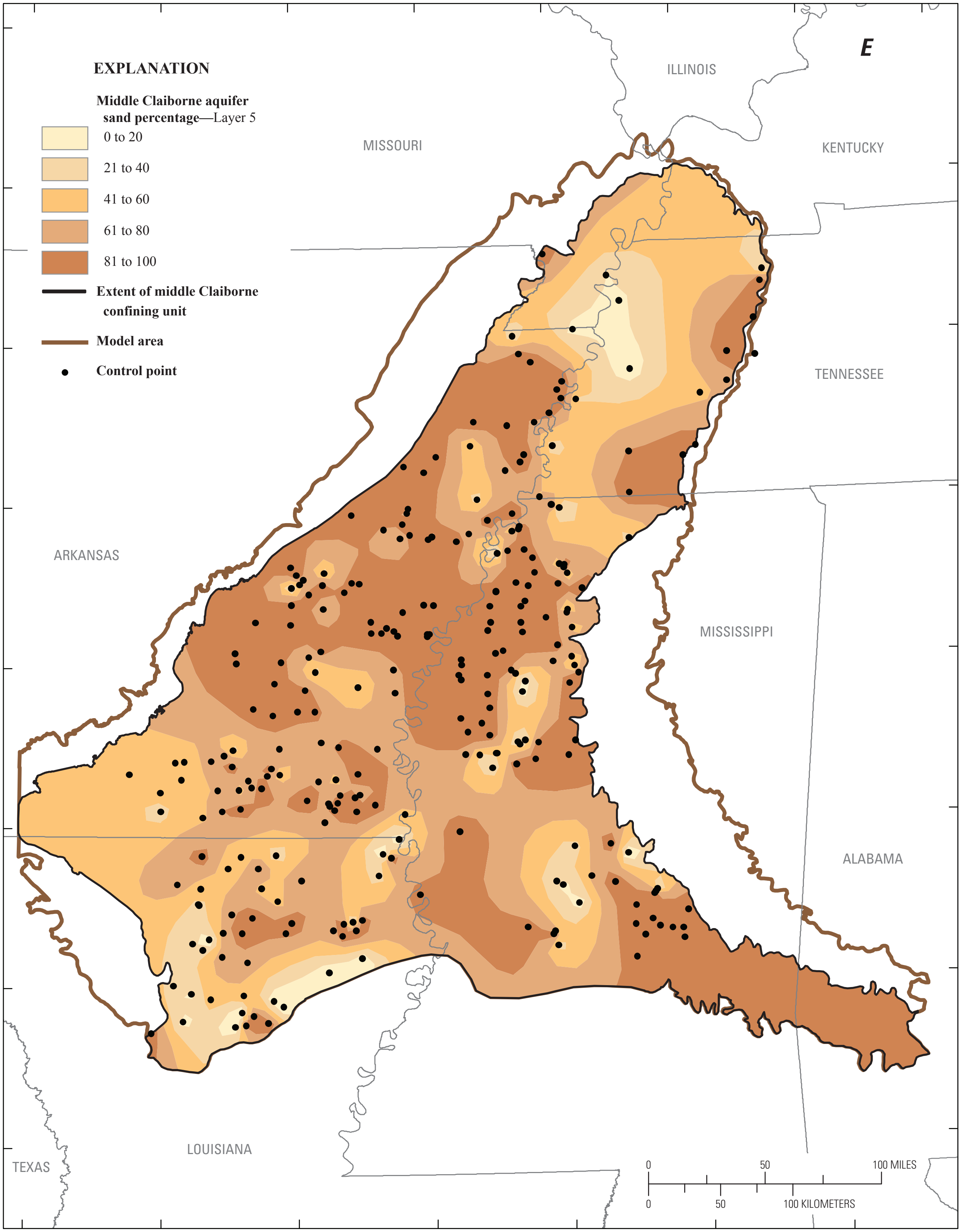

Figure 14. Sand percentage for select hydrogeologic units in the Mississippi Embayment Regional Aquifer Study area.—Continued

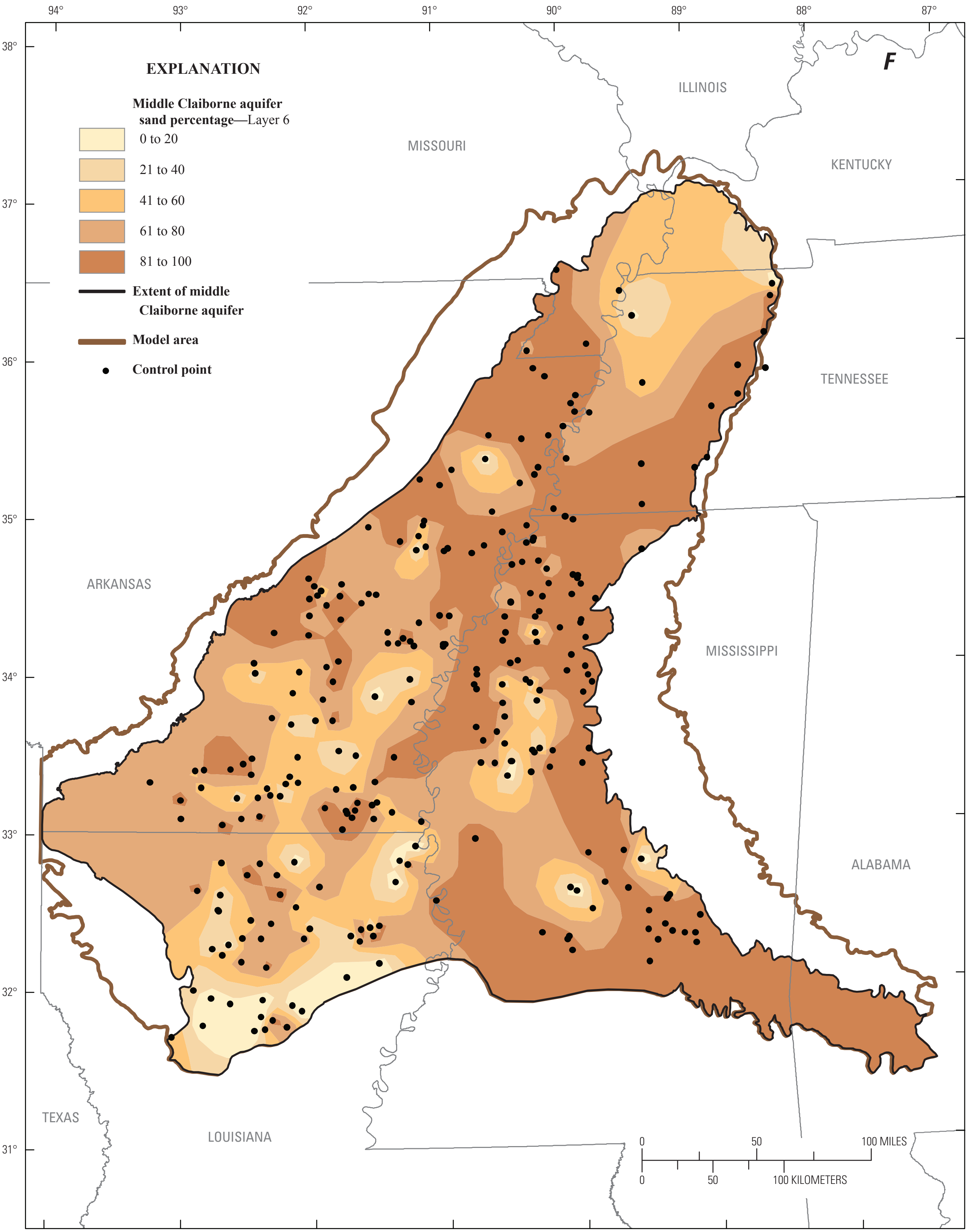

Figure 14. Sand percentage for select hydrogeologic units in the Mississippi Embayment Regional Aquifer Study area.—Continued

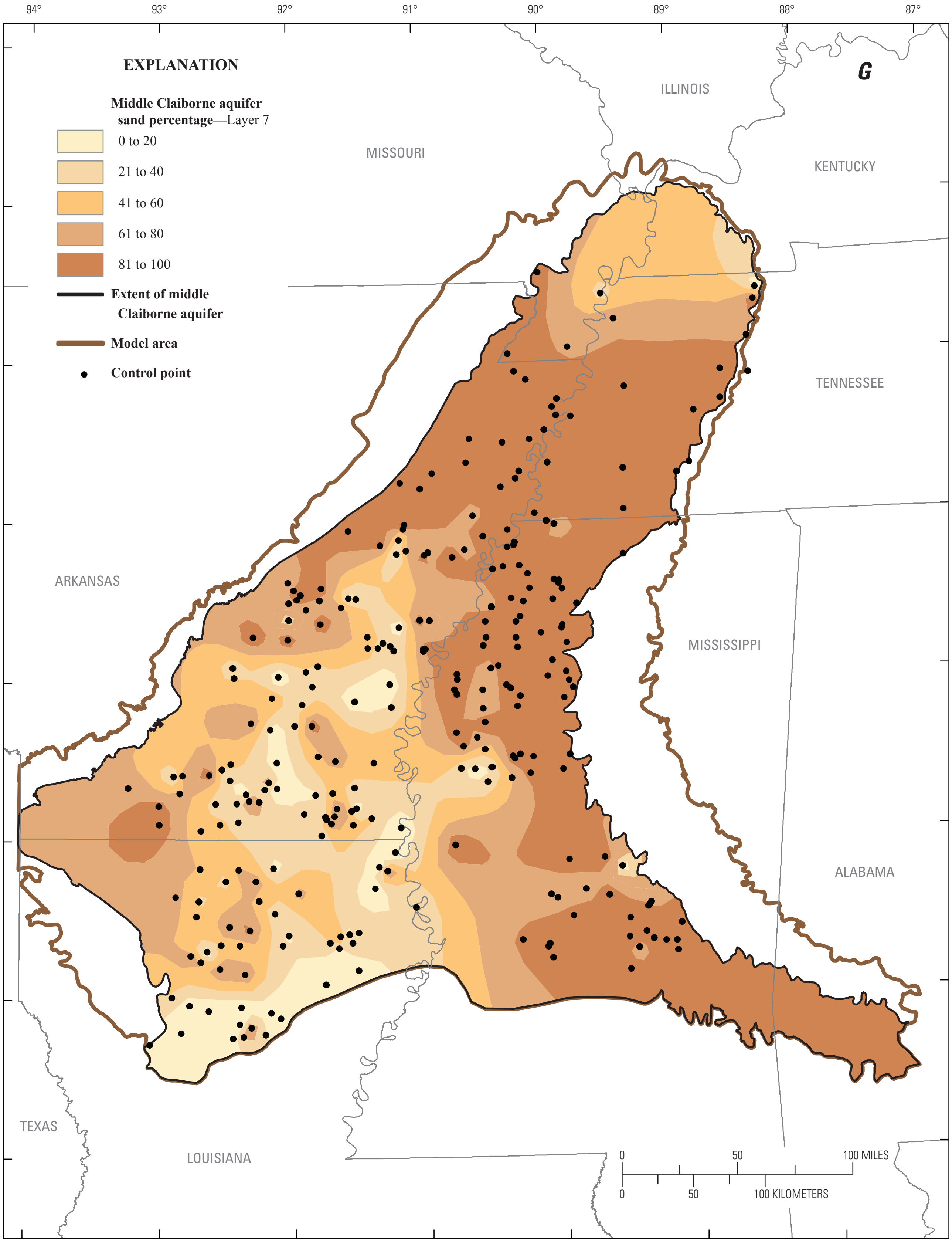

Figure 14. Sand percentage for select hydrogeologic units in the Mississippi Embayment Regional Aquifer Study area.—Continued

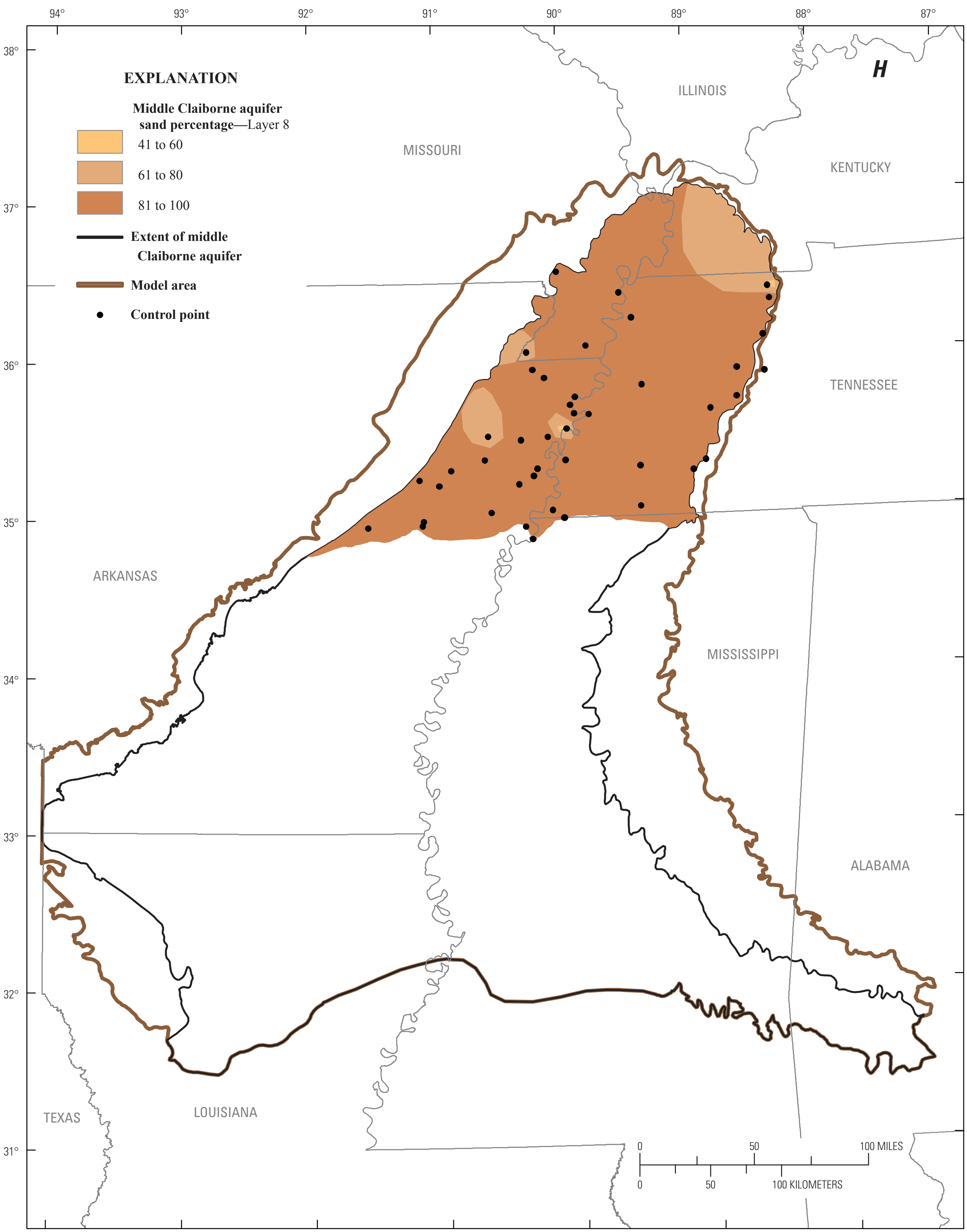

Figure 14. Sand percentage for select hydrogeologic units in the Mississippi Embayment Regional Aquifer Study area.—Continued

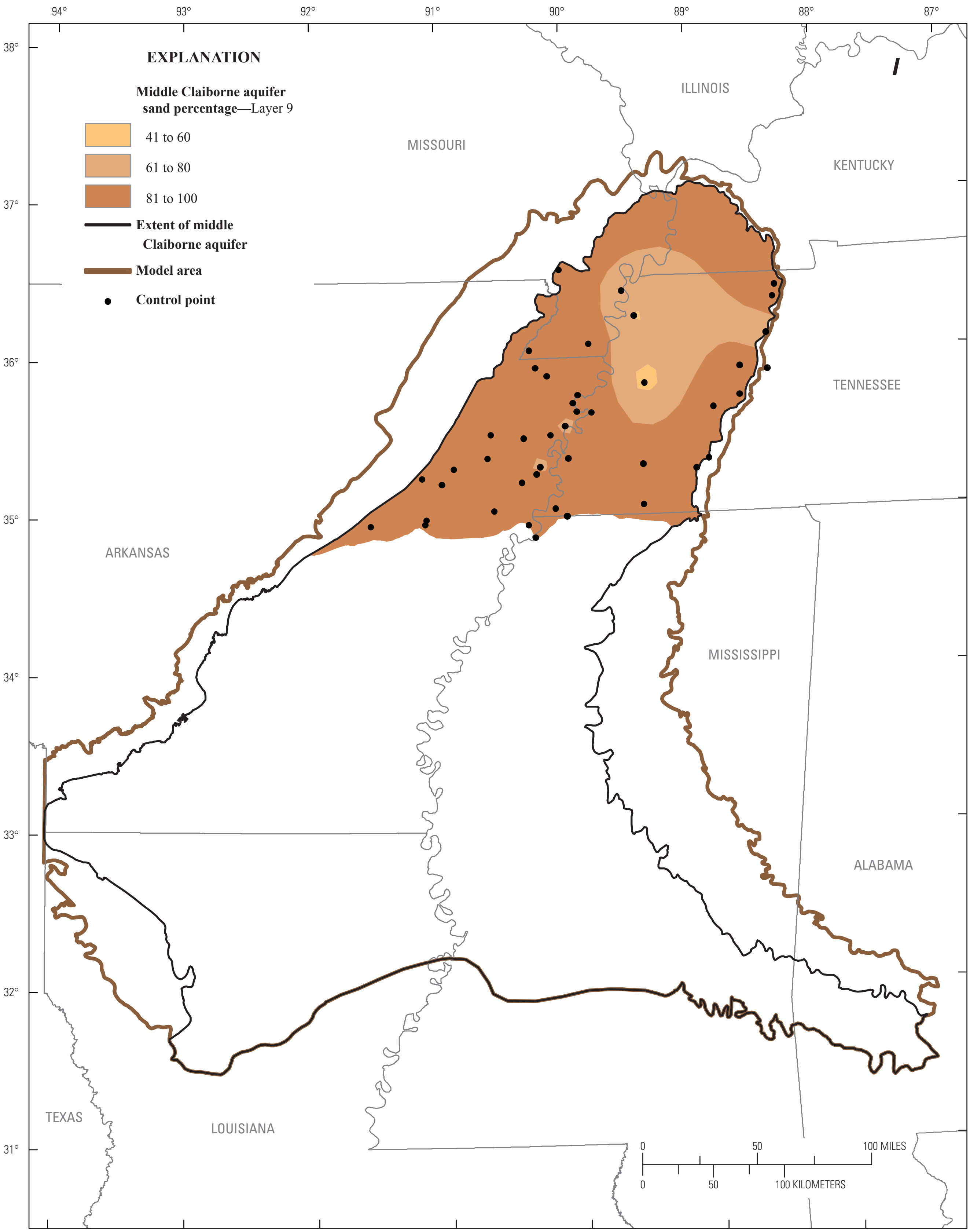

Figure 14. Sand percentage for select hydrogeologic units in the Mississippi Embayment Regional Aquifer Study area.—Continued

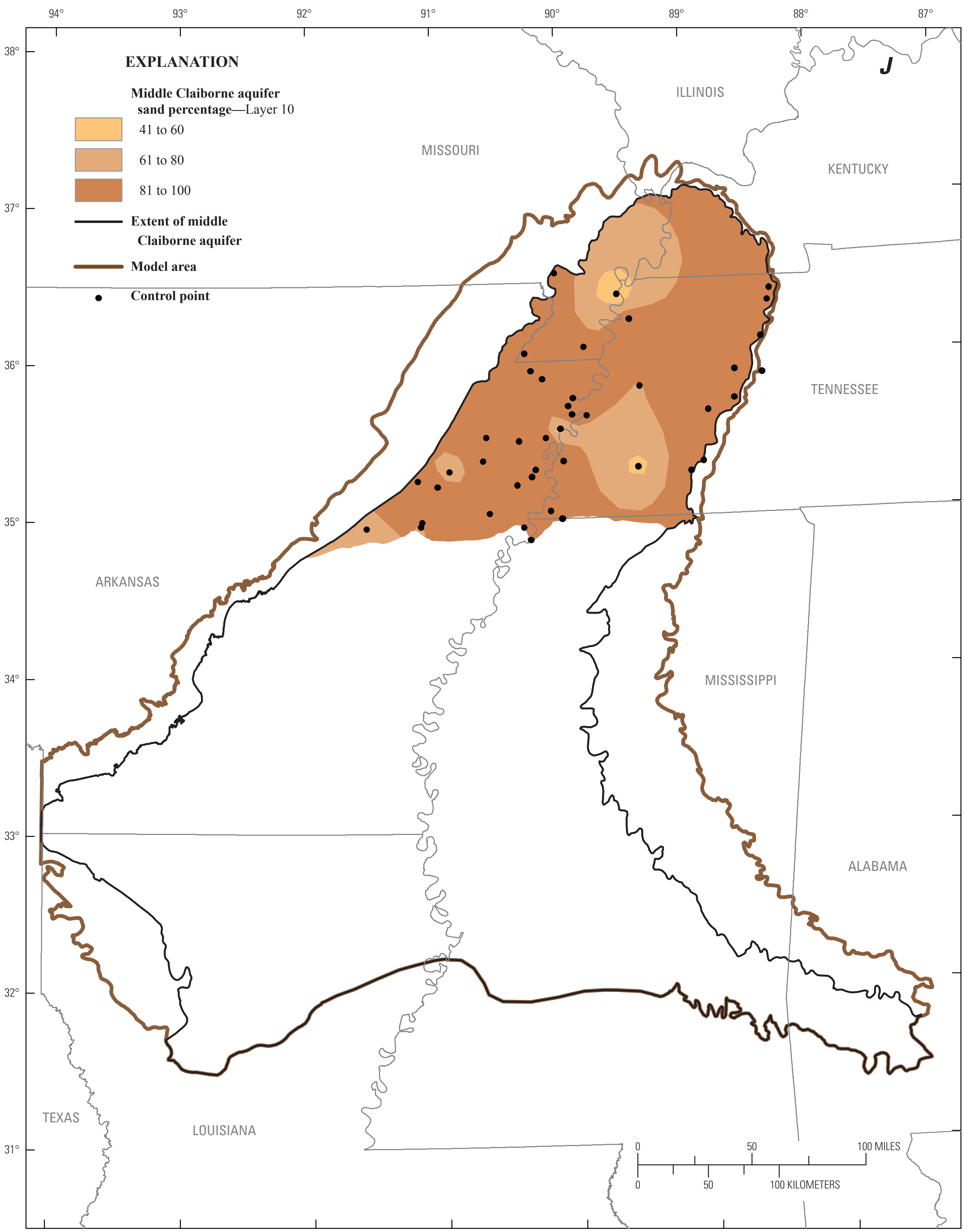

Figure 14. Sand percentage for select hydrogeologic units in the Mississippi Embayment Regional Aquifer Study area.—Continued

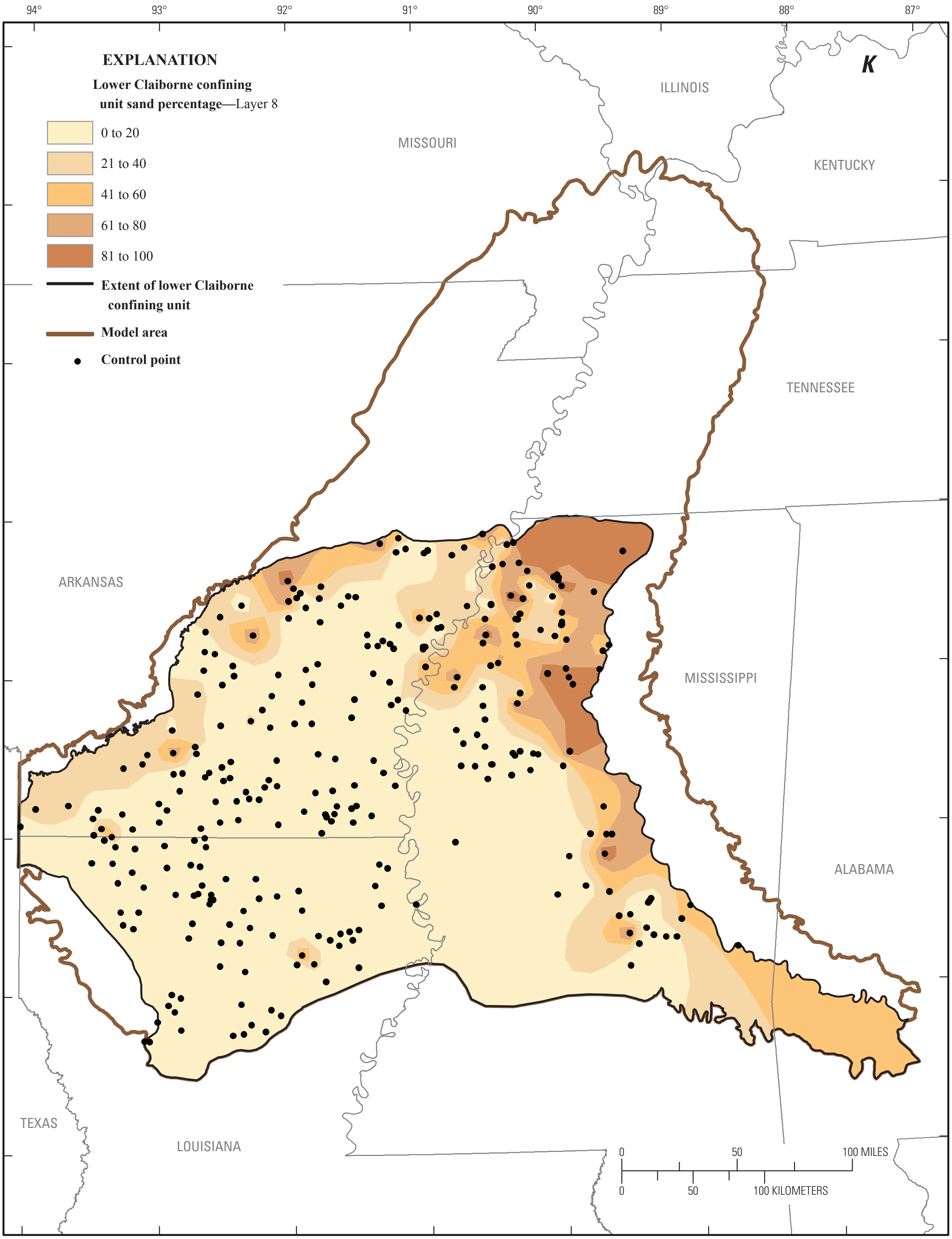

Figure 14. Sand percentage for select hydrogeologic units in the Mississippi Embayment Regional Aquifer Study area.—Continued

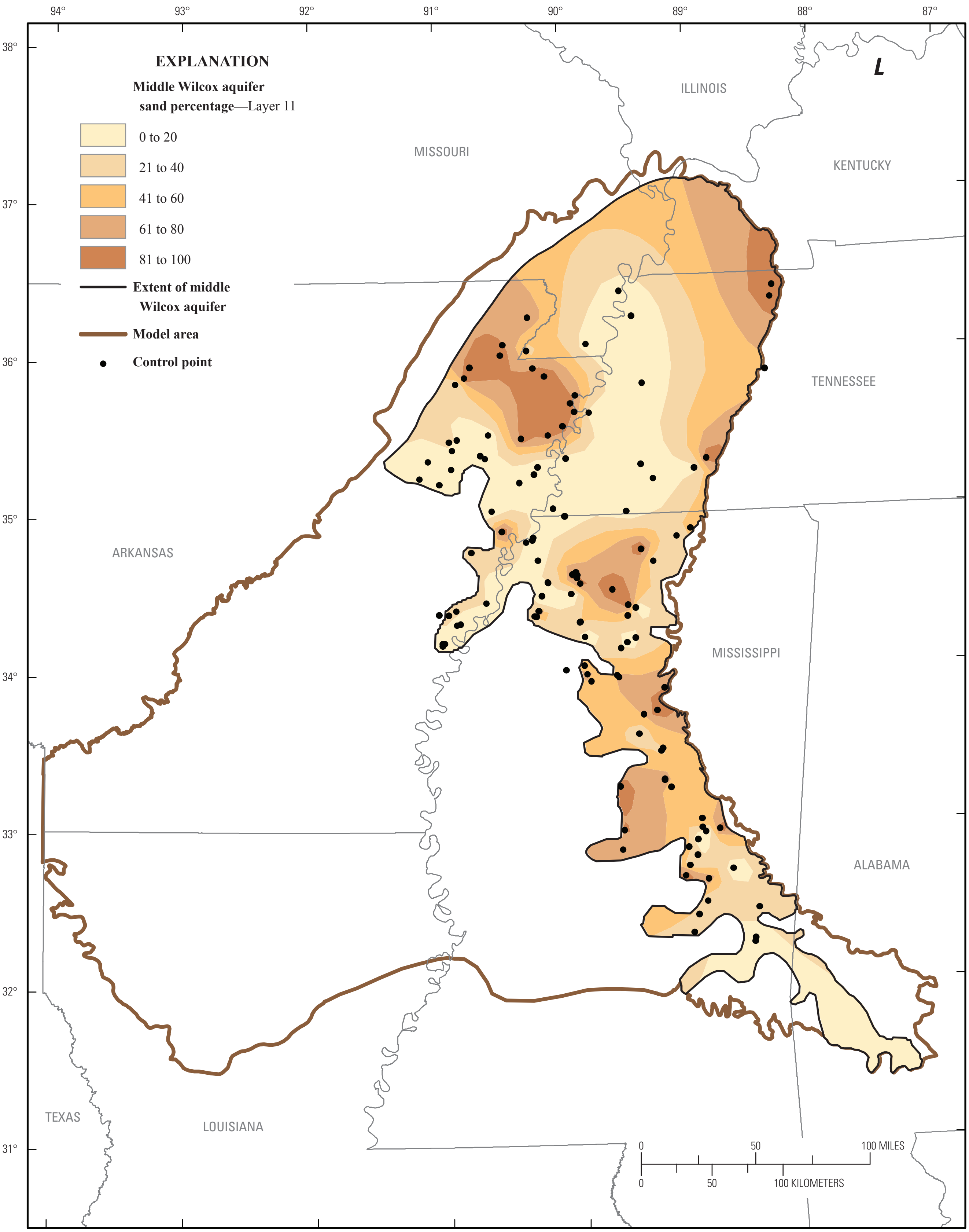

Figure 14. Sand percentage for select hydrogeologic units in the Mississippi Embayment Regional Aquifer Study area.—Continued

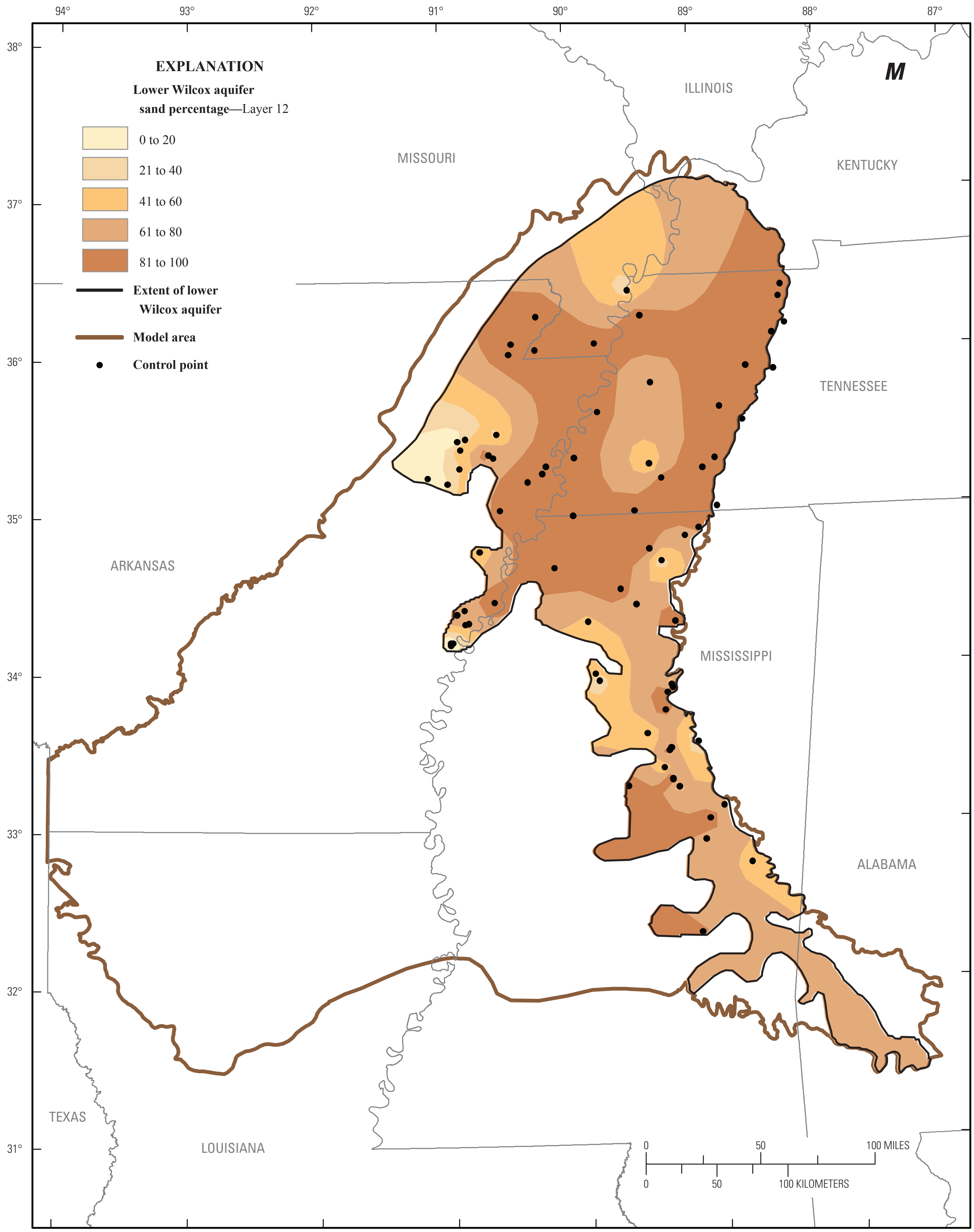

Figure 14. Sand percentage for select hydrogeologic units in the Mississippi Embayment Regional Aquifer Study area.—Continued

Model Calibration

The ability of the MERAS model to simulate measured conditions was accomplished by a combination of manual changes to parameter values and automated calibration methods. Automated parameter estimation was achieved through alternate use of UCODE-2005 (Poeter and others, 2005) and PEST (Doherty, 2008) for all 104 parameters. Simulations with UCODE-2005 were used primarily to examine the sensitivity of observations to various parameters during manual simulations. PEST automatically adjusted input parameters (hydraulic conductivity, vertical anisotropy, specific storage, specific yield, recharge, riverbed conductance, and hydraulic conductance of faults) in a series of model simulations. After each model simulation, simulated hydraulic-head values, total streamflow, and stream leakage were compared automatically to measured hydraulic-head values, total flow, and stream leakage. The simulations continued until a best fit between simulated hydraulic head and stream leakage with measured hydraulic head and stream leakage was attained. The calibration approach used here differs from traditional non-linear regression parameter estimation in two areas by using: (1) Tikhonov regularization (Tikhonov, 1963; Doherty, 2003; Fienen and others, 2009); and (2) hybrid singular value decomposition (Tonkin and Doherty, 2005; Hunt and others, 2007), also referred to as SVD-Assist (SVDA) in Doherty (2008). Additional information regarding the overview of the advantages of using these more sophisticated tools for parameter estimation are discussed by Hunt and others (2007); the tools were applied using the guidelines given by Doherty and Hunt (2009).

Weighted Hydraulic-Head Observations

Hydraulic-head observations were weighted to reduce the influence of hydraulic-head observations that are less accurate and to increase the influence of observations that are more accurate. Weights on observation data account for potential measurement error associated with the method of determining land surface, effects of recent pumpage, unknown screened intervals of wells, and other factors. In theory, weights of the observation values used in the regression procedure can be calculated from estimates of the variance or standard deviation of measurement error (Hill, 1998). The weights are calculated by dividing one by the square of the standard deviation (or variance) of the measurement errors for the observation. To estimate these standard deviations, the measurement errors can be assumed to have a normal distribution, and a 95-percent confidence interval for the measurement can be constructed. The 95-percent confidence interval spans a range equal to the measurement ±1.96 times the standard deviation (square root of the variance). Examples and detailed calculations of weights are given by Hill (1998).

For this report, standard deviations associated with land surface were calculated for hydraulic-head observations based on coordinate accuracy (how well the location of a well is known) and altitude accuracy (how well the land surface altitude of a measurement point of a well is known). The coordinate and altitude accuracy for wells are documented in the USGS National Water Inventory System (NWIS). Wells with coordinate accuracies better than ±5 seconds were included in the standard deviation calculation. Altitude accuracies other than those obtained from topographic maps were not included in the standard deviation because other methods generally were reasonably accurate. All wells that were not assigned a standard deviation based on the criteria above were assigned a standard deviation of one, which corresponds to a weight of one.

The standard deviation associated with coordinate accuracy was calculated by creating a radius around each well equal to the length of the well's coordinate accuracy value in degrees. The standard deviation of the land-surface altitude within the radius of each well was calculated. The standard deviation associated with the altitude accuracy was calculated by dividing half of the NWIS value of altitude accuracy (assuming the altitude accuracy equals the contour interval adjacent the well location) by 1.65 (where 1.65 is the critical value of a 90 percent confidence interval assuming that the error is normally distributed) (Hill and Tiedeman, 2007).

Each standard deviation was then converted to a variance (square root of standard deviation) so that the coordinate and altitude variances could be summed for each well. The final calculation converted the variance at each well back to a standard deviation. The resultant standard deviations of all wells range from 1 to 43.8 ft with an average of 1.9 ft.

Streamflow Measurements as Observations

Streamflow measurements, flow characteristics, and stream leakage estimates from previous studies were used as observations in the MERAS model. Flow characteristics were used for predevelopment observations and streamflow measurements were used for at least one additional observation late in the simulation period for each selected gage. Predevelopment observations were assumed to be the 50th percentile of daily streamflow (Wolock, 2003). Additional total streamflow measurement values were obtained from the USGS NWIS (U.S. Geological Survey, 2008c). Streamflow measurements used as observations were weighted using a method similar to that of weighting hydraulic head observations. Most predevelopment observations were assigned a standard deviation of 100,000 ft^3/d. The exception is the predevelopment observation on the White River, which was assigned a standard deviation of 1,000,000 ft^3/d because of the much greater difference in flow of the White River compared to most other streams. The standard deviation of postdevelopment observations was calculated by assuming a 90 percent probability that the streamflow measurements were within 5 percent of the true value. The standard deviation equals 5 percent of the streamflow value divided by 1.65 (see the "Weighted Hydraulic-Head

Observations” section) (Hill and Tiedeman, 2007). Stream leakage estimates were scarce in the model area as multiple factors (reservoir regulation, stream diversions, return flow from irrigation, etc.) combine to make true stream leakage estimates very difficult. Stream leakage estimates from Nyman (1965) were used to constrain the model in a local area on Nonconnah Creek in western Tennessee (fig. 3). Additionally, in 1998, streamflow measurements were made along a 40-mi segment of the White River in eastern Arkansas. The White River streamflow measurements indicated a 13 percent loss in streamflow from the upstream to downstream measurements (Jaysson E. Funkhouser, U.S. Geological Survey, written commun., 2006). The locations of the upstream and downstream measurements were used to extract information from the model to calculate the percent of streamflow that discharges to the aquifer through the use of UCODE-2005. Streamflow observation locations are shown in figure 3; total streamflow and stream leakage estimates and simulated values are presented in the “Streamflow Observations and Errors” section.

Model Evaluation

Optimal Parameter Estimates

The final parameter estimates of the model (table 3) are considered reasonable estimates for the type of material and conditions found in the Mississippi embayment aquifer system. For aquifers, horizontal hydraulic conductivity values of 3.7 to 600 ft/d are within the expected range of hydraulic conductivities for silty to clean sand (Freeze and Cherry, 1979), and also near the range of values used by McKee and Clark (2003), Stanton and Clark (2003), and Arthur (2001) for middle Claiborne and alluvial models. For confining units, horizontal hydraulic conductivity values of 0.00453 to 2.4 ft/d are within the expected range of hydraulic conductivities for marine clay to silt or loess (Freeze and Cherry, 1979). Generally, values for hydraulic conductivity are within the same order of magnitude for a given hydrogeologic unit and represent average values for large areas in the Mississippi embayment aquifer system. Horizontal hydraulic conductivities of horizontal flow barriers representing faults range from 0.0001 ft/d to 1.5536 ft/d. Specific yield values throughout the model range from 0.10 to 0.30. Specific storage values range from 2.59×10^{-7}/ft to 6.25×10^{-3}/ft. Final vertical anisotropy values range from 22.3 in surficial units to 2,297.1 in the El Dorado confining unit. Streambed conductances for each stream varied by stream reach, according to streambed hydraulic conductivity, streambed thickness, stream length, and stream width within each stream reach. The final values of streambed hydraulic conductivity range from 1.09×10^{-2} ft/d to 16.1 for streams simulated in the model. The fraction of precipitation (multiplier) that makes up recharge from infiltration ranges from 1.25×10^{-4} to 7.06×10^{-2} (table 4), which results in a range of recharge values of 0.003 to 5.73 in/yr. Comparatively, values of recharge in studies outside the embayment, range from 1.6 to 4.6 in/yr through a silt, clay, and sand confining unit over the Floridan aquifer system (Murray, 2007), and from 0.008 to 4.4 in/yr in the High Plains aquifer system (McMahon and others, 2006).

Model Fit and Model Error

Hydraulic Head Observations and Errors

Simulated heads were generally in good agreement with observed hydraulic-heads with 46,249 simulated values within ± 25 ft of the observed value. Simulated heads were compared to 55,786 observed hydraulic-head measurements from 3,245 wells in the MERAS model area. Values of mean, minimum, maximum, root mean square error (RMSE), and absolute mean error were computed for each year from residuals (table 5). RMSE in feet is determined using the equation:

$$\text{RMSE} = [\text{Sum of } (h_s - h_o)^2 / n]^{0.5}$$

where h_s is simulated hydraulic head, in feet,
h_o is observed hydraulic head, in feet, and
n is number of observations.

Values of RMSE between simulated and observed hydraulic heads of all observations ranged from 8.33 ft in 1919 to 47.65 ft in 1951, though only six annual RMSE values are greater than 40 ft for the entire simulation period (table 5). The six greatest RMSE values also occur in sequence from 1949 to 1954 and are attributed to the lack of pumping data for the pre-1960 time period. The RMSE for all observations in the model is 23.18 ft over a range in observed hydraulic head of 741.66 ft, where the range equals the difference between the highest and lowest observed hydraulic-head. The two principal aquifers, the alluvial aquifer and the middle Claiborne aquifer, are shown as individual statistics in table 5 because these aquifers make up the bulk of the information about the system. The RMSE for alluvial observations is 16.43 over a range in observed hydraulic head of 297.25 ft. The RMSE for the middle Claiborne aquifer is 35.78 over a range in observed hydraulic head of 634.94 ft. The mean of residuals indicates model bias depending on the magnitude and direction of the mean away from zero. The closer the mean is to zero, indicating a balance between positive and negative residuals, the less model bias occurs. A positive mean indicates the model tends to overpredict (simulated hydraulic heads greater than observed) water-level altitude, and a negative mean indicates underprediction (simulated hydraulic heads less than observed) of water levels. The mean residual approached zero with an absolute value less than 20 ft during 75 of the 88 years for which residuals were calculated. Out of 55,786 observations, 24,256 residuals were greater than or equal to

Table 3. Final calibrated hydraulic parameter values.

[* considered a confining unit within the parameter extent]

Parameter group	Parameter description	Parameter name	Final value	Units	Reference for parameter extent	Model layer	Composite-scaled sensitivity
Hydraulic conductivity in horizontal direction	Alluvial aquifer in zone 101	HK_alvm101	600	feet/day	fig. 9 zone 101	1 to 13	8.979×10^{-1}
	Alluvial aquifer in zones 102 and 108	HK_alvm102	166.7	feet/day	fig. 9 zones 102 and 108	1 to 13	2.744
	Alluvial aquifer in zone 103	HK_alvm103	135.4	feet/day	fig. 9 zone 103	1 to 13	1.382
	Alluvial aquifer in zone 104	HK_alvm104	458.5	feet/day	fig. 9 zone 104	1 to 13	1.078
	Alluvial aquifer in zone 105	HK_alvm105	425.4	feet/day	fig. 9 zone 105	1 to 13	1.554×10^{-1}
	Alluvial aquifer in zone 106	HK_alvm106	400	feet/day	fig. 9 zone 106	1 to 13	1.691
	Alluvial aquifer in zone 107	HK_alvm107	88.4	feet/day	fig. 9 zone 107	1 to 13	8.075×10^{-1}
	Loess undifferenitated	HK_loss	27.9	feet/day	fig. 9 zones 2 and 10	1 to 13	2.282
	Fluvial sediments undifferentiated	HK_fluv	200	feet/day	fig. 9 zone 2, where Vicksburg-Jackson confining unit (fig. 14 B) does not exist	2 to 10	8.797×10^{-1}
	Vicksburg-Jackson confining unit	HK_vkbg	1	feet/day	fig. 14 B	2	1.156
	Undifferientiated Claiborne Group	HK_clbr	48.7	feet/day	fig. 11, zone 150	3 to 10	5.070×10^{-1}
	Upper Claiborne aquifer	HK_cckf	26.3	feet/day	fig. 14 C; fig. 10, zone 30	3	2.690
	Middle Claiborne onfining unit	HK_ckmn	0.154	feet/day	fig. 11, zone 40	4	4.192
	Middle Claiborne aquifer in zone 50	HK_sprt1	146.1	feet/day	fig. 12, zone 50	5 to 7	4.867
	Middle Claiborne aquifer in zone 51	HK_sprt2	34.8	feet/day	fig. 12, zone 51	5 to 7	1.194
	Middle Claiborne aquifer in zone 52	HK_sprt3	27.2	feet/day	fig. 12, zone 52	5 to 7	1.782

Table 3. Final calibrated hydraulic parameter values.—Continued

[* considered a confining unit within the parameter extent]

Parameter group	Parameter description	Parameter name	Final value	Units	Reference for parameter extent	Model layer	Composite-scaled sensitivity
	Middle Claiborne aquifer in zone 61	HK_sprt3_5	3.7	feet/day	fig. 12, zone 61	6	2.096
	Middle Claiborne aquifer in zone 53	HK_sprt4	10.2	feet/day	fig. 12, zone 53	5 to 7	3.608
	El Dorado confining unit	HK_spcl	0.00453	feet/day	fig. 12, zone 61 (layer 6)	6	1.186
	El Dorado Sand	HK_spes	59	feet/day	fig. 12, zone 70 (layer 7)	7	7.397
	Lower Claiborne confining unit	HK_crvr	0.0883	feet/day	fig. 14 K	8	2.773
	Winona-Tallahatta aquifer	HK_wnth	26.9	feet/day	fig. 6	9	6.503×10^{-1}
	Lower Claiborne aquifer	HK_crrz	25	feet/day	fig. 13	10	9.737×10^{-1}
	Wilcox aquifer in zone 110	HK_wlcx	5.6	feet/day	fig. 13 zone 110	11 to 13	5.486
	Middle Wilcox aquifer*	HK_flid	2.4	feet/day	fig. 14 L	11	1.132
	Lower Wilcox aquifer	HK_lwaq	24.6	feet/day	fig. 14 M	12	1.714
	Old Breastworks confining unit	HK_odbx	1.4	feet/day	fig. 7	13	3.797×10^{-1}
Vertical anisotropy	Alluvial aquifer	VANI_alvm	100	dimensionless	fig. 9 zones 101-108	1 to 13	1.167×10^{-1}
	Loess undifferenitated	VANI_loss	22.3	dimensionless	fig. 9 zones 2 and 10	1 to 13	6.933×10^{-2}
	Vicksburg-Jackson confining unit	VANI_vkbg	1,475	dimensionless	fig. 14 B	2	1.127
	Undifferientiated Claiborne Group	VANI_clbr	23.4	dimensionless	fig. 11, zone 150	3 to 10	5.908×10^{-2}
	Upper Claiborne aquifer	VANI_cckf	612.8	dimensionless	fig. 14 C	3	2.938×10^{-1}
	Middle Claiborne confining unit	VANI_ckmn	564.6	dimensionless	fig. 14 D	4	4.194
	Middle Claiborne aquifer in zone 50	VANI_sprt1	243.4	dimensionless	fig. 12, zone 50	5 to 7	2.101×10^{-1}

Table 3. Final calibrated hydraulic parameter values.—Continued

[* considered a confining unit within the parameter extent]

Parameter group	Parameter description	Parameter name	Final value	Units	Reference for parameter extent	Model layer	Composite-scaled sensitivity
	Middle Claiborne aquifer in zones 51 and 53	VANI_sprt2	680	dimensionless	fig. 12 zones 51 and 53	5 to 7	1.339
	Middle Claiborne aquifer in zone 52	VANI_sprt3	798.8	dimensionless	fig. 12, zone 52	5 to 7	9.769×10^{-1}
	El Dorado confining unit	VANI_spcl	2,297.1	dimensionless	fig. 12, zone 61 (layer 6)	6	1.175
	El Dorado Sand	VANI_spes	254.2	dimensionless	fig. 12, zone 70 (layer 7)	7	8.046×10^{-2}
	Lower Claiborne confining unit	VANI_crvr	334.5	dimensionless	fig. 14 K	8	2.738
	Winona-Tallahatta aquifer	VANI_wnth	28	dimensionless	fig. 6	9	6.344×10^{-2}
	Lower Claiborne aquifer	VANI_crrz	23	dimensionless	fig. 13	10	6.958×10^{-2}
	Wilcox aquifer in zone 110	VANI_wlcx	402.8	dimensionless	fig. 13, zone 110	11 to 13	6.082×10^{-1}
	Middle Wilcox aquifer*	VANI_flid	617.8	dimensionless	fig. 14 L	11	9.910×10^{-1}
	Lower Wilcox aquifer	VANI_lwaq	27.7	dimensionless	fig. 14 M	12	6.780×10^{-2}
	Old Breastworks confining unit	VANI_odbx	478.4	dimensionless	fig. 7	13	1.274×10^{-1}
Specific storage	Alluvial aquifer in zone 101	SS_alvm101	3.50×10^{-3}	1/foot	fig. 9 zone 101	1 to 13	7.812×10^{-1}
	Alluvial aquifer in zones 102 and 108	SS_alvm102	4.03×10^{-3}	1/foot	fig. 9 zones 102 and 108	1 to 13	1.443
	Alluvial aquifer in zone 103	SS_alvm103	3.34×10^{-3}	1/foot	fig. 9 zone 103	1 to 13	5.152×10^{-1}
	Alluvial aquifer in zone 104	SS_alvm104	5.74×10^{-3}	1/foot	fig. 9 zone 104	1 to 13	2.839
	Alluvial aquifer in zone 105	SS_alvm105	2.85×10^{-3}	1/foot	fig. 9 zone 105	1 to 13	1.353×10^{-1}
	Alluvial aquifer in zone 106	SS_alvm106	4.33×10^{-3}	1/foot	fig. 9 zone 106	1 to 13	3.132
	Alluvial aquifer in zone 107	SS_alvm107	6.25×10^{-3}	1/foot	fig. 9 zone 107	1 to 13	8.637×10^{-1}
	Loess undifferenitated	SS_loss	1.36×10^{-3}	1/foot	fig. 9 zones 2 and 10	1 to 13	7.095×10^{-1}
	Vicksburg-Jackson confining unit	SS_vkbg	3.46×10^{-7}	1/foot	fig. 14 B	2	6.974×10^{-2}

Table 3. Final calibrated hydraulic parameter values.—Continued

[* considered a confining unit within the parameter extent]

Parameter group	Parameter description	Parameter name	Final value	Units	Reference for parameter extent	Model layer	Composite-scaled sensitivity
	Undifferientiated Claiborne Group	SS_clbr	3.68×10^{-7}	1/foot	fig. 11, zone 150	3 to 10	7.170×10^{-2}
	Upper Claiborne aquifer	SS_cckf	2.59×10^{-7}	1/foot	fig. 14 C	3	6.030×10^{-2}
	Middle Claiborne confining unit	SS_ckmn	2.88×10^{-7}	1/foot	fig. 14 D	4	8.166×10^{-2}
	Middle Claiborne aquifer in zone 50	SS_sprt1	8.51×10^{-6}	1/foot	fig. 12, zone 50	5 to 7	5.986×10^{-1}
	Middle Claiborne aquifer in zones 51 and 53	SS_sprt2	1.03×10^{-6}	1/foot	fig. 12 zones 51 and 53	5 to 7	5.312×10^{-1}
	Middle Claiborne aquifer in zone 52	SS_sprt3	9.92×10^{-7}	1/foot	fig. 12, zone 52	5 to 7	1.900
	El Dorado confining unit	SS_spcl	3.65×10^{-7}	1/foot	fig. 12, zone 61 (layer 6)	6	1.346×10^{-1}
	El Dorado Sand	SS_spes	2.44×10^{-6}	1/foot	fig. 12, zone 70 (layer 7)	7	1.341
	Lower Claiborne confining unit	SS_crvr	3.08×10^{-7}	1/foot	fig. 14 K	8	2.347×10^{-1}
	Winona-Tallahatta aquifer	SS_wnth	2.81×10^{-7}	1/foot	fig. 6	9	9.998×10^{-2}
	Lower Claiborne aquifer	SS_crrz	2.79×10^{-7}	1/foot	fig. 13	10	7.827×10^{-2}
	Wilcox aquifer in zone 110	SS_wlcx	3.65×10^{-7}	1/foot	fig. 13, zone 110	11 to 13	4.353×10^{-1}
	Middle Wilcox aquifer*	SS_flid	3.36×10^{-7}	1/foot	fig. 14 L	11	8.174×10^{-2}
	Lower Wilcox aquifer	SS_lwaq	3.39×10^{-7}	1/foot	fig. 14 M	12	5.892×10^{-2}
	Old Breastworks confining unit	SS_odbx	3.23×10^{-7}	1/foot	fig. 7	13	5.238×10^{-2}
Specific yield	Alluvial aquifer in zoness 101-105	SY_alvm	0.3	dimensionless	fig. 9 zones 101-105	1	4.310
	Alluvial aquifer in zone 106	SY_alvm106	0.1	dimensionless	fig. 9 zone 106	1	2.514
	Loess undifferenitated	SY_loss	0.3	dimensionless	fig. 9 zones 2 and 10	1 to 13	8.710×10^{-1}
Recharge multiplier	Alluvial aquifer in zone 101	RCHALM101	3.80×10^{-2}	dimensionless	fig. 9 zone 101	1 to 13	2.412

Table 3. Final calibrated hydraulic parameter values.—Continued

[* considered a confining unit within the parameter extent]

Parameter group	Parameter description	Parameter name	Final value	Units	Reference for parameter extent	Model layer	Composite-scaled sensitivity
	Alluvial aquifer in zone 102	RCHALM102	4.46×10^{-2}	dimension-less	fig. 9 zone 102	1 to 13	3.292
	Alluvial aquifer in zone 103	RCHALM103	5.10×10^{-2}	dimension-less	fig. 9 zone 103	1 to 13	4.482
	Alluvial aquifer in zone 104	RCHALM104	2.88×10^{-2}	dimension-less	fig. 9 zone 104	1 to 13	3.084
	Alluvial aquifer in zone 105	RCHALM105	5.11×10^{-2}	dimension-less	fig. 9 zone105	1 to 13	2.140×10^{-1}
	Alluvial aquifer in zone 106	RCHALM106	1.30×10^{-4}	dimension-less	fig. 9 zone 106	1 to 13	6.813×10^{-2}
	Alluvial aquifer in zone 107	RCHALM107	1.02×10^{-2}	dimension-less	fig. 9 zone 107	1 to 13	5.931×10^{-1}
	Alluvial aquifer in zone 108	RCHALM108	3.42×10^{-3}	dimension-less	fig. 9 zone 108	1 to 13	5.170×10^{-1}
	Various clay	RCHCLAY	1.25×10^{-4}	dimension-less	fig. 9 zones 3, 5, and 7	2, 4, and 8	1.299×10^{-1}
	Loess undifferenitated	RCHLOSS	1.23×10^{-2}	dimension-less	fig. 9 zone 2	multiple	3.542
	Upper Claiborne aquifer	RCHCCKF	2.35×10^{-3}	dimension-less	fig. 14 C	3	1.100
	Middle Claiborne aquifer in western part of model area	RCHSPTW	1.16×10^{-3}	dimension-less	fig. 9 zone 6	5	1.979×10^{-1}
	Middle Claiborne aquifer in eastern part of model area	RCHSPTE	6.38×10^{-3}	dimension-less	fig. 9 zone 61	5	4.439×10^{-1}
	Lower Claiborne aquifer	RCHCRRZ	8.60×10^{-3}	dimension-less	fig. 9, zone 8	10	1.053
	Wilcox aquifer undif-ferentiated in eastern part of model area	RCHWXE	7.02×10^{-3}	dimension-less	fig. 9, zone 9	11	1.527
	Wilcox aquifer undif-ferentiated in western part of model area	RCHWXW	7.06×10^{-2}	dimension-less	fig. 9, zone 11	11	5.226
	Terrace deposits undif-ferntiated	RCHTRRC	1.16×10^{-2}	dimension-less	fig. 9, zone 10	multiple	7.401
Streambed conductance	Selected rivers	RIVCON	1.458×10^{-1}	feet/day	fig. 4	multiple	1.495
	Arkansas River	RIVARK	0.09	feet/day	fig. 4	multiple	1.190
	Mississippi River	RIVMISS	15.4	feet/day	fig. 4	multiple	0.000
	Ouachita River	RIVOUACH	16.1	feet/day	fig. 4	multiple	7.891×10^{-2}
	White River	RIVWHT	13.8	feet/day	fig. 4	multiple	6.187×10^{-2}
	L'Anguille River	RIVLANG	0.99	feet/day	fig. 4	multiple	7.128×10^{-1}

Table 3. Final calibrated hydraulic parameter values.—Continued

[* considered a confining unit within the parameter extent]

Parameter group	Parameter description	Parameter name	Final value	Units	Reference for parameter extent	Model layer	Composite-scaled sensitivity
	Saline River	RIVSALIN	1.03	feet/day	fig. 4	multiple	8.998×10^{-2}
	Cache River	RIVCACH	1.14	feet/day	fig. 4	multiple	7.139×10^{-1}
	Selected rivers	RIVLOW	1.099×10^{-2}	feet/day	fig. 4	multiple	1.198
	Selected rivers	RIVMEMP	1	feet/day	fig. 4	multiple	5.116×10^{-1}
Horizontal flow barrier	Fault set in southeastern Arkansas	mod_mck	1.0×10^{-4}	feet/day	fig. 12	5 to 13	2.398
	Fault set in south-central Arkansas	mrdata_1	1.5536	feet/day	fig. 12	5 to 13	5.902×10^{-2}
	Fault set in south-central Arkansas	union_fault	5.928×10^{-3}	feet/day	fig. 12	5 to 13	1.098×10^{-1}
	Fault set in Mississippi	pickens	0.00504	feet/day	fig. 12	5 to 13	1.117×10^{-1}
Precipitation value	Predevelopment precipitation	predevrch	2.647×10^{-3}	feet/day	fig. 9 all zones	multiple	6.668

Table 4. Recharge parameter values and corresponding range of recharge.

Zone number	Parameter name (see table 3)	Range in precipitation (inches)	Fraction of recharge	Range in recharge amount (inches per year)
101	RCHALM101	29 to 85	3.80×10^{-2}	1.09 to 3.25
102	RCHALM102	27 to 85	4.46×10^{-2}	1.23 to 3.79
103	RCHALM103	29 to 83	5.10×10^{-2}	1.47 to 4.25
104	RCHALM104	28 to 84	2.88×10^{-2}	0.81 to 2.43
105	RCHALM105	28 to 79	5.11×10^{-2}	1.45 to 4.03
106	RCHALM106	27 to 85	1.30×10^{-4}	0 to 0.01
107	RCHALM107	28 to 86	1.02×10^{-2}	0.29 to 0.87
108	RCHALM108	28 to 85	3.42×10^{-3}	0.1 to 0.29
2	RCHLOSS	26 to 80	1.23×10^{-2}	0.32 to 0.99
10	RCHTRRC	26 to 85	1.16×10^{-2}	0.3 to 0.99
3	RCHCLAY	30 to 80	1.25×10^{-4}	0 to 0.01
4	RCHCCKF	30 to 83	2.35×10^{-3}	0.07 to 0.19
5	RCHCLAY	29 to 85	1.25×10^{-4}	0 to 0.01
6	RCHSPTW	27 to 85	1.16×10^{-3}	0.03 to 0.1
61	RCHSPTE	29 to 80	6.38×10^{-3}	0.18 to 0.51
7	RCHCLAY	27 to 83	1.25×10^{-4}	0 to 0.01
8	RCHCRRZ	27 to 84	8.60×10^{-3}	0.23 to 0.72
9	RCHWXE	31 to 84	7.02×10^{-3}	0.22 to 0.59
11	RCHWXW	27 to 81	7.06×10^{-2}	1.9 to 5.73

Table 5. Summary of weighted hydraulic-head residual statistics for model calibration for all observations, alluvial observations, and middle Claiborne aquifer observations.

[--, no value]

	All observations								Alluvial observations			Middle Claiborne observations		
Year	Mean (feet)	Minimum residual (feet)	Maximum residual (feet)	Root mean square error (RMSE) (feet)	Mean absolute error (feet)	Number of observa-tions	Range (feet)	Ratio of RMSE to range	Root mean square error (feet)	Number of observa-tions	Range (feet)	Root mean square error (feet)	Number of observa-tions	Range (feet)
1902	0.20	0.20	0.20	--	0.20	1	--	--	--	1	--	--	--	--
1911	7.44	7.44	7.44	--	7.44	1	--	--	--	--	--	--	--	--
1913	-72.37	-72.37	-72.37	--	72.37	1	--	--	--	--	--	--	--	--
1916	-25.87	-25.87	-25.87	--	25.87	1	--	--	--	--	--	--	1	--
1918	28.35	28.35	28.35	--	28.35	1	--	--	--	1	--	--	--	--
1919	1.88	-8.67	9.84	8.33	7.90	4	85.5	0.1	--	1	--	--	1	--
1925	-4.07	-4.07	-4.07	--	4.07	1	--	--	--	--	--	--	1	--
1927	-8.68	-17.19	-0.16	12.16	8.68	2	6.06	2.01	12.16	2	6.06	--	--	--
1928	3.56	-34.64	26.05	16.42	13.90	30	88.3	0.19	16.37	27	78.7	16.84	3	74.31
1929	2.12	-45.55	21.77	15.61	12.90	37	146.2	0.11	16.03	34	76.41	9.71	3	111.66
1930	2.21	-30.32	23.01	14.26	11.88	37	95.98	0.15	15.05	33	81.35	--	1	--
1931	3.85	-20.97	23.32	13.67	12.01	32	78.92	0.17	13.86	31	78.92	--	1	--
1932	3.69	-33.45	28.53	15.47	12.84	34	97.52	0.16	15.92	32	77.99	3.42	2	81.53
1933	3.91	-26.90	26.51	15.51	13.62	32	103.75	0.15	15.99	30	81.79	3.49	2	86.01
1934	5.30	-23.81	30.56	15.93	14.15	35	99.25	0.16	16.38	33	78.2	3.44	2	83.27
1935	9.91	-21.90	35.78	17.70	15.36	52	110.34	0.16	18.03	50	90.65	3.88	2	83.6
1936	10.59	-25.13	35.82	18.32	16.15	56	170.27	0.11	18.78	53	170.27	5.77	3	81.98
1937	8.46	-58.02	83.43	21.38	16.85	74	225.17	0.09	20.94	69	225.17	26.71	5	81.87
1938	9.64	-38.50	84.07	21.26	17.27	88	226.84	0.09	21.43	74	226.84	10.47	6	111.13
1939	11.45	-39.38	84.09	24.10	18.82	107	233.19	0.1	21.55	76	227.4	37.13	13	166.51
1940	9.11	-56.32	84.12	23.04	18.16	111	234.51	0.1	20.60	76	226.75	26.18	17	208.96
1941	10.05	-55.30	84.34	22.03	17.45	107	233.7	0.09	20.71	77	226.31	15.30	11	209.05
1942	9.97	-54.64	84.12	21.85	17.45	107	235.61	0.09	21.35	77	228.92	15.37	13	207.05
1943	10.34	-51.77	84.76	21.90	17.57	102	258.95	0.08	21.59	73	228.71	15.25	11	230.98

Table 5. Summary of weighted hydraulic-head residual statistics for model calibration for all observations, alluvial observations, and middle Claiborne aquifer observations.—Continued

[--, no value]

	All observations								Alluvial observations			Middle Claiborne observations		
Year	Mean (feet)	Minimum residual (feet)	Maximum residual (feet)	Root mean square error (RMSE) (feet)	Mean absolute error (feet)	Number of observa-tions	Range (feet)	Ratio of RMSE to range	Root mean square error (feet)	Number of observa-tions	Range (feet)	Root mean square error (feet)	Number of observa-tions	Range (feet)
1944	9.75	-52.08	85.54	22.53	18.43	110	228.64	0.1	22.30	79	228.64	17.20	14	198.43
1945	11.56	-52.26	85.99	24.04	19.03	66	201.56	0.12	23.75	37	147.13	17.51	12	166.95
1946	15.84	-50.50	206.21	37.96	22.93	85	398.5	0.1	21.79	48	231.23	72.54	16	369.58
1947	15.43	-50.20	226.49	38.50	23.27	111	390.33	0.1	21.78	73	151.62	76.00	20	390.33
1948	13.24	-53.92	227.10	36.51	23.13	131	390.86	0.09	21.49	82	181.28	66.86	27	390.86
1949	14.30	-54.03	224.87	41.56	24.61	166	415.52	0.1	21.30	96	180.51	71.40	44	415.52
1950	17.33	-51.53	224.70	45.17	26.60	156	417.06	0.11	21.85	87	229.17	75.14	46	416.72
1951	18.56	-54.84	210.66	47.65	27.80	148	404.17	0.12	21.74	85	181.41	79.87	44	404.17
1952	14.56	-51.83	196.12	40.37	23.74	152	390.37	0.1	21.16	88	176.78	67.59	42	390.37
1953	7.32	-144.11	233.67	47.17	26.34	247	543.97	0.09	18.19	172	228.36	83.36	43	428.38
1954	7.83	-152.77	216.43	40.56	22.80	336	518.11	0.08	18.82	252	235	75.70	44	398.84
1955	6.71	-145.51	229.54	34.13	18.54	483	539.54	0.06	16.84	389	247.41	76.95	48	424.81
1956	5.84	-154.95	229.69	32.03	17.33	548	548.36	0.06	16.15	440	236.93	69.54	59	426.2
1957	4.93	-77.03	225.27	25.96	14.36	657	649.65	0.04	15.59	543	256.72	68.11	60	422.46
1958	0.36	-131.78	229.46	26.92	15.57	742	627.6	0.04	17.61	606	254	61.87	72	428.26
1959	-1.12	-142.28	232.95	24.02	14.58	770	635.34	0.04	17.16	628	256.49	48.71	76	508.2
1960	-0.63	-143.97	234.68	23.70	14.34	774	532.46	0.04	16.76	634	255.27	49.72	73	438.33
1961	-0.40	-85.58	236.30	23.88	14.17	694	547.58	0.04	14.95	542	243.09	43.43	90	545.9
1962	-1.78	-90.73	230.30	22.79	13.92	696	637.97	0.04	15.29	545	247.28	46.44	87	455.59
1963	-0.44	-143.12	234.33	23.61	13.65	682	559.53	0.04	14.31	533	255.24	46.28	89	554.25
1964	0.73	-93.77	223.30	22.61	13.39	652	570.47	0.04	13.50	501	253.74	43.93	103	564.12
1965	1.40	-83.09	222.85	23.55	14.17	643	570.8	0.04	14.05	475	257.9	43.10	121	570.8
1966	2.27	-81.50	197.99	24.48	15.17	630	555.76	0.04	14.67	442	245.76	42.48	127	555.76
1967	2.93	-125.74	191.32	25.16	15.92	668	574.97	0.04	14.97	436	253.21	41.22	155	574.97
1968	1.95	-139.10	189.84	25.16	16.49	755	592.92	0.04	16.05	453	253.19	38.45	209	592.92

Table 5. Summary of weighted hydraulic-head residual statistics for model calibration for all observations, alluvial observations, and middle Claiborne aquifer observations.—Continued

[--, no value]

	All observations								Alluvial observations			Middle Claiborne observations		
Year	Mean (feet)	Minimum residual (feet)	Maximum residual (feet)	Root mean square error (RMSE) (feet)	Mean absolute error (feet)	Number of observa-tions	Range (feet)	Ratio of RMSE to range	Root mean square error (feet)	Number of observa-tions	Range (feet)	Root mean square error (feet)	Number of observa-tions	Range (feet)
1969	0.05	-80.33	137.15	23.62	16.20	887	712.15	0.03	16.32	575	251.89	36.22	216	599.25
1970	0.21	-82.93	130.91	23.04	15.88	889	567.24	0.04	16.33	563	252.67	34.67	219	567.24
1971	0.86	-81.05	129.78	21.50	14.59	929	558.63	0.04	14.97	593	245.75	32.66	229	558.63
1972	2.29	-80.98	131.49	21.26	14.30	846	560.56	0.04	14.70	505	254.68	29.83	227	560.56
1973	2.64	-89.71	133.78	23.17	16.20	788	552.26	0.04	16.35	426	253.1	30.20	239	552.26
1974	2.06	-92.86	168.09	24.15	16.75	809	550.26	0.04	17.00	443	254.15	31.63	251	550.26
1975	1.52	-94.96	189.05	23.59	16.76	882	613.19	0.04	17.33	493	276.03	29.58	265	543.14
1976	3.43	-89.82	157.20	23.10	15.96	887	633.45	0.04	15.88	469	279.83	30.31	264	549.21
1977	2.49	-143.18	161.85	26.01	17.42	891	633.64	0.04	17.81	455	282.01	31.79	267	547.14
1978	0.96	-146.27	176.66	26.22	17.26	987	637.76	0.04	17.01	535	281.35	33.06	280	553.92
1979	-1.93	-152.20	192.64	25.29	16.94	1053	663.75	0.04	17.42	565	280.05	29.24	294	580.4
1980	-1.47	-156.12	173.55	23.23	15.65	1204	630.89	0.04	16.45	760	254.28	26.54	289	558.11
1981	-0.33	-149.08	176.91	22.39	14.69	1274	659.58	0.03	14.76	804	256.8	27.27	280	552.35
1982	-0.17	-162.75	141.78	20.73	13.94	1300	658.53	0.03	14.92	864	254.26	26.52	264	560.17
1983	-2.04	-91.38	135.07	19.86	14.21	1401	662.79	0.03	15.85	936	273.93	24.72	291	564.44
1984	-0.94	-117.79	144.29	19.63	13.54	1643	678.65	0.03	14.79	1162	277.23	28.63	297	572.35
1985	-1.37	-117.74	142.11	20.00	13.85	1676	684.11	0.03	15.42	1197	282.45	28.53	303	580.76
1986	-0.47	-116.65	165.29	20.30	13.90	1700	669.82	0.03	15.35	1218	292.18	29.94	310	566.3
1987	-0.80	-128.37	164.25	20.27	14.00	1703	685.84	0.03	14.88	1227	275.73	30.05	298	585.98
1988	-0.54	-121.80	170.77	20.45	14.01	1610	689.15	0.03	14.71	1198	239.01	32.55	249	588.12
1989	-2.22	-124.29	181.39	20.53	13.66	1622	668.78	0.03	14.15	1160	246.95	30.61	302	567.71
1990	-3.02	-134.63	175.72	20.50	13.42	1561	672.85	0.03	14.60	1178	243.74	31.92	234	566.44
1991	-5.02	-139.39	68.75	18.37	12.49	1249	669.75	0.03	14.79	1048	231.73	31.24	57	565.53
1992	-4.97	-140.86	189.55	20.05	13.28	1360	711.91	0.03	15.54	1186	237.8	42.71	81	605.38
1993	-3.36	-141.81	197.39	20.68	13.43	1279	701.87	0.03	14.49	984	250.9	32.86	206	593.6

Table 5. Summary of weighted hydraulic-head residual statistics for model calibration for all observations, alluvial observations, and middle Claiborne aquifer observations.—Continued

[--, no value]

	All observations								Alluvial observations			Middle Claiborne observations		
Year	Mean (feet)	Minimum residual (feet)	Maximum residual (feet)	Root mean square error (RMSE) (feet)	Mean absolute error (feet)	Number of observa-tions	Range (feet)	Ratio of RMSE to range	Root mean square error (feet)	Number of observa-tions	Range (feet)	Root mean square error (feet)	Number of observa-tions	Range (feet)
1994	-5.49	-114.28	82.53	17.92	12.20	1198	707.32	0.03	16.35	1069	251.51	29.20	55	600.44
1995	-3.86	-93.32	183.95	19.57	13.33	1137	717.69	0.03	14.60	855	243.79	27.93	202	612.58
1996	-6.64	-122.67	111.77	21.30	14.18	1145	722.29	0.03	16.43	922	242.13	33.67	82	615.36
1997	-3.88	-137.83	84.07	20.61	14.27	953	623.85	0.03	15.66	659	243.15	30.14	231	623.85
1998	-6.37	-80.03	93.93	19.71	14.17	902	625.92	0.03	18.37	789	239.46	28.21	89	625.92
1999	-3.10	-93.59	89.16	20.40	14.45	919	626.11	0.03	15.76	668	241.32	29.89	223	626.11
2000	-5.81	-93.36	109.24	22.08	15.22	1083	631.29	0.03	18.35	851	245.28	31.26	130	631.29
2001	-3.19	-84.22	97.03	21.59	15.24	950	612.12	0.04	16.30	657	235.66	30.40	259	612.12
2002	-7.88	-89.04	100.45	21.33	14.99	887	627.24	0.03	20.06	777	235.85	30.34	73	627.24
2003	-5.84	-96.30	106.67	23.86	16.45	965	619.76	0.04	17.65	613	237.5	30.57	249	619.76
2004	-9.89	-91.53	112.45	23.20	16.32	854	625.54	0.04	21.37	732	237.19	35.46	84	625.54
2005	-7.88	-109.77	106.44	24.66	17.47	913	616.28	0.04	19.76	609	229.74	33.01	264	616.28
2006	-10.86	-98.92	110.53	25.23	17.78	904	627.42	0.04	22.11	722	228.24	36.60	83	627.42
2007	-8.61	-138.78	99.14	30.70	22.47	391	545.55	0.06	23.99	149	226.11	35.80	210	545.55
All	-1.15	-162.75	236.30	23.18	15.14	55786	741.66	0.03	16.43	39732	297.25	35.78	10265	634.94

zero (overprediction) and 31,530 residuals were less than zero (underprediction), resulting in a mean residual of -1.15 ft. The maximum and minimum residuals were 236.30 ft and -162.75 ft, respectively.

Streamflow Observations and Errors

Simulated streamflow generally is lower than measured streamflow for streams with streamflow less than 1,000 ft^3/s and greater than measured streamflow for streams with streamflow more than 1,000 ft^3/s (fig. 15). Simulated streamflow is underpredicted for 18 observations and overpredicted for 10 observations in the model. Four observations are not shown on figure 15—stream leakage for the White River and Nonconnah Creek and streamflow for the White River for pre- and post-development. The fraction of streamflow that is stream leakage for the White River was simulated as -0.042, which indicates by the negative value that flow is into the White River from the aquifer (4.2 percent of streamflow was gained from the groundwater system). The fraction of streamflow that is stream leakage for the White River was estimated by measurements to be 0.13 (13 percent of streamflow was lost to the aquifer). Stream leakage for Nonconnah Creek was simulated as 0.073 ft^3/s and the estimated stream leakage value for Nonconnah Creek was 0.100 ft^3/s (Nyman, 1965). While the simulated stream leakage for Nonconnah Creek closely matches the estimated value, the fraction of streamflow that is leakage for the White River is into the river (gaining) instead of out of the river (losing) as the estimated value indicates. One possible reason for the discrepancy includes pumping directly from the river. This pumping would remove water from the river resulting in a measured loss of streamflow that would appear to occur as leakage. Pre- and post-development streamflow for the White River was simulated as 4.02×10^4 ft^3/s and 2.47×10^4, respectively. Pre- and postdevelopment streamflow for the White River was measured as 1.85×10^4 and 1.27×10^4, respectively. Though the absolute differences between simulated and measured streamflow on the White River are great, the simulated values are considered a reasonable fit given the discretization of the simulated streams and other factors contributing to streamflow. These differences also illustrate the uncertainty in model inputs such as predevelopment recharge, overland flow, pumpage (from stream and aquifer), precipitation, and observation weights. Uncertainty in simulated streamflow values is compounded by the simulated hydraulic head in the surrounding aquifer. For example, if the simulated hydraulic head in the surrounding aquifer is slightly underpredicted, streamflow may simply be lost to the aquifer, instead of the stream gaining water from the aquifer. In these cases, a difference of a few feet may account for large differences in streamflow.

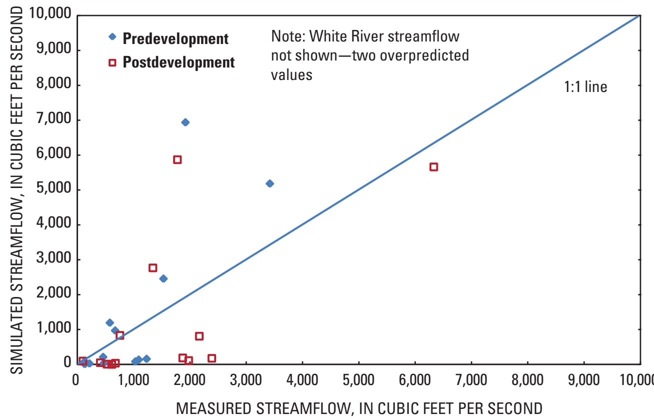

Figure 15. Simulated and measured streamflow.

Simulated and Observed Hydrographs

Simulated and observed hydrographs of hydraulic-head values completed in the alluvial aquifer and the middle Claiborne aquifer were used to examine the temporal trends of the model at selected wells in the model area (fig. 16). Hydrograph comparisons for the alluvial aquifer were based on wells used by Ackerman (1989). Most hydrograph comparisons for the middle Claiborne aquifer were based on wells used by Arthur and Taylor (1990). Though the simulated and observed hydrographs generally show declines in water levels, some hydrographs show slight increases in recent years (fig. 16 G, I, and J). Water-level increases can be attributed to various factors: water conservation, alternative water supplies, or the redistribution of well fields to pump from locations farther from the selected hydrograph wells (Freiwald and Johnson, 2007; Kingsbury, 1996).

The simulated and observed hydrographs show good agreement for most locations with relatively long periods of record (fig. 16). Some with a poorer fit to observed conditions (fig. 16 A and F) predict higher hydraulic heads throughout the period of measurement, or a steep decline in heads that observations do not reflect. Many of these differences are likely because of the placement and timing of pumping wells in the model, which are dependent on the accuracy of pumping data, as well as uncertainty in hydraulic property values.

Simulated and Observed Potentiometric Surfaces

Simulated potentiometric surfaces for 2007 generally agree with observed potentiometric surfaces (fig. 17). An embayment-wide potentiometric surface for the middle Claiborne aquifer was constructed representing the spring of 2007 (Schrader, 2007). The potentiometric surface was constructed using water-level measurements from 309 wells in Arkansas, 7 wells in Kentucky, 116 wells in Louisiana, 150 wells in Mississippi, 6 wells in Missouri, and 160 wells in Tennessee.

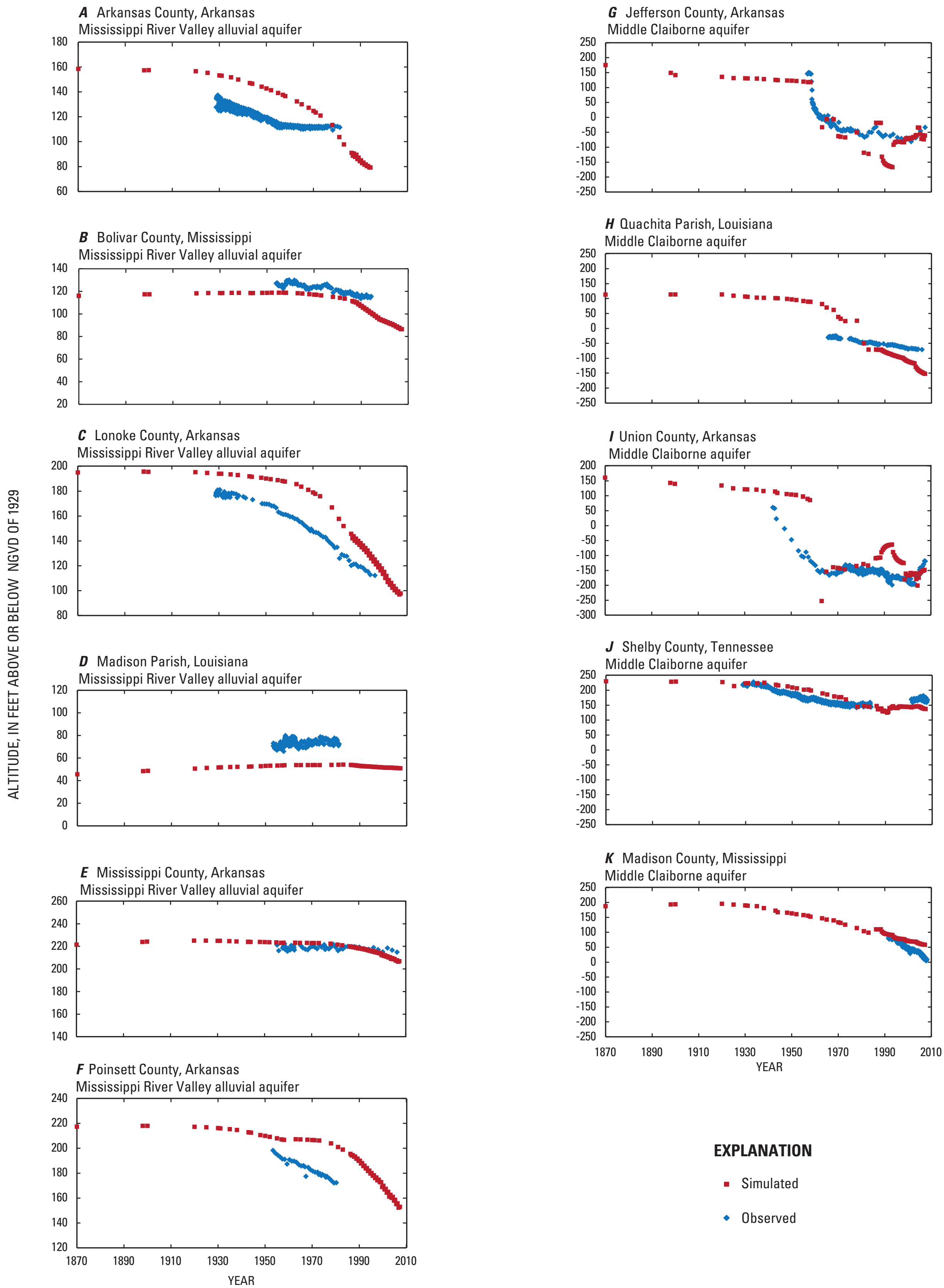

Figure 16. Simulated and observed hydrographs of hydraulic head in selected wells.

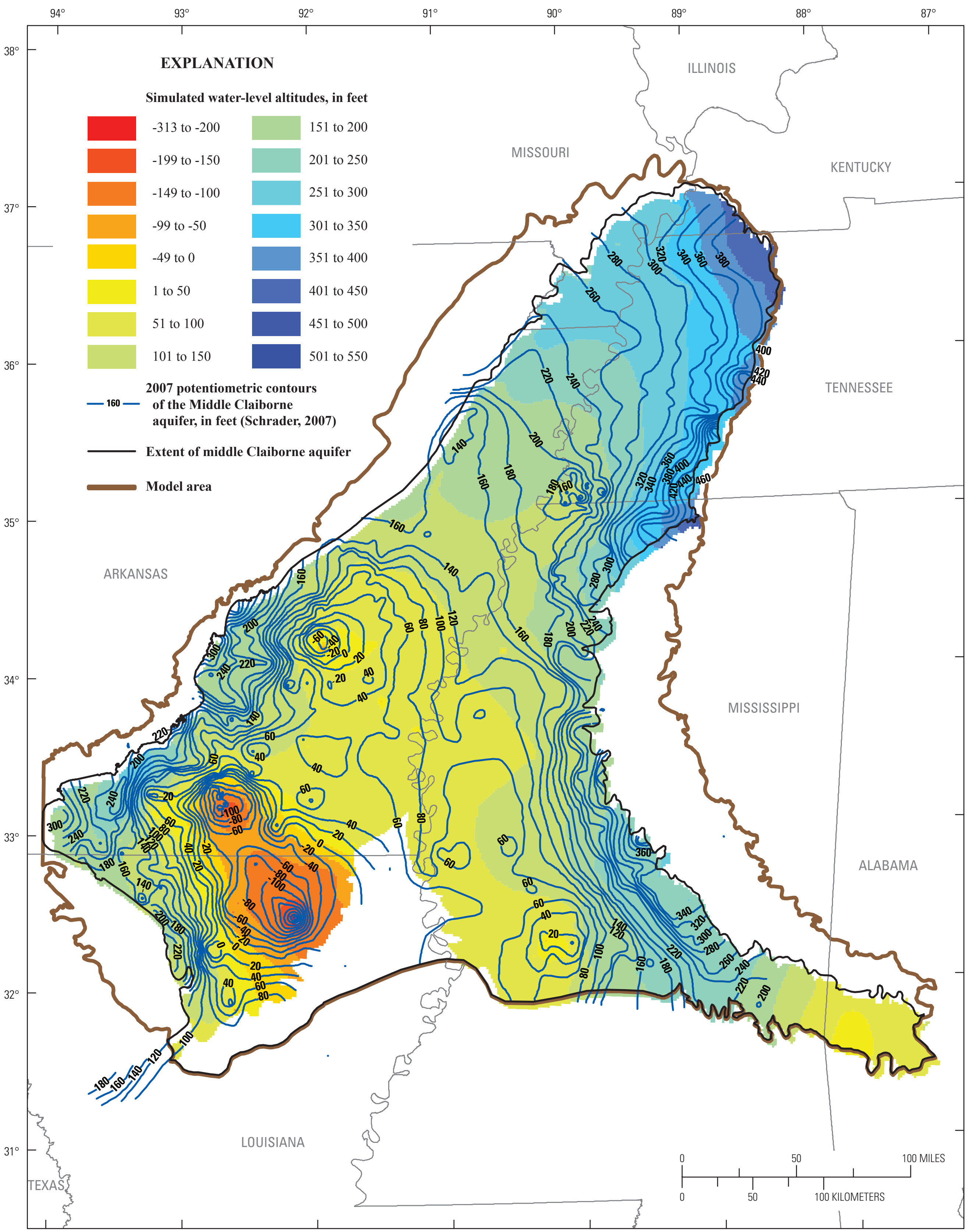

Potentiometric contours from Schrader (2007)

Figure 17. Potentiometric surface and simulated water levels for the middle Claiborne aquifer, 2007.

This potentiometric surface indicates a relief in water-level altitude of over 700 ft from the highest to lowest water level in the middle Claiborne aquifer. Potentiometric-surface contours for spring 2007, overlain on simulated hydraulic heads, give a reasonable qualitative match to cones of depression in central and southern Arkansas, northern Louisiana, and southern Mississippi (fig. 17). The simulated hydraulic heads also approximate large gradients in southern Arkansas, thought to be influenced by faulting in the area.

Sensitivity Analysis

The sensitivity of hydraulic heads to various model parameters was calculated using UCODE-2005 (Poeter and others, 2005). Composite scaled sensitivities (CSS) were calculated for all 104 parameters (table 3). CSS values aid in determining if there is adequate information in the calibration data to estimate a particular parameter. CSS values less than about 0.01 times the largest CSS indicate that the regression may not be able to estimate the parameter (Hill, 1998).

The CSS calculated using initial parameter values provided an indication of which model parameters were most important to estimate in the nonlinear-regression procedure and which should be set to fixed values. However, the CSS values are dependent on the parameter values because the sensitivities are a nonlinear function of the model parameters. Two of the defined parameters have CSS values greater than 10 (fig. 18): hydraulic conductivity of the middle Claiborne aquifer in the southwestern part of the model area (HK_sprt3) and hydraulic conductivity of the middle Claiborne aquifer primarily in the central part of the model area (HK_sprt2). The next highest parameters with a CSS over 6 are recharge to terrace deposits (RCHTRRC), hydraulic conductivity of the El Dorado Sand (HK_spes), and predevelopment precipitation (predevrch) (table 3).

Normality of Weighted Residuals

Normality of weighted residuals is a prerequisite for a valid regression. If the model accurately represents the system, the weighted residuals are expected to be random, independent, and normally distributed (Hill, 1998). The independence and normality of the weighted residuals can be assessed through use of (1) the summary statistic, R_N^2, which represents the correlation coefficient between the ordered weighted residuals and order statistics from the normal probability distribution function (Hill and others, 2000) and (2) a histogram of the weighted residuals. The weighted residuals are thought to be independent and normally distributed if the computed value of R_N^2 for a calibration is higher than the tabulated critical value. The critical value of R_N^2 is 0.987 for a set of 200 observations (maximum number of observations for which a value has been tabulated). The value of R_N^2 for hydraulic heads in the model calibration is 0.95, which is smaller than the critical value; however Hill and Tiedeman (2007) state “correlations less than these critical values may

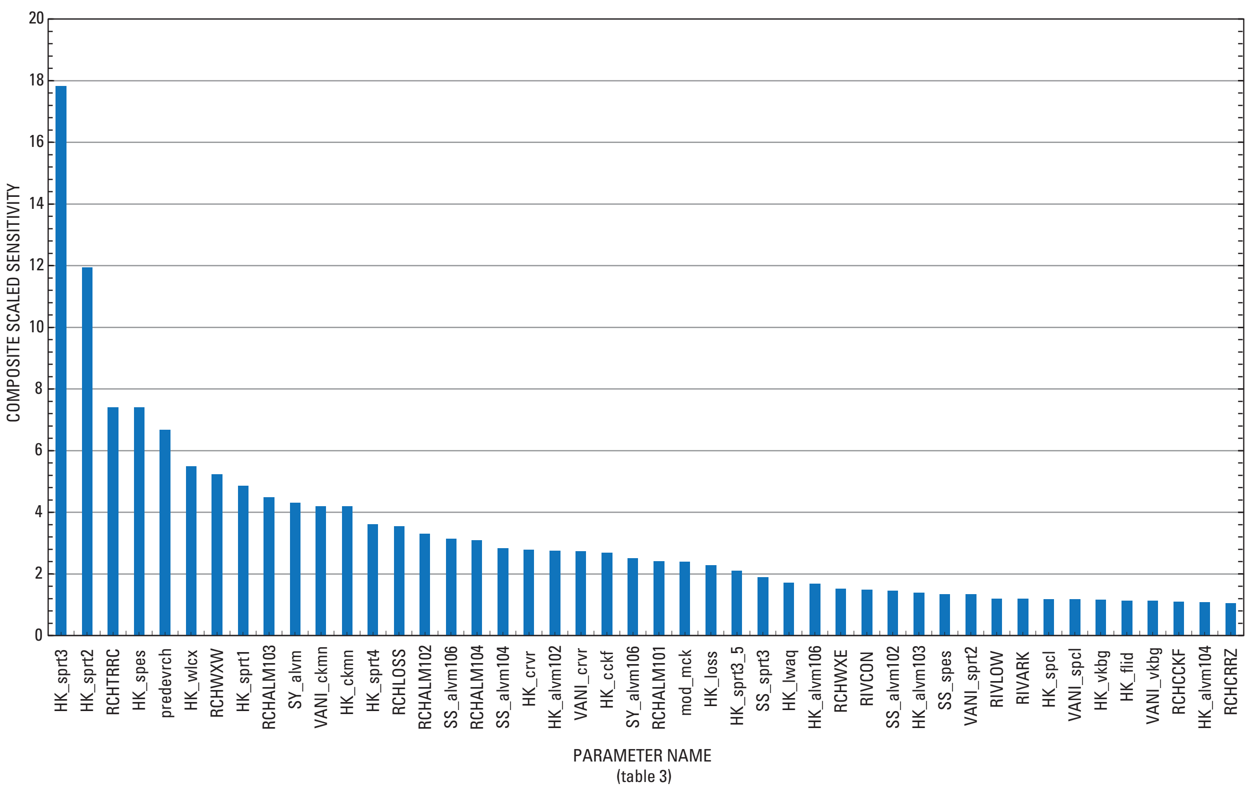

Figure 18. Composite scaled sensitivity values.

be acceptable…”. A histogram (fig. 19) of all 55,786 weighted residuals shows an approximately normal distribution with the mode occurring in the -25 ft to 25 ft interval.

Parameter correlations were computed using the approximate covariance matrix for the parameters, which is calculated as part of the nonlinear-regression method (Hill and others, 2000). If a pair of parameters has a correlation coefficient near 1.0 or -1.0, independent estimation of the two parameters is not possible given the calibration data set used in the regression. In the calibration, eight parameter pairs have correlations greater than 0.85.

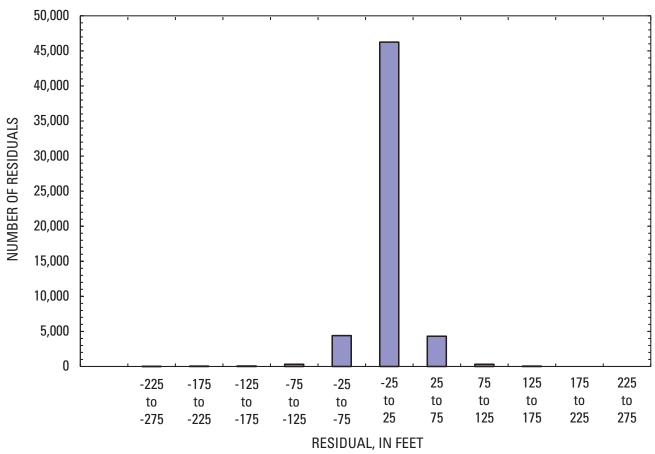

Figure 19. Histogram of weighted residuals.

Typically, correlations greater than 0.95 suggest problems with parameter nonuniqueness (Hill, 1998), and there were not enough observation data to independently estimate the model parameters. In these cases, the model may only be estimating the ratio or sum of the highly correlated parameters. HK_ckmn, VANI_ckmn, HK_crvr, and VANI_crvr (table 3) have the largest absolute correlations of any parameter pair at 1.0 each. However, through the use of SVDA during the calibration process of PEST, it was possible to estimate values for combinations of these parameters.

Graphical analyses of the weighted residuals facilitate assessment of model bias or error and of model fit to the calibration data. These analyses include plots of the weighted observed and weighted simulated values and of the spatial and temporal distribution of the weighted hydraulic-head residuals.

The plot of weighted observed and weighted simulated equivalents for an unbiased model ideally should show a random distribution of the weighted residuals above and below zero for all weighted simulated equivalents. In this case, the model fit is generally similar over the entire range of available hydraulic head values, and the calibration has, in general, the desired random distribution of weighted residuals (fig. 20).

Additional assessments of model error are accomplished through analysis of the spatial and temporal distribution of weighted residuals for years after 2000 (fig. 21). Different ranges in residuals are represented by a variety of geometric symbols for visual analysis of model bias. Residuals representing observation data following the year 2000 provide the best guide during model calibration because of (1) improved water-use data for later years and (2) the high number and uniform distribution of wells. Positive residuals, shown in blue, indicate simulated hydraulic heads that are higher than observed,

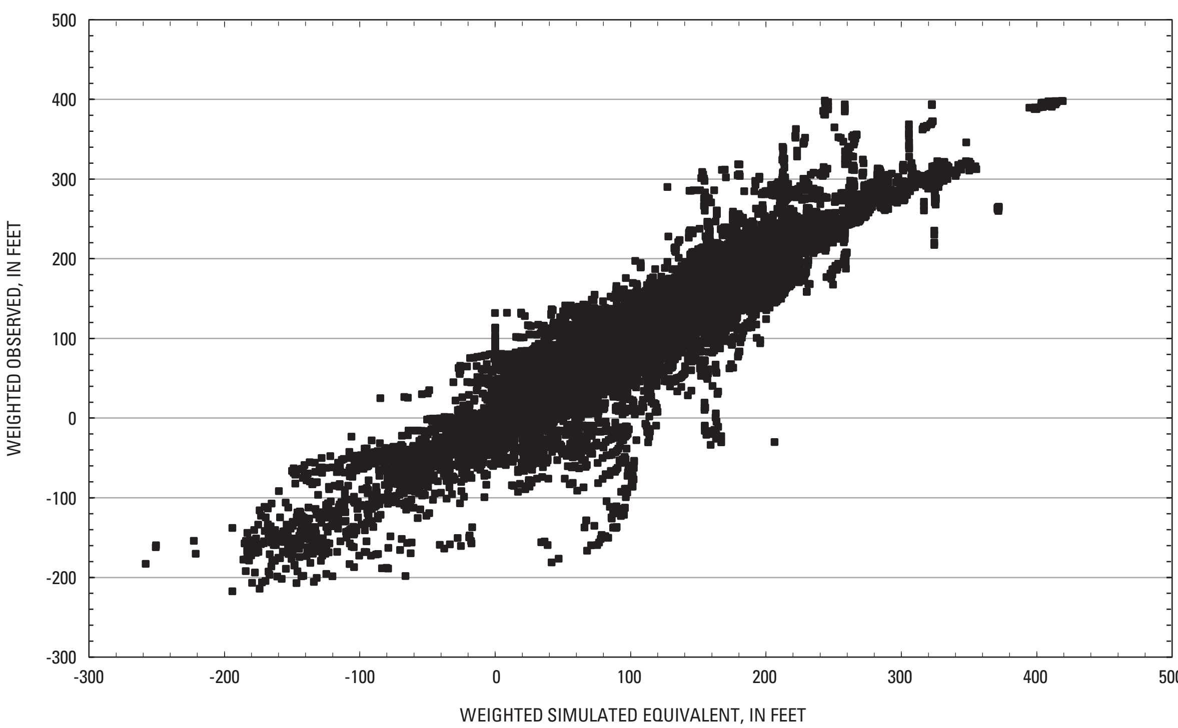

Figure 20. Weighted simulated equivalent plotted against weighted observed.

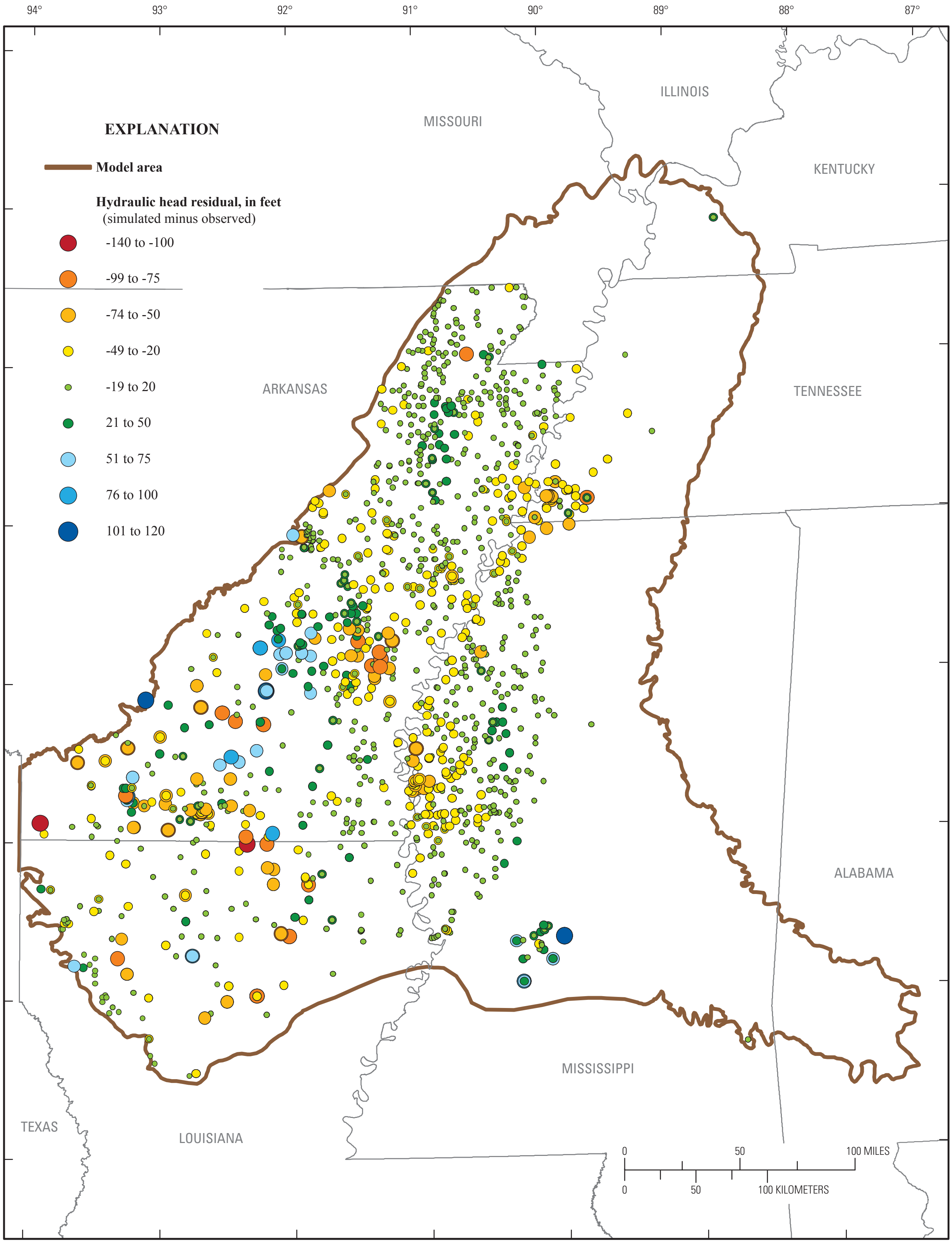

Figure 21. Spatial distribution of hydraulic-head residuals after 2000.

while negative residuals indicate simulated hydraulic heads that are lower than observed.

Ideally, negative and positive weighted residuals should be small and randomly distributed in space. Clustering of residuals with similar magnitudes and signs is indicative of model bias. Overall, residuals (fig. 19) appear to be well distributed in both magnitude and sign (±). In many cases, insufficient reporting of well completion data makes it difficult to determine in which aquifer the well is screened or whether it is screened in both aquifers. The uncertainty of the aquifer assignment to a well may result in inaccurate assignment of the well within the model layers, which can affect the simulated water level and residual.

Geologic structure and averaging of pumpage data can affect model bias. A possible cause of model bias occurs in southern Arkansas where geologic studies suggest considerably more heterogeneity in geologic conditions and faulting than is presently mapped and represented by the simple zones and flow boundaries in the current model. In addition, model bias through time may be caused by the temporal averaging of groundwater withdrawals to obtain the mean annual pumpage used in each stress period and the spatial averaging of pumpage from several wells located in a single model cell.

The weighted residuals ideally should show no temporal bias and be balanced around zero. All of the weighted residuals are less than 250 ft in absolute value. Upward trends with time may occur because of some wells having hydraulic-head measurements only at later times in the simulation. For each year, the number of positive residuals is approximately equal to negative residuals, and there appears to be a slight trend through time from overprediction to underprediction as indicated by the mean for all observations (table 5).

Groundwater-Flow Budget

The groundwater-flow budget indicates changes in flow into (inflows) and out of (outflows) the model area from the predevelopment period (pre-1870) to 2007 (fig. 22). Negative rates indicate outflows from the groundwater system, and positive rates indicate inflows to the groundwater system. Total flow (sum of inflows or outflows) through the model ranged from about 600 Mgal/d in predevelopment to 18,197 Mgal/d near the end of the simulation. This increase in simulated flow through the model reflects increases in pumpage and inflow from the predevelopment condition. There are three inflows to the model listed from largest to smallest: withdrawal from storage, areal recharge, and stream leakage. There are three discharges or outflows listed from largest to smallest: pumpage from wells, addition to storage, and stream leakage. The pumpage from wells represents the largest outflow components with a net rate of 18,197 Mgal/d near the end of the model simulation in 2006. Groundwater outflows are offset primarily by inflow from aquifer storage.

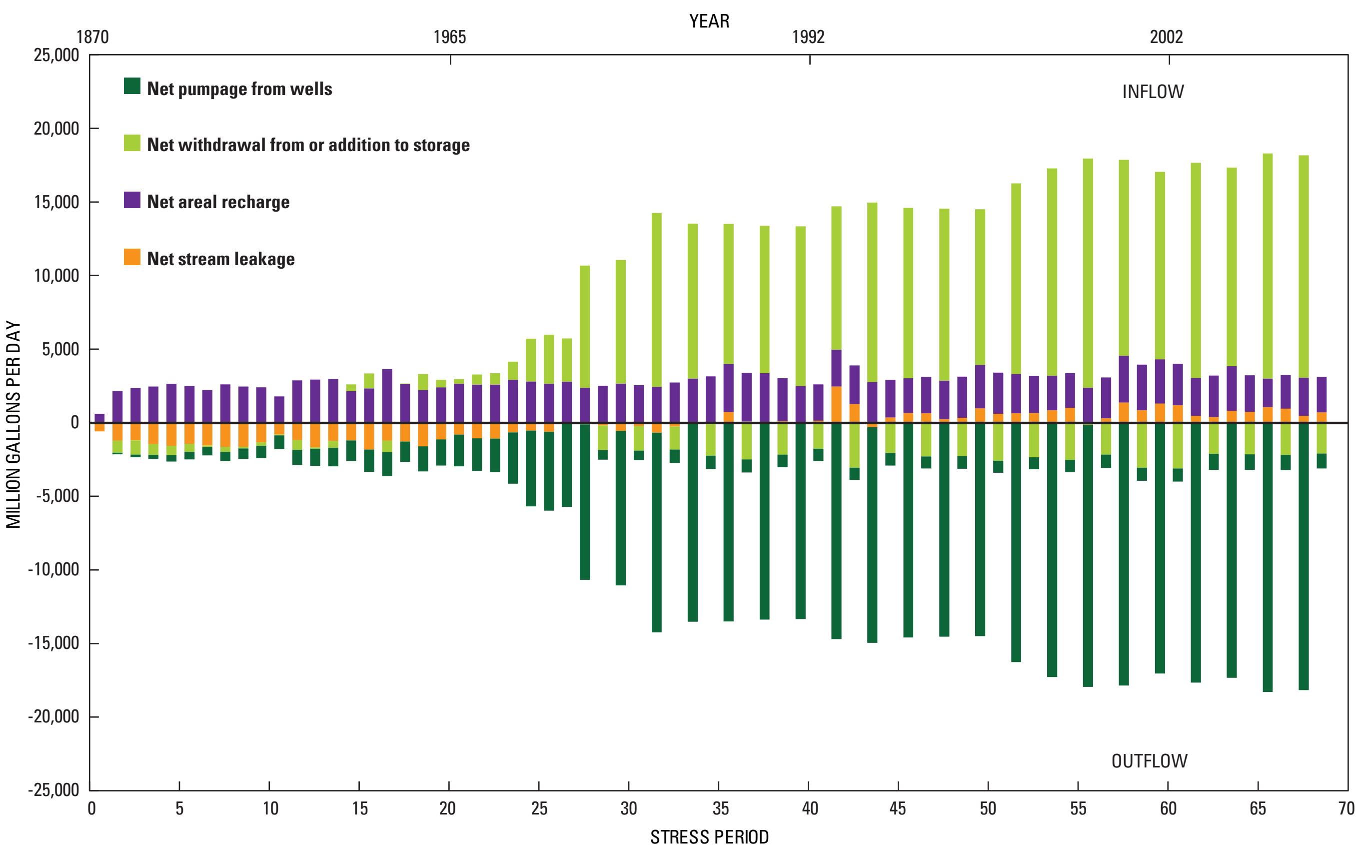

Figure 22. Groundwater-flow budget.

Limitation of Analyses

An understanding of model limitations is essential to effectively use flow and hydraulic head simulation results. The accuracy of a groundwater model is limited by simplification of complexities within the flow system (conceptual model), space and time discretization effects, and assumptions made in the formulation of the governing flow equations. Model accuracy also is affected by cell size, number of layers, accuracy of boundary conditions, accuracy and availability of hydraulic property data, accuracy of withdrawal and areal recharge estimates, historical data for calibration, parameter sensitivity, and the interpolations and extrapolations that are inherent in using data in a model. Although a model might be calibrated, the calibration parameter values are not unique in yielding acceptable distributions of hydraulic head.

Results of the MERAS model must be evaluated while taking into account the resolution of these limitations. The placement and timing of pumping wells in the model, which are dependent on the accuracy of pumping data, play a crucial role in the simulated hydraulic head and flow values. Much of the pumping data in the model is based on 5-year county totals and trend analysis from these 5-year totals. Very little site-specific pumping data are available relative to the temporal and spatial extent of the model area. Additionally, few data exist pertaining to wells that are screened through multiple hydrogeologic units. Though the model is capable of simulating multi-screened wells, assumptions were made regarding the number and location of these wells and number of hydrogeologic units through which they are screened. Data regarding predevelopment conditions for streamflow and hydraulic head are sparse to nonexistent, therefore model calibration to predevelopment conditions are not well constrained. The temporal disrectization of the model is determined, in part, by data resolution and, therefore, varies from 6 months to 28 years in stress period length. Each stress period incorporates average input values for pumpage, streamflow, and precipitation for the given time interval. Groundwater flow from underlying or adjacent systems is not well defined, though the contribution from such systems is considered negligible compared to the overall flow within the Mississippi embayment aquifer system. Model framework, which includes the altitude and thickness of hydrogeologic units, are based on available geophysical information, which varies spatially and vertically throughout the model area. Areas of sparse geophysical information may affect model results through assumptions in the altitude and thickness of these hydrogeologic units, and the lack of definition of structural controls that may affect groundwater movement. The horizontal hydraulic conductivity values assigned to many hydrogeologic units also are modified based on an assumption of sand percentage evaluated through the use of geophysical logs. The assumption of a no-flow boundary at the freshwater-saltwater interface and constant density of water may not be entirely valid, thus the need for simulations including variable density may be warranted in local areas where high salinity water is problematic.

The goal of the MERAS model was to develop a model capable of suitable accuracy at regional scales. The intent was not to reproduce individual local-scale details, which are typically not possible given the uniform cell size of 1 mi^2. Although the MERAS model may not represent each local-scale detail, it is relevant for a better understanding of the regional flow system.

Summary

The Mississippi Embayment Regional Aquifer Study (MERAS) was conducted with support from the Groundwater Resources Program of the U.S. Geological Survey Office of Groundwater. This report documents the model construction and calibration for use as a tool to quantify groundwater availability within the Mississippi embayment. To approximate the differential equations governing three-dimensional groundwater flow, the MERAS model used the U.S. Geological Survey's modular three-dimensional finite-difference code, MODFLOW-2005; the preconditioned conjugate gradient solver was used for the numerical solution technique. The model area boundary is approximately 78,000 mi^2 and includes eight States with approximately 6,900 mi of simulated streams, 70,000 well locations, and 10 primary hydrogeologic units. The finite-difference grid consists of 414 rows, 397 columns, and 13 layers. Each model cell is 1 mi^2 with varying thickness by cell and by layer. The simulation period extends from January 1, 1870, to April 1, 2007, for a total of 137 years and 69 stress periods. The first stress period is simulated as steady state to represent predevelopment conditions.

Areal recharge is applied throughout the MERAS model area using the MODFLOW-2005 Recharge Package. Recharge rates were estimated as a fraction (ranging from 1.25×10^{-4} to 7.06×10^{-2}) of precipitation based on typical literature values and soil type and modified during calibration of the regional model. Irrigation, municipal, and industrial wells are simulated using the Multi-Node Well Package. Pumpage from each multi-node well was input from site-specific data, 5-year water-use reports, and trend analysis. There are 43 streams simulated by the MERAS model. Each stream or river in the model area was simulated using the Streamflow-Routing Package of MODFLOW-2005. The base of the flow system is represented in the MERAS model as a no-flow boundary, which coincides with the top of the Midway confining unit. The downgradient limit of each model layer is a no-flow boundary, which approximates the extent of water with less than 10,000 mg/L dissolved solids. Initial conditions are simulated with a steady-state stress period (representing conditions prior to January 1, 1870) at the beginning of the simulation.

The MERAS model was calibrated by making manual changes to parameter values and examining residuals for hydraulic heads and streamflow. Additional calibration was achieved through alternate use of UCODE-2005 and PEST. Simulated heads were compared to 55,786 hydraulic-head measurements from 3,245 wells in the MERAS model area. Values of root mean square error between simulated and observed hydraulic heads ranged from 8.33 in 1919 to 47.65 in 1951, though only six annual root mean square error values are greater than 40 feet for the entire simulation period. The root mean square error for all observations in the model was 23.18 ft with a range in hydraulic-head altitudes of 741.66 ft. Simulated streamflow generally is lower than measured streamflow for streams with streamflow less than 1,000 ft^3/s, and greater than measured the streamflow for streams with streamflow more than 1,000 ft^3/s. Simulated streamflow is underpredicted for 18 observations and overpredicted for 10 observations in the model. These differences in streamflow illustrate the large uncertainty in model inputs such as predevelopment recharge, overland flow, pumpage (both from stream and aquifer), and precipitation, and observation weights.

The groundwater-flow budget indicates changes in flow into (inflows) and out of (outflows) the model area during the pregroundwater-irrigation period (pre-1870) to 2007. Total flow (sum of inflows or outflows) through the model ranged from about 600 million gallons per day in predevelopment to 18,197 million gallons per day near the end of the simulation. This increase in simulated flow through the model reflects increases in withdrawals and inflow from the pre-groundwater irrigation condition. The multi-node wells represent the largest outflow components with a net rate of 18,197 million gallons per day near the end of the model simulation in 2006. Groundwater outflows are offset primarily by inflow from aquifer storage and recharge.

Acknowledgments

The compilation of data for thousands of pumping and observations wells, miles of simulated rivers, streamflow, and the hydrogeologic framework for an area of this size in a relatively short period of time into a manageable model was not a trivial task. The authors would like to thank those who have given their time and expertise in model simulations and construction: Arlen Harbaugh, Tom Reilly, Connor Haugh, and Randy Hunt, as well as many others who have contributed to this investigation.

References Cited

Ackerman, D.J., 1989, Hydrology of the Mississippi River Valley alluvial aquifer, south-central United States – A preliminary assessment of the regional flow system: U.S. Geological Survey Water-Resources Investigations Report 88-4028, 80 p.

Ackerman, D.J., 1996, Hydrology of the Mississippi River Valley alluvial aquifer, South-Central United States: U.S. Geological Survey Professional Paper, 1416-D, 56 p.

Albin, D.R., 1964, Geology and ground-water resources of Bradley, Calhoun, and Ouachita Counties, Arkansas: U.S. Geological Survey Water Supply Paper 1779-G, 32 p.

Arthur, J.K., and Taylor, R.E., 1998, Ground-water flow analysis of the Mississippi embayment aquifer system, south-central United States: U.S. Geological Survey Professional Paper, 1416-I, 148 p.

Arthur, J.K., and Taylor, R.E., 1990, Definition of the geohydrologic framework and preliminary simulation of ground-water flow in the Mississippi embayment aquifer system, Gulf Coastal Plain, United States: U.S. Geological Survey Water Resources Investigations Report, 86-4364, 97 p.

Arthur, J.K., 2001, Hydrogeology, model description, and flow analysis of the Mississippi River alluvial aquifer in northwestern Mississippi: U.S. Geological Survey Water-Resources Investigations Report, 2001-4035, 47 p.

Beckman, J.D., and Williamson, A.K., 1990, Salt-dome locations in the Gulf Coastal Plain, South-Central United States: U.S. Geological Survey Water-Resources Investigations Report 90-4060, 44 p.

Brahana, J.V., and Broshears, R.E., 2001, Hydrogeology and ground-water flow in the Memphis and Fort Pillow aquifers in the Memphis area, Tennessee: U.S. Geological Survey Water-Resources Investigations Report 89-4131, 56 p.

Brahana, J.V., and Mesko, T.O., 1988, Hydrogeology and preliminary assessment of regional flow in the upper Cretaceous and adjacent aquifers in the northern Mississippi embayment: U.S. Geological Survey Water-Resources Investigations Report, 87-4000, 65 p.

Clark, B.R., Landon, M.K., Kauffman, L.J., and Hornberger, G.Z., 2008, Simulations of ground-water flow, transport, age, and particle tracking near York, Nebraska, for a study of transport of anthropogenic and natural contaminants (TANC) to public supply wells: U.S. Geological Survey Scientific Investigations Report 2007–5068, 48 p.

Cushing, E.M., Boswell, E.H., Speer, P.R., and Hosman, R.L., 1970, Availability of water in the Mississippi embayment: U.S. Geological Survey Professional Paper, 448-A, 11 p.

Daly, C., Taylor, G.H., Gibson, W.P., Parzybok, T.W., Johnson, G.L, Pasteris, P., 2000, High-quality spatial climate data sets for the United States and beyond: Transactions of the American Society of Agricultural Engineers, V. 43, p. 1957-1962.

Doherty, John, 2008, PEST model-independent parameter estimation user manual: 5th ed., Watermark Numerical Computing, accessed October 28, 2008 at http://www.grac.org/pest.html

Doherty, John, 2003, Ground water model calibration using pilot points and regularization: Ground Water v. 41, no. 2, p. 170-177.

Doherty, J., and Hunt, R.J., 2009, Two statistics for evaluating parameter identifiability and error reduction. Journal of Hydrology v. 366, p. 119-127.

Fenneman, N.M., and Johnson, D.W., 1946, Physical divisions of the United States (Map): Washington, D.C., U.S. Geological Survey.

Fetter, C.W., 1994, Applied hydrogeology, (3d ed.): New York, MacMillan College Publishing Co., Inc., 691 p.

Fienen, M.N., Muffles, C.T., and Hunt, R.J., 2009, On constraining pilot point calibration with regularization in PEST: Ground Water, 2009, accessed September 29, 2009, at http://www3.interscience.wiley.com/cgi-bin/fulltext/122343976/HTMLSTART

Fitzpatrick, D.J., Kilpatrick, J.M., and McWreath, H.,1990, Geohydrologic characteristics and simulated response to pumping stresses in the Sparta aquifer in east-central Arkansas: U.S. Geological Survey Water-Resources Investigations Report 88-4201, 50 p.

Freeze, R.A., and Cherry, J.A., 1979, Groundwater: Englewood Cliffs, New Jersey, Prentice-Hall, 604 p.

Freiwald, D.A., and Johnson, S.F., 2007, Monitoring of Sparta aquifer recovery in southern Arkansas and northern Louisiana, 2003-07: U.S. Geological Survey Fact Sheet 2007-3102, 4 p.

Halford, K.J. and Hanson, R.T., 2002, User guide for the drawdown-limited, multi-node well (MNW) package for the U.S. Geological Survey's modular three-dimensional finite-difference ground-water flow model, versions MODFLOW-96 and MODFLOW-2000: U.S. Geological Survey Open-File Report 02-293, 33 p.

Hall, D.H., 1989, Estimated use of water in Missouri during 1985: U.S. Geological Survey Water-Resources Investigations Report 89-4038, 1 sheet.

Hanson, R.T, Li, Zhen, and Faunt, C.C., 2004, Documentation of the Santa Clara Valley regional ground-water/surface-water flow model, Santa Clara County, California: U.S. Geological Survey Scientific Investigations Report 2004-5231, 75 p.

Harbaugh, A.W., 2005, MODFLOW-2005, the U.S. Geological Survey modular ground-water model—The ground-water flow process: U.S. Geological Survey Techniques and Methods 6-A16, variously paged.

Hart, R.M., Clark, B.R., and Bolyard, S.E., 2008, Digital hydrogeologic surface and thickness for the hydrogeologic units of the Mississippi Embayment Regional Aquifer Study (MERAS): U.S. Geological Survey Scientific Investigations Report 2008-5098, 33 p., accessed December 4, 2008, at http://pubs.usgs.gov/sir/2008/5098/pdf/SIR2008-5098.pdf

Hart, R.M., and Clark, B.R., 2008a, Geophysical well-log database for the Mississippi Embayment Regional Aquifer Study (MERAS): U.S. Geological Survey Scientific Investigations Report 2008-5192, 8 p., accessed December 4, 2008, http://pubs.usgs.gov/sir/2008/5192/pdf/SIR2008-5192.pdf

Hart, R.M. and Clark, B.R., 2008b, Automated method using geophysical logs to determine hydrogeologic unit sand percent for ground-water model development: *in* Poeter, E.P., Zheng, C., Hill, M.C., eds. Proceedings, Modflow and more 2008, Ground Water and Public Policy: Golden, CO, Colorado School of Mines, May 19-21, 2008, p. 138-142.

Hays, P.D, Lovelace, J.K., and Reed, T.B., 1998, Simulated response to pumping stress in the Sparta aquifer of southeastern Arkansas and north-central Louisiana, 1998-2027: U.S. Geological Survey Water-Resources Investigations Report 98-4121, 25 p.

Hill, M.C., 1990, Preconditioned conjugate-gradient 2 (PCG2), a computer program for solving ground-water flow equations: U.S. Geological Survey Water-Resources Investigations Report 90-4048, 43 p.

Hill, M.C., 1998, Methods and guidelines for effective model calibration: U.S. Geological Survey Water-Resources Investigations Report 98-4005, 90 p.

Hill, M.C., Banta, E.R., Harbaugh, A.W., Anderman, E.R., 2000, MODFLOW-2000, The U.S. Geological Survey modular ground-water model-user guide to the observation, sensitivity, and parameter-estimation processes and three post-processing programs: U.S. Geological Survey Open-File Report 00-184, 209 p.

Hill, M.C., and Tiedeman, C.R., 2007, Effective groundwater model calibration: Hoboken, New Jersey, John Wiley & Sons, Inc., , 455 p.

Holland, T.W., 1999, Water use in Arkansas, 1995: U.S. Geological Survey Open-File Report 99-188, 1 sheet.

Hosman, R.L., 1982, Outcropping Tertiary units in southern Arkansas: U.S. Geological Survey Miscellaneous Investigations Series I-1405, scale 1:250,000.

Hosman, R.L., 1988, Geohydrologic framework of the Gulf Coastal Plain: U.S. Geological Survey Hydrologic Investigations Atlas 695, scale 1:2,500,000, 2 sheets.

Hosman, R.L., 1996, Regional stratigraphy and subsurface geology of Cenozoic deposits, Gulf Coastal Plain, South-Central United States: U.S. Geological Survey Professional Paper 1416-G, 35 p.

Hosman, R.L., and Weiss, J.S., 1991, Geohydrologic units of the Mississippi embayment and Texas Coastal Uplands aquifer systems, South-Central Unites States: U.S. Geological Survey Professional Paper 1416-B, 19 p.

Hunt, R.J., Doherty, J., and Tonkin, M.J., 2007, Are models too simple? Arguments for increased parameterization: Ground Water, v. 45, no. 3, 254-262.

Hutson, S.S., Barber, N.L., Kenny, J.F., Linsey, K.S., Lumia, D.S., and Maupin, M.A., 2004, Estimated use of water in the United States in 2000: U.S. Geological Survey Circular 1268, 46 p.

Johnson, P.M., 1994, Estimated water withdrawals in Mississippi during 1990: U.S. Geological Survey Fact Sheet 94-060, 2 p.

Kingsbury, J.A., 1996, Altitude of the potentiometric surfaces, September 1995, and historical water-level changes in the Memphis and Fort Pillow aquifers in the Memphis area, Tennessee: U.S. Geological Survey Water-Resources Investigations Report 96-4278, 1 sheet.

Kingsbury, J.A., and Parks, W.S., 1993, Hydrogeology of the principal aquifers and relation of faults to interaquifer leakage in the Memphis area, Tennessee: U.S. Geological Survey Water-Resources Investigations Report 93-4075, 22 p.

Kleiss, B.A., Coupe, R.H., Gonthier, G.J., and Justus, B.J., 2000, Water quality in the Mississippi embayment, Mississippi, Louisiana, Arkansas, Missouri, Tennessee, and Kentucky, 1995–98: U.S. Geological Survey Circular 1208, 36 p., online at http://pubs.water.usgs.gov/circ1208/

Lloyd, O.B., Jr., and Lyke, W.L., 1995, Ground water atlas of the United States: Segment 10, Illinois, Indiana, Kentucky, Ohio, Tennessee: U.S. Geological Survey Hydrologic Atlas 730-K.

Mahon, G.L., and Ludwig, A.H., 1990, Simulation of ground-water flow in the Mississippi River alluvial aquifer in eastern Arkansas: U.S. Geological Survey Water-Resources Investigations Report 89-4145, 57 p.

Mahon, G.L., and Poynter, D.T., 1993, Development, calibration, and testing of ground-water flow models for the Mississippi River Valley alluvial aquifer in eastern Arkansas using one-square-mile cells: U.S. Geological Survey Water-Resources Investigations Report 92-4106, 33.

Mancini, E.A., and Tew, B.H., 1994, Claiborne-Jackson Group contact (Eocene) in Alabama and Mississippi: Gulf Coast Association of Geological Societies Transactions, v. 44, p. 431-439.

McKee, P.W., and Clark, B.R., 2003, Development and calibration of a ground-water flow model for the Sparta aquifer of southeastern Arkansas and north-central Louisiana and simulated response to withdrawals, 1998-2027: U.S. Geological Survey Water-Resources Investigations Report 03-4132, 71 p.

McMahon, P.B., Dennehy, K.F., Bruce, B.W., Böhlke, J.K., Michel, R.L., Gurdak, J.J., and Hurlbut, D.B., 2006, Storage and transit time of chemicals in thick unsaturated zones under rangeland and irrigated cropland, High Plains, United States: Water Resources Research, v. 42, no. 3, p. 1-18.

Mehl, S.W., and Hill, M.C., 2007, MODFLOW-2005, The U.S. Geological Survey modular ground-water model—Documentation of the multiple-refined-areas capability of Local Grid Refinement (LGR) and the Boundary Flow and Head (BFH) Package: U.S. Geological Survey Techniques and Methods 6-A21, 13 p.

Mooty, W.S., and Richardson, J.R., 1998, Water use in Alabama, 1995: U.S. Geological Survey Water-Resources Investigations Report 98-4154, 92 p.

Murray, L.C. Jr., 2007, Analysis of water-level differentials and variations in recharge between the surficial and Upper Floridan aquifers in east-central and northeast Florida: U.S. Geological Survey Scientific Investigations Report, 2007-5081, 58 p.

National Oceanic and Atmospheric Administration, 2009, NOAA Southern Regional Climate Center, accessed January 13, 2009 at http://www.srcc.lsu.edu/southernClimate/atlas/

Nyman, D.J., 1965, Predicted hydrologic effects of pumping from the Lichterman well field in the Memphis area, Tennessee: U.S. Geological Survey Water Supply Paper 1819-B, 26 p.

Parks, W.S., 1990, Hydrogeology and preliminary assessment of the potential for contamination of the Memphis aquifer in the Memphis area, Tennessee: U.S. Geological Survey Water-Resources Investigations Report 90-4092, 39 p.

Parks, W.S. and Lounsbury, R.W., 1976, Summary of some current and possible future environmental problems related to geology and hydrology at Memphis, Tennessee: U.S. Geological Survey Water-Resource Investigations, 4-76, 34 p.

Payne, J.N., 1968, Hydrologic significance of the lithofacies of the Sparta Sand in Arkansas, Louisiana, Mississippi, and Texas: U.S. Geological Survey Professional Paper 569-A, 17 p.

Petersen, J.C., Broom, M.E., and Bush, W.V., 1985, Geohydrologic units of the Gulf Coastal Plain in Arkansas: U.S. Geological Survey Investigations Report 85-4116, 20 p.

Pettijohn, R.A., Weiss, J.S., and Williamson, A.K., 1988, Distribution of dissolved-solids concentrations and temperature in ground water of the Gulf Coast aquifer systems, South-Central United States: U.S. Geological Survey Water-Resources Investigations Report 88-4082, scale 1:3,500,000, 5 sheets.

Poeter, E.P., Hill, M.C., Banta, E.R., Mehl, Steffen, and Christensen, Steen, 2005, UCODE_2005 and six other computer codes for universal sensitivity analysis, calibration, and uncertainty evaluation: U.S. Geological Survey Techniques and Methods 6-A11, 283 p.

PRISM Group, 2006, PRISM Group, accessed September 12, 2006, at www.ocs.orst.edu/prism/.

Prudic, D.E., Konikow, L.F., and Banta, E.R., 2004, A new streamflow-routing (SFR1) package to simulate stream-aquifer interaction with MODFLOW-2000: U.S. Geological Survey Open-File Report 2004-1042, p. 95.

Prudic, D.E., 1991, Estimates of hydraulic conductivity from aquifer-test analyses and specific capacity data, Gulf Coast Regional Aquifer Systems, South-Central United States: U.S. Geological Survey Water-Resources Investigations Report 90-4121, 38 p.

Reed, T.B., 2003, Recalibration of a ground-water flow model of the Mississippi River Valley alluvial aquifer of northeastern Arkansas, 1918-1998, with simulations of water levels caused by projected ground-water withdrawals through 2049: U.S. Geological Survey Water-Resources Investigations Report 2003-4109, 58 p.

Reed, J.E., 1972, Analog simulation of water-level declines in the Sparta Sand, Mississippi embayment: U.S. Geological Survey Hydrologic Atlas, HA 434, 5 maps.

Sargent, B.P., 2007, Water use in Louisiana, 2005: Louisiana Department of Transportation and Development Water Resources Special Report no. 16, 133 p.

Saucier, R.T., 1994, Geomorphology and Quaternary geologic history of the Lower Mississippi Valley, Volume I: U.S. Army Corps of Engineers Waterways Experiment Station, Vicksburg, Mississippi, 400 p.

Scheiderer, R.M. and Freiwald, D.A., 2006, Monitoring the recovery of the Sparta aquifer in southern Arkansas and northern Louisiana: U.S. Geological Survey Fact Sheet 2006-3090, 4 p.

Schrader, T.P., 2007, Potentiometric surface in the Sparta-Memphis aquifer of the Mississippi Embayment, spring 2007: U.S. Geological Survey Scientific Investigations Map 3014, 1 sheet.

Schrader, T.P., 2001, Status of water levels and selected water-quality conditions in the Mississippi River valley alluvial aquifer in eastern Arkansas, 2000: U.S. Geological Survey Water-Resources Investigations Report, 2001-4124, 52 p.

Sholar, C.J., and Wood, P.A., 1995, Water use in Kentucky, 1990: U.S. Geological Survey Water-Resources Investigations Report 95-4032, 51 p.

Spiers, C.A., 1977, The Winona-Tallahatta aquifer in Mississippi: U.S. Geological Survey Water-Resources Investigations Report 77-125, 1 map.

Stanton, G.P., and Clark, B.R., 2003, Recalibration of a ground-water flow model of the Mississippi River Valley alluvial aquifer in southeastern Arkansas, 1918-1998, with simulations of hydraulic heads caused by projected ground-water withdrawals through 2049: U.S. Geological Survey Water-Resources Investigations Report 03-4232, 48 p.

Stephenson, L.W., Logan, W.N., Waring, G.A., and Howard, C.S., 1928, The ground-water resources of Mississippi, with discussions of the chemical character of the waters: U.S. Geological Survey Water Supply Paper 576, 515 p.

Stuart, M., Klotz, C., and Kascak, C., 1996, Agricultural resources and environmental indicators: U.S. Department of Agriculture Economic Research Service Number 17, 4 p.

Sumner, D.M., and Wasson, B.E., 1990, Geohydrology and simulated effects of large ground-water withdrawals on the Mississippi River alluvial aquifer in northwestern Mississippi: U.S. Geological Survey Water Supply Paper 2292, 60 p.

Tikhonov, A.N., 1963, Solution of incorrectly formulated problems and the regularization method: Soviet Mathematics, Doklady, v. 4, p. 1035–1038.

Tonkin, M. J., and Doherty, J., 2005, A hybrid regularized inversion methodology for highly parameterized environmental models, Water Resources Research, v. 41, no. 10, p. 1-16.

U.S. Geological Survey, 2008a, Office of Ground Water (OGW), accessed October 15, 2008, at http://water.usgs.gov/cgi/rasabiblio/?category=11&form=introduction.

U.S. Geological Survey, 2008b, The USGS Land Cover Institute (LCI), accessed October 15, 2008, at http://landcover.usgs.gov/natllandcover.php.

U.S. Geological Survey, 2008c, USGS water data for the Nation, accessed February 6, 2007, at http://waterdata.usgs.gov/nwis

Veach, A.C., 1906, Geology and underground water resources of northern Louisiana and southern Arkansas: U.S. Geological Survey Professional Paper 46, 422 p.

Warwick, P.D., SanFilipo, J.R., Crowley, S.S., Thomas, R.E., Freid, J., and Tulley, J.K., 1997, Map showing outcrop of the coal-bearing units and land use in the Gulf Coast Region: U.S. Geological Survey Open-File Report 97-172, 1 sheet.

Williamson, A.K., Grubb, H.F., and Weiss, J.S., 1990, Groundwater flow in the Gulf Coast aquifer systems, South-Central United States – A preliminary analysis: U.S. Geological Survey Water-Resources Investigations Report 89-4071, 134 p.

Williams, T.A., and Williamson, A.K., 1989, Estimating water-table altitudes for regional ground-water flow modeling, U.S. Gulf Coast: Ground Water v. 27, no. 3, p. 333-340.

Wolock, D., 2003, Flow characteristics at U.S. Geological Survey streamgages in the conterminous United States: U.S. Geological Survey Open-File Report 2003-146, vector digital data.

Publishing support provided by:
Lafayette and Rolla Publishing Service Centers

For more information concerning the research described in the report:

U.S. Geological Survey
Arkansas Water Science Center
401 Hardin Road
Little Rock, AR 72211-3528
(501) 228-3600

http://ar.water.usgs.gov

USGS

Clark and Hart—**The Mississippi Embayment Regional Aquifer Study (MERAS)**—Scientific Investigations Report 2009–5172